



# INVESTIGATION OF FEP TEFLON AS A COVER FOR SILICON SOLAR CELLS

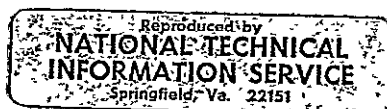
by

S. A. Greenberg, M. McCargo, and W. L. Palmer

LOCKHEED PALO ALTO RESEARCH LABORATORY

prepared for

NATIONAL AERONAUTICS AND SPACE ADMINISTRATION



NASA Lewis Research Center  
Contract NAS 3-14398  
Americo F. Forestieri, Project Manager

FACILITY FORM 602	N71-35231	
	(ACCESSION NUMBER)	(THRU)
	69 (PAGES)	63. (CODE)
	CR-72970 (NASA CR OR TMX OR AD NUMBER)	03 (CATEGORY)

1. Report No. NASA CR-72970		2. Government Accession No.		3. Recipient's Catalog No.	
4. Title and Subtitle INVESTIGATION OF FEP TEFLON AS A COVER FOR SILICON SOLAR CELLS				5. Report Date August 1971	
				6. Performing Organization Code	
7. Author(s) S. A. Greenberg, M. McCargo, and W. L. Palmer				8. Performing Organization Report No. LMSC-D243070	
9. Performing Organization Name and Address Lockheed Palo Alto Research Laboratory Palo Alto, California				10. Work Unit No.	
				11. Contract or Grant No. NAS 3-14398	
12. Sponsoring Agency Name and Address National Aeronautics and Space Administration Washington, D. C. 20546				13. Type of Report and Period Covered Contractor Report	
				14. Sponsoring Agency Code	
15. Supplementary Notes Project Manager, Americo F. Forestieri, NASA Lewis Research Center, Cleveland, Ohio					
16. Abstract  A program was executed for the purpose of demonstrating the feasibility of using FEP Teflon as a cover for silicon solar cells. A process for heat sealing Type C FEP to silicon solar cells was developed and optimized. Abbreviated and extended environmental tests were conducted on the optimized cells. The effects of high humidity and temperature, thermal shock, and ultraviolet proton and electron irradiation were evaluated. The process was extended to 15-cell modules, which were evaluated under similar environmental conditions. The performance of the FEP-covered cells was encouraging and compared favorably with that of conventional cover glasses.					
17. Key Words (Suggested by Author(s))  Solar cells FEP Teflon Environmental effects				18. Distribution Statement  Unclassified - unlimited	
19. Security Classif. (of this report)  Unclassified		20. Security Classif. (of this page)  Unclassified		21. No. of Pages  69	
				22. Price*  \$3.00	

## FOREWORD

This document was prepared by the Thermophysics Group of the Engineering Sciences Directorate, Lockheed Palo Alto Research Laboratory and by the Manufacturing Research Group, Lockheed Missiles & Space Company, for the Lewis Research Center of the National Aeronautics and Space Administration as the final report of the research activities carried out under Contract NAS 3-14398, from July 1970 through May 1971. The work was administered under the technical direction of A. F. Forestieri of the Lewis Research Center.

PRECEDING PAGE BLANK NOT FILMED

#### ABSTRACT

A program was executed for the purpose of demonstrating the feasibility of using FEP Teflon as a cover for silicon solar cells. A process for heat sealing 5-mil Type C FEP to silicon solar cells was developed and optimized. Abbreviated and extended environmental tests were conducted on the optimized cells. The resistance of the FEP/solar cell package to high humidity and temperature, thermal shock, and ultraviolet, proton, and electron irradiation was evaluated. The process was extended to 15-cell flexible modules, which were evaluated under similar environmental conditions. The performance of the FEP-covered cells was encouraging and compared favorably with that of conventional cover glasses.

## ILLUSTRATIONS

Figure		Page
1	Spectral transmittance of FEP Teflon — 0.013-cm (5-mil) thickness	5
2	FEP bond strength as a function of dwell time	8
3	FEP bond strength as a function of pressing temperature	9
4	Comparison of cell output in the bare and covered conditions	12
5	Effect of surface defects on cell output	13
6	UV exposure 52 ESH on FEP-covered cell	16
7	UV exposure 52 ESH on bare cell	17
8	Proton flux profile	18
9	Proton exposure on bare cell	19
10	Proton exposure on FEP-covered cell	20
11	Effect of $10^{16}$ e <sup>-</sup> /cm <sup>2</sup> on FEP-covered cell with catastrophic failure	21
12	Effect of $10^{16}$ e <sup>-</sup> /cm <sup>2</sup> on FEP-covered cell with delamination	22
13	Effect of $10^{16}$ e <sup>-</sup> /cm <sup>2</sup> on bare cell	23
14	Thermal cycling profile	26
15	Effect of uv exposure on output of FEP-covered cell	27
16	Effect of protons on short-circuit current	28
17	Effect of $10^{16}$ e <sup>-</sup> /cm <sup>2</sup> on FEP-covered cell with silicon oxide removal	31
18	Effect of $10^{16}$ e <sup>-</sup> /cm <sup>2</sup> on FEP-covered cell with delamination	32
19	Effect of $10^{16}$ e <sup>-</sup> /cm <sup>2</sup> on bare cell	33
20	Effect of $10^{15}$ e <sup>-</sup> /cm <sup>2</sup> on FEP-covered cell	34
21	Effect of $10^{15}$ e <sup>-</sup> /cm <sup>2</sup> on bare cell	35
22	Effect of $10^{14}$ e <sup>-</sup> /cm <sup>2</sup> on FEP-covered cell	36
23	Effect of $10^{14}$ e <sup>-</sup> /cm <sup>2</sup> on bare cell	37
24	Tooling for five-cell submodules	39
25	Water-cooled heat sink	41

PRECEDING PAGE BLANK NOT FILMED

## CONTENTS

Section	Page
1 INTRODUCTION	1
2 STUDIES ON SINGLE SILICON SOLAR CELL/FEP PACKAGES	3
2.1 Objectives	3
2.2 Materials	3
2.3 Cleaning Procedures	4
2.4 Heat-Sealing Optimization	4
2.5 Abbreviated Environmental Tests	14
2.6 Full Environmental Tests	24
3 STUDIES ON MULTICELL MODULES	38
3.1 Objectives	38
3.2 Module Fabrication	38
3.3 Full Environmental Tests	45
4 DISCUSSION AND CONCLUSIONS	58
5 RECOMMENDATIONS FOR FUTURE STUDIES	60
6 REFERENCES	61
Appendix	
A EXPERIMENTAL APPARATUS	62
A.1 Static Ultraviolet Exposure Apparatus	62
A.2 Proton Exposure Facility	63
A.3 Solar Simulator	63
A.4 Thermal Cycling Apparatus	67
B SPACE ENVIRONMENTAL CONSIDERATIONS	68
B.1 Solar Ultraviolet Radiation	68
B.2 Thermal Cycling	68
B.3 Low-Energy Protons	68
B.4 Electron Irradiation	69

Figure		Page
26	FEP-covered submodules	42
27	Circuitry interconnect pattern	43
28	FEP-covered module	44
29	Effect of uv on FEP-covered module	47
30	Effect of $1 \times 10^{13}$ p <sup>+</sup> /cm <sup>2</sup> on FEP-covered module	48
31	Effect of $1 \times 10^{15}$ p <sup>+</sup> /cm <sup>2</sup> on FEP-covered module	49
32	Effect of $1 \times 10^{17}$ p <sup>+</sup> /cm <sup>2</sup> on FEP-covered module	50
33	Effect of $2 \times 10^{17}$ p <sup>+</sup> /cm <sup>2</sup> on FEP-covered module	51
34	Effect of $1 \times 10^{15}$ e <sup>-</sup> /cm <sup>2</sup> on FEP-covered module	53
35	Effect of $1 \times 10^{14}$ e <sup>-</sup> /cm <sup>2</sup> on FEP-covered module	54
36	Effect of $4 \times 10^{14}$ e <sup>-</sup> /cm <sup>2</sup> on FEP-covered module	55
37	Total hemispherical emittance of FEP compared with fused silica	57
38	Combined environments chamber	64
39	Comparison of solar simulator with the Johnson solar spectrum	65
40	Spectral deviation of simulator	66

## TABLES

Table		Page
1	Time-temperature profile of cells in press	7
2	Optimum processing parameters	10
3	Angular dependence on short-circuit current as a function of surface finish	11
4	Comparison of optical properties of conventional and FEP-covered modules	56
5	Comparison of FEP and fused silica covers	59
6	Electrons at synchronous altitudes	69

## Section 1

### INTRODUCTION

The primary purposes of solar cell covers are to provide protection from penetrating radiation and to lower the operating temperature of the cells via high infrared emittance. Conventional silicon solar cell arrays employ covers of 6- to 20-mil glass or fused silica, adhesive bonded to the front surface of the cells. To protect the adhesive from optical degradation induced by solar ultraviolet radiation, it is generally necessary to coat the rear surface of the cover glass with a multilayer film that does not transmit uv radiation. In addition, the front surface of the cover glass is provided with a low refractive index coating such as  $\text{MgF}_2$  ( $n \cong 1.38$ ) to minimize front surface reflectance losses.

Although conventionally protected solar arrays have been relatively successful in providing reliable power for numerous spacecraft missions, the application procedures, material, and coating costs of conventional cover glasses represent a major portion of solar array fabrication costs. The use of FEP Teflon (fluorinated ethylene propylene) as a solar cell cover material provides a novel approach to solar cell radiation protection and temperature control. The flexible dielectric film is suitable for application to large-area solar arrays by direct heat-sealing techniques. The favorable cost, simplicity, ease of fabrication can provide a major advance in the state-of-the-art of solar array manufacturing.

This program was designed to evaluate the feasibility of utilizing FEP as a replacement for conventional silicon solar cell covers. The investigations were conducted for single FEP/solar cell packages and 15-cell modules in three tasks.

Task I was concerned with optimization of the heat-sealing process. The effects of time, temperature, pressure, cleaning, and other controllable processing parameters were investigated. Initial efforts were made using 2- by 2-cm n-on-p silicon solar cells in an attempt to reproducibly produce generally spaceworthy individual Teflon/solar cell packages with good bonding and high electrical output.

Task II was devoted to evaluation of the effectiveness of the process with regard to bond integrity, optical transmission of the covers, cell damage, mechanical strength, electrical output under simulated sunlight, and other characteristics pertinent to overall space worthiness.

Task III was concerned with environmental testing of the individual Teflon/solar cell packages and modules. Abbreviated testing of the covered cells included high humidity and temperature, thermal shock, ultraviolet, and proton and electron irradiation. Full environmental tests of the same parameters were also conducted but were more extensive and provided detailed performance data of individual cell packages and modules as a function of exposure duration.



## Section 2

### STUDIES ON SINGLE SILICON SOLAR CELL/FEP PACKAGES

#### 2.1 OBJECTIVES

The goal of the initial efforts under this program was to optimize the heat-sealing techniques for individual silicon solar cell/FEP packages. The parameters investigated included temperature, pressure, time, cleaning techniques and parting materials.

#### 2.2 MATERIALS

##### 2.2.1 Solar Cells

Studies under this program were conducted with 14-mil thick, 2- by 2-cm n-on-p silicon solar cells. The cells supplied by Centralab Semiconductor Division, Globe Union, Inc., were solderless, with a base resistivity of 1 to 3  $\Omega$ cm and minimum average current of 123 mA at 0.470 V. For reasons of economy, some of the initial optimization studies were conducted with Class II mechanical cells of the same type.

The use of solderless cells was dictated by the fact that the bonding temperature required for FEP heat sealing exceeds the melting point of conventional solders, leading to solder splaying. Investigation of high-temperature solder materials was outside the scope of this program.

##### 2.2.2 FEP Teflon

Fluorinated ethylene propylene (FEP) Teflon film is soft and pliable and poses no significant handling problems except for the requirement of reasonable care to prevent surface scratches. The material supplied by Du Pont comes in several forms. Type A FEP is untreated and nonwetting and can be thermally bonded only above its melting point (548°K; 275°C). Type C FEP has one surface treated by a Du Pont proprietary process that promotes wetting and allows heat sealing to occur in the 473°K (200°C) range. Type C-20 has both surfaces treated in this manner. Although the nature of the surface treatment is proprietary, it is speculated that a thin layer ( $\sim 1 \mu$ ) of foreign material is applied to the surface. The Type C shows a reduction of a few percent in transmittance below 4000 Å compared with Type A of the same thickness. FEP Type CX, recently introduced, is similar to Type C but with a modified surface treatment.

The FEP used exclusively throughout this program was Type C FEP with a 5-mil (0.013 cm; 0.005 in.) thickness. All studies were conducted using FEP cut from a single roll in order to eliminate variations in material properties.

## 2.3 CLEANING PROCEDURES

Prior to establishing heat-sealing criteria, it was necessary to develop cleaning procedures for the as-received FEP film that would be consistent with good bonding practice and would be practical and reproducible.

Initial attempts at cleaning utilized ultrasonic agitation with the film immersed in various solvents. Methyl alcohol, ethyl alcohol, Freon TWD, and methylene chloride were investigated as solvents. In all cases, some residue and/or particles remained on the surface after immersion. The FEP surface is somewhat electrostatic in nature and tends to attract and hold dust particles.

Agitation of the film in an aqueous detergent solution followed by rinsing with flowing distilled water was found to provide an adequate technique for removal of dust particles. However, examination under a microscope (200x) revealed residual brown spots of an organic nature.

Ultimately, it was determined that reproducible cleaning of the FEP could be achieved by immersion of the material in boiling ethyl alcohol. This technique provided for rapid drying without residue or dust accumulation. Since the tests were not conducted under clean-room conditions, dust accumulation following cleaning dictated either immediate usage or storage in a clean container. Storage tests indicated that the cleaned film could be kept for 14 days without accumulating contamination. In most cases, however, freshly cleaned FEP was employed.

Transmission spectra of the freshly cleaned 5-mil Type C FEP are presented in Figure 1. No detectable difference in spectral transmittance could be observed between the clean and the as-received FEP except in the case where excessive dust was intentionally placed on the film.

## 2.4 HEAT-SEALING OPTIMIZATION

### 2.4.1 Heat-Sealing Approach

Two basic approaches to heat sealing of FEP to individual silicon solar cells were initially evaluated: platen press forming and vacuum bagging. Vacuum bagging was considered to provide less flexibility in process parameter evaluation than the platen press technique, particularly in the area of applied pressure studies. Therefore, primary emphasis was placed on using platen press techniques for process optimization. Subsequently, during the course of this program, it was demonstrated that the optimum process parameters are such that either technique may be viable. However, within the scope of this program, the decision was made to concentrate on platen press techniques.

### 2.4.2 Parting Materials

In order to heat seal the FEP to the surface of a silicon solar cell in a reproducible manner, it is necessary to cover the FEP with a slip sheet that is easily parted from the FEP and does not degrade the properties of the FEP, particularly the optical

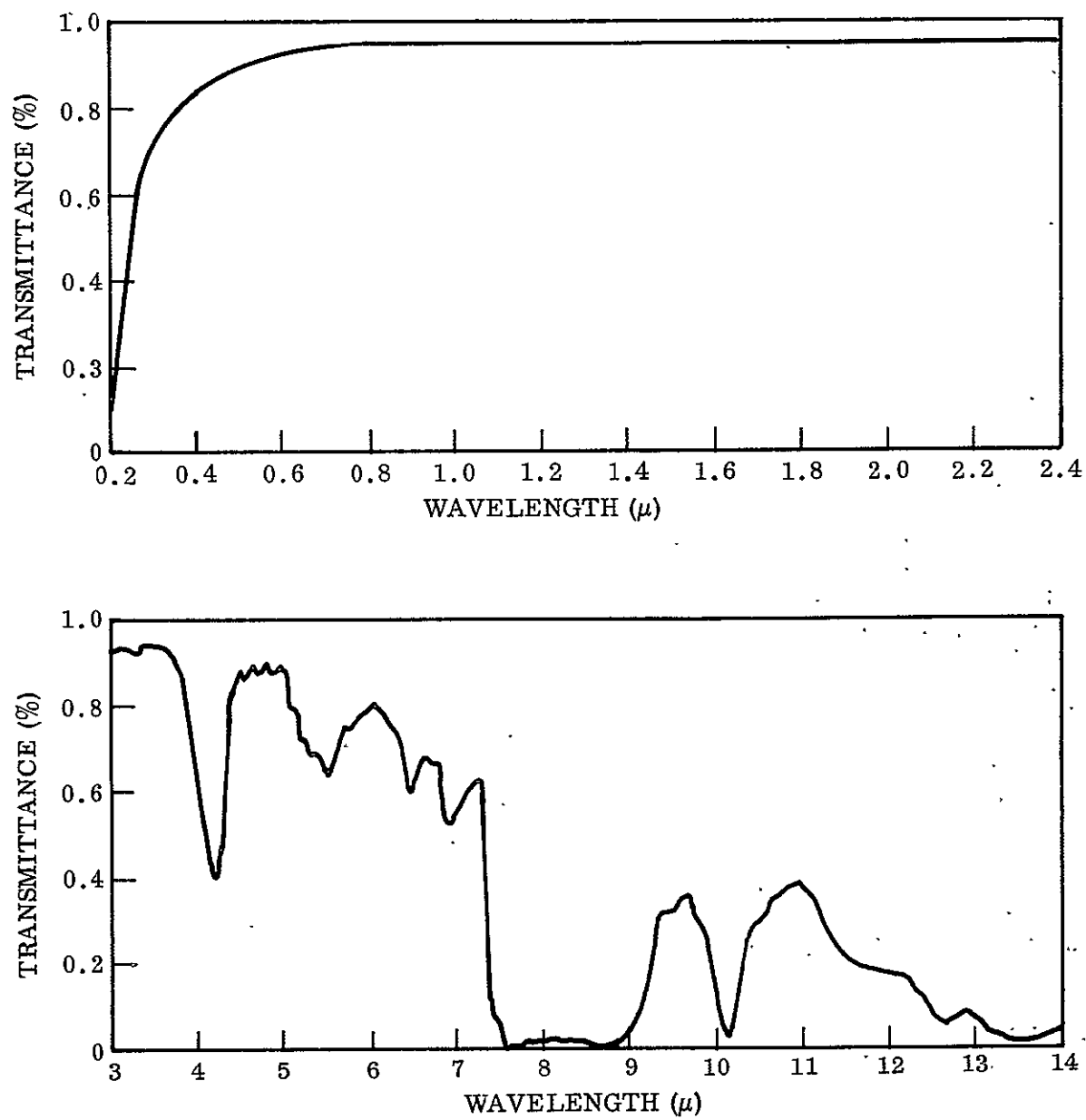


Figure 1. - Spectral transmittance of FEP Teflon - 0.013-cm (5-mil) thickness

transmission. Below the melting point of the bulk FEP ( $\sim 548^\circ\text{K}$ ;  $275^\circ\text{C}$ ), virtually any film with a good surface finish may be used that does not melt or deform significantly. However, at temperatures approaching  $548^\circ\text{K}$  ( $275^\circ\text{C}$ ), the additional requirement of poor adhesion between the FEP and parting material is imposed. Of available film materials, only polyimide (Kapton) and TFE Teflon were judged to meet all the requirements.

Initial heat sealing tests between  $473^\circ\text{K}$  ( $200^\circ\text{C}$ ) and  $573^\circ\text{K}$  ( $300^\circ\text{C}$ ) were conducted using TFE Teflon and polyimide films as parting materials. The polyimide film (1 mil) produced FEP/solar cell packages with smooth surfaces that had negligible adhesion to the slip sheet. Using the TFE Teflon as the slip sheet (2 mils), the resulting packages had diffuse surface finishes. At temperatures above  $558^\circ\text{K}$  ( $285^\circ\text{C}$ ), some difficulty was encountered in separating the FEP from the TFE. Presumably the FEP flowed into the somewhat rough TFE surface.

Based on these tests, it was determined that Kapton provided an ideal parting material in all respects. Kapton slip sheets were used exclusively throughout the remainder of the program, and no problems related to the use of this material were encountered.

#### 2.4.3 Bonding Procedures

The establishment of Kapton as an adequate parting material for heat sealing FEP allowed a standardized platen press heat-sealing procedure to be established. The technique initially employed consisted of laying up a silicone rubber pad [0.159 cm (1/16 in.) thick], a Kapton slip sheet, and a solar cell. A precut strip of clean FEP Teflon was aligned over the cell to cover all but the bus strip on the top edge. Another Kapton sheet was placed over the assembly and covered with a second silicone rubber pad. The sandwich assembly was placed between heated platens in a press, and pressure was applied for a given period. Upon release of pressure, the FEP/cell package was removed and trimmed as required. Modifications of this technique were employed where process parameter investigations dictated.

#### 2.4.4 Temperature Effects

To evaluate the effects of pressing temperature on the sealing process, correlation tests between the temperature of the heated upper and lower press platens and the temperature of the silicon solar cell in the sandwich assembly were run. The platen temperatures were monitored using copper-constantan thermocouples with an ice water reference junction. Thermocouples were placed on the upper and lower faces of the solar cells during pressing. The time required to bring the cells up to preheated platen temperatures were measured using an arbitrary pressure of  $3.5 \times 10^6 \text{ N/m}^2$  (500 psi). The results are shown in Table 1.

From Table 1, it can be seen that over the operational temperature range the cells reach platen temperature in less than 60 sec. Study of temperature requirements for heat sealing therefore necessitated dwell times in the hot press of a minimum of 60 sec at the higher temperatures and 30 sec in the lower temperature region [ $513^\circ\text{K}$  ( $\sim 240^\circ\text{C}$ )].

TABLE 1. — TIME-TEMPERATURE PROFILE OF CELLS IN PRESS

Platen Temperature	Time Required for Cell to Reach Temperature, sec
473°K(200°C)	25
493°K(220°C)	27
513°K(240°C)	30
533°K(260°C)	34
553°K(280°C)	40
573°K(300°C)	48

To establish a temperature range for effective bonding, five cells were heat sealed with FEP at temperature increments of 10°K in the range 493° — 553°K (220° — 280°C). At 493°K(220°C), negligible bond strength occurred and the FEP could be lifted from the cell easily. At 503°K(230°C), two of the five cells showed incomplete lamination, particularly at the edges. Tests at all other temperatures resulted in good adherent, optically clear FEP/solar cell packages. The tests were repeated at 508°K(235°C) in an attempt to establish a lower limit for heat-sealing temperature. Complete, adherent bonds were obtained at this temperature, indicating that the bonding threshold is in the temperature region 503° — 508°K(230° — 235°C).

These data appear to be compatible with data supplied by Du Pont (ref. 1), as shown in Figure 2. In this figure, it can be seen that the limiting strength of Type C FEP bonded to itself is obtained after a 1-min dwell time at 506°K(233°C). Figure 3, however, indicates that the ultimate bond strength is not reached until 508°K(235°C), but that the limiting strength is approached for longer dwell times at lower temperatures. For the purposes of this program, long dwell times are not desirable, and the minimum acceptable pressing temperature is 508°K(235°C).

#### 2.4.5 Pressure Effects

The effect of applied pressure on the bonding performance of FEP was evaluated in detail. At a fixed temperature of 518°K(245°C), silicon solar cells were bonded in triplicate under pressures of  $17 \times 10^4$ ,  $34 \times 10^4$ ,  $69 \times 10^4$ ,  $34 \times 10^5$ ,  $69 \times 10^5$ ,  $14 \times 10^6$ , and  $34 \times 10^6$  N/m<sup>2</sup> (25, 50, 100, 1000, 2000, and 5000 psi). The cells were held at temperature for 60 sec and rapidly quenched by removal from the hot press to a room-temperature, water-cooled heat sink.

At applied pressures above  $69 \times 10^4$  N/m<sup>2</sup> (100 psi) all cells were uniformly covered and could not easily be stripped by a manual pull test. At  $17 \times 10^4$  and  $34 \times 10^4$  N/m<sup>2</sup> (25 and 50 psi), two and three cells in each case showed incomplete lamination and were easily peeled. Repetition of the tests at these pressure produced identical results, indicating that the effective bonding threshold was above  $34 \times 10^4$  N/m<sup>2</sup> (50 psi). Repetition of the pressure effect tests at dwell times of 2, 3, 5, and 10 min

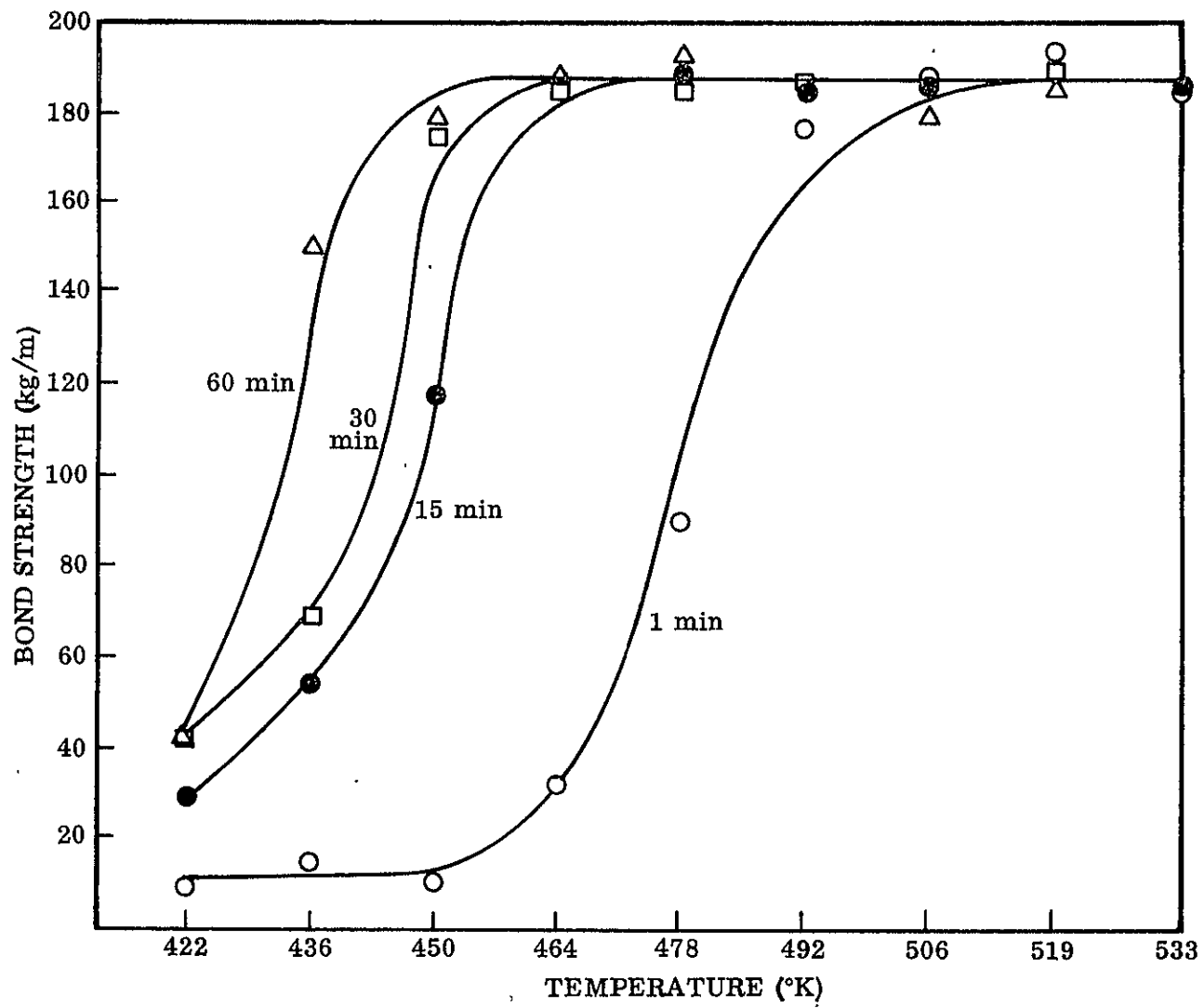


Figure 2. - FEP bond strength as a function of dwell time

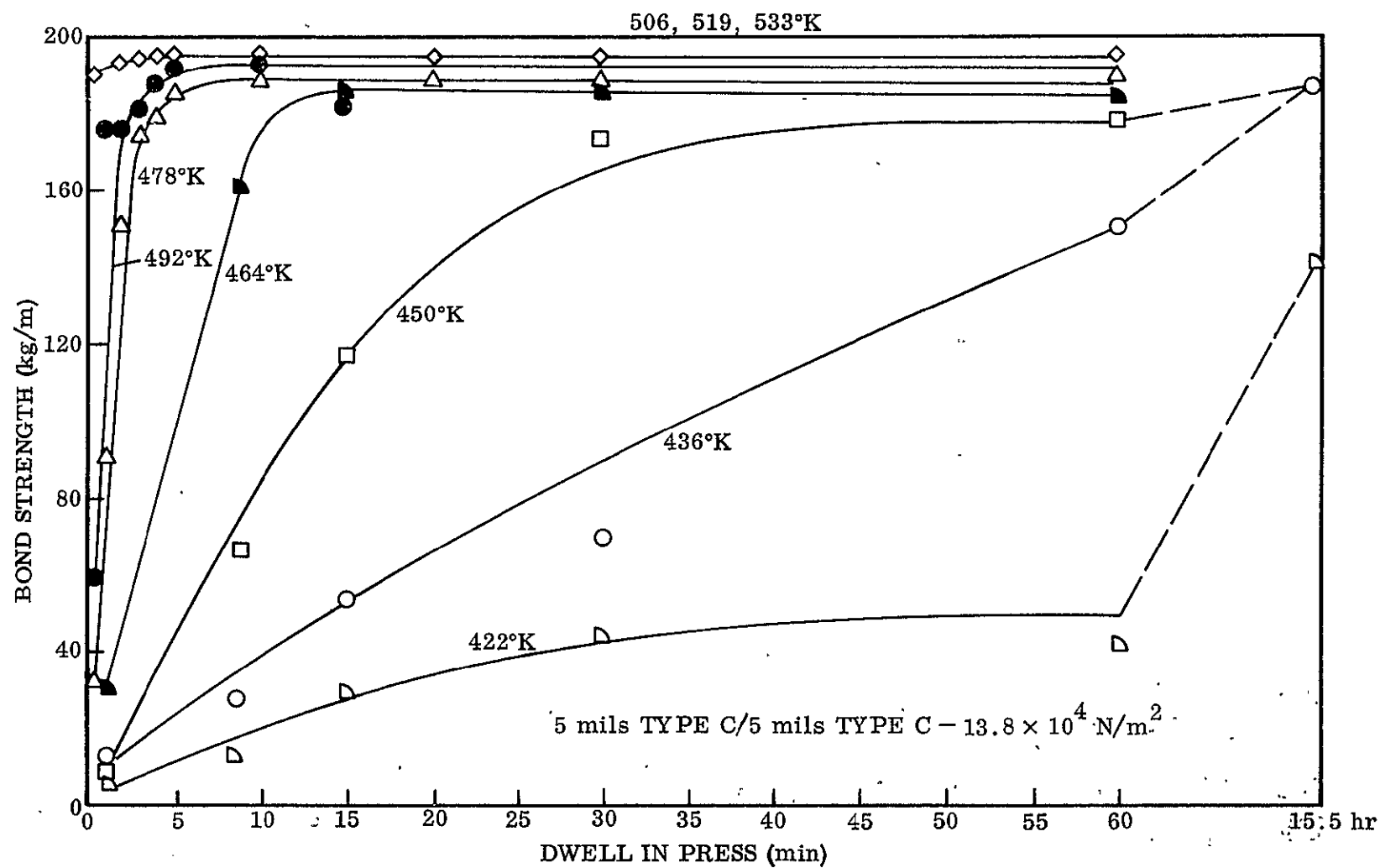


Figure 3. - FEP bond strength as a function of pressing temperature

produced good-quality cells, with only a single bond failure at the 5-min dwell time for  $69 \times 10^4 \text{ N/m}^2$  (100 psi).

To assess concurrently the effects of temperature and pressure, triplicate samples were fabricated at seven pressures between  $34 \times 10^4$  and  $34 \times 10^6 \text{ N/m}^2$  (50 and 5000 psi) at 503°, 513°, 523°, 533°, and 543°K (230°, 240°, 250°, 260°, and 270°C). At 503°K (230°C), random bond failures occurred over the entire pressure range, indicating insufficient temperature. For all the other conditions, excellent cell packages resulted except for several edge delaminations for pressures below  $69 \times 10^4 \text{ N/m}^2$  (100 psi).

#### 2.4.6 Optimum Processing Parameters

The results of the parametric study of processing parameters indicates that the process of heat-sealing FEP to silicon solar cells is rather insensitive to processing parameters if the critical temperature and pressure are exceeded. Quench cooling of covered cells at zero load has been found to provide somewhat superior adhesion compared with cooling under pressure, although qualitatively both techniques yield adequately strong bonds.

The selection of unique processing conditions remains somewhat arbitrary; however, nominally optimum conditions have been selected on the basis of convenience and tend to lie near the midrange of valid operating conditions. Table 2 summarizes the operational and optimum conditions for heat sealing of FEP to individual silicon solar cells.

TABLE 2. — OPTIMUM PROCESSING PARAMETERS

Parameter	Operating range	Nominal optimum value
Temperature	508°–553°K (235°–280°C)	523°K(250°C)
Applied pressure	$69 \times 10^4$ – $34 \times 10^6 \text{ N/m}^2$ 100–5000 psi	$34 \times 10^5$ – $69 \times 10^5 \text{ N/m}^2$ 500–1000 psi
Dwell time at temperature	30 sec – 10 min	60 sec
Parting material	Polyimide (Kapton) 0.0013 cm (0.5 mil)	—
Pressing pad	Silicone rubber 0.16 cm (1/16 in.)	—
Cleaning	Boiling ethyl alcohol	—
Solar cell condition	Solderless	



To assess the reproducibility of the optimized process and to evaluate the bond quality and the effect of heat sealing of FEP on the output of the solar cells, 10 cells were processed separately. Examination of the cells revealed that the surfaces were of uniformly high quality, free from scratches, bubbles, and wrinkles. Probing with a sharp scalpel at the edges and near the center failed to initiate any tears or delaminations. It was essentially impossible to remove the heat-sealed FEP from the cells without cracking the solar cells.

Curves of current versus voltage of the optimized covered cells under simulated solar radiation (see Appendix A) were compared with current/voltage curves for the same cells measured prior to covering. Without exception, the latter were identical to the curves for the bare cells within the reproducibility of the solar simulator and measuring equipment. Figure 4 shows a typical set of curves and provides an indication of the performance of the FEP cover. This performance can be compared with that of a conventional fused silica adhesive bonded cover glass, which imposes a short circuit current loss of about 2% over that for the bare cell.

Although this optimized set of cells was free from surface defects, experience had indicated that cells containing wrinkles, scratches, or bubbles were occasionally produced. To assess the effects of these defects on cell performance, a cell having gross surface irregularities was produced by melting the FEP film (at 583°K; 310°C) and intentionally deforming the surface. Figure 5 shows that no appreciable diminution of cell output resulted, despite the nonuniform thickness and the wrinkles and bubbles in the FEP cover.

To assess further the effects of surface finish on the electrical and optical properties of the Teflon cover, comparisons were made between a smooth-finish (optimized) covered cell and a matte-finish cell produced by interposing a nickel mesh during heat sealing. The ratio of short-circuit current at normal incidence (90°) to that at 60° and 30° incidence for each cell is given in Table 3.

TABLE 3. - ANGULAR DEPENDENCE ON SHORT-CIRCUIT CURRENT  
AS A FUNCTION OF SURFACE FINISH

Angle of incidence $\theta$ , deg	Smooth-finish short-circuit current, mA	Ratio $\frac{I(\theta)}{I(90^\circ)}$	Matte-finish short-circuit current, mA	Ratio $\frac{I(\theta)}{I(90^\circ)}$
90	148	1.00	138.5	1.0
60	128	0.865	120	0.865
30	72	0.486	68	0.490

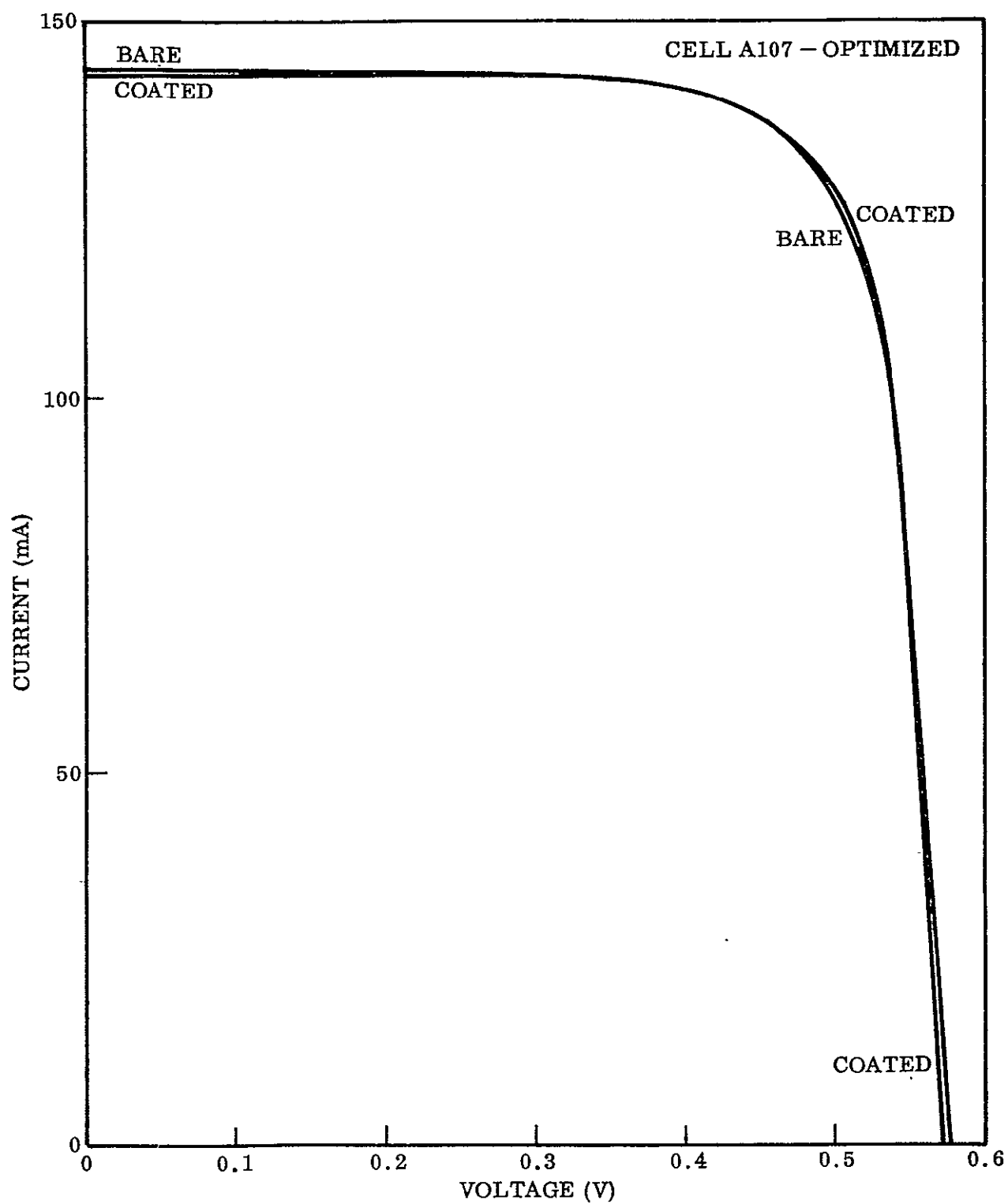


Figure 4. — Comparison of cell output in the bare and covered conditions

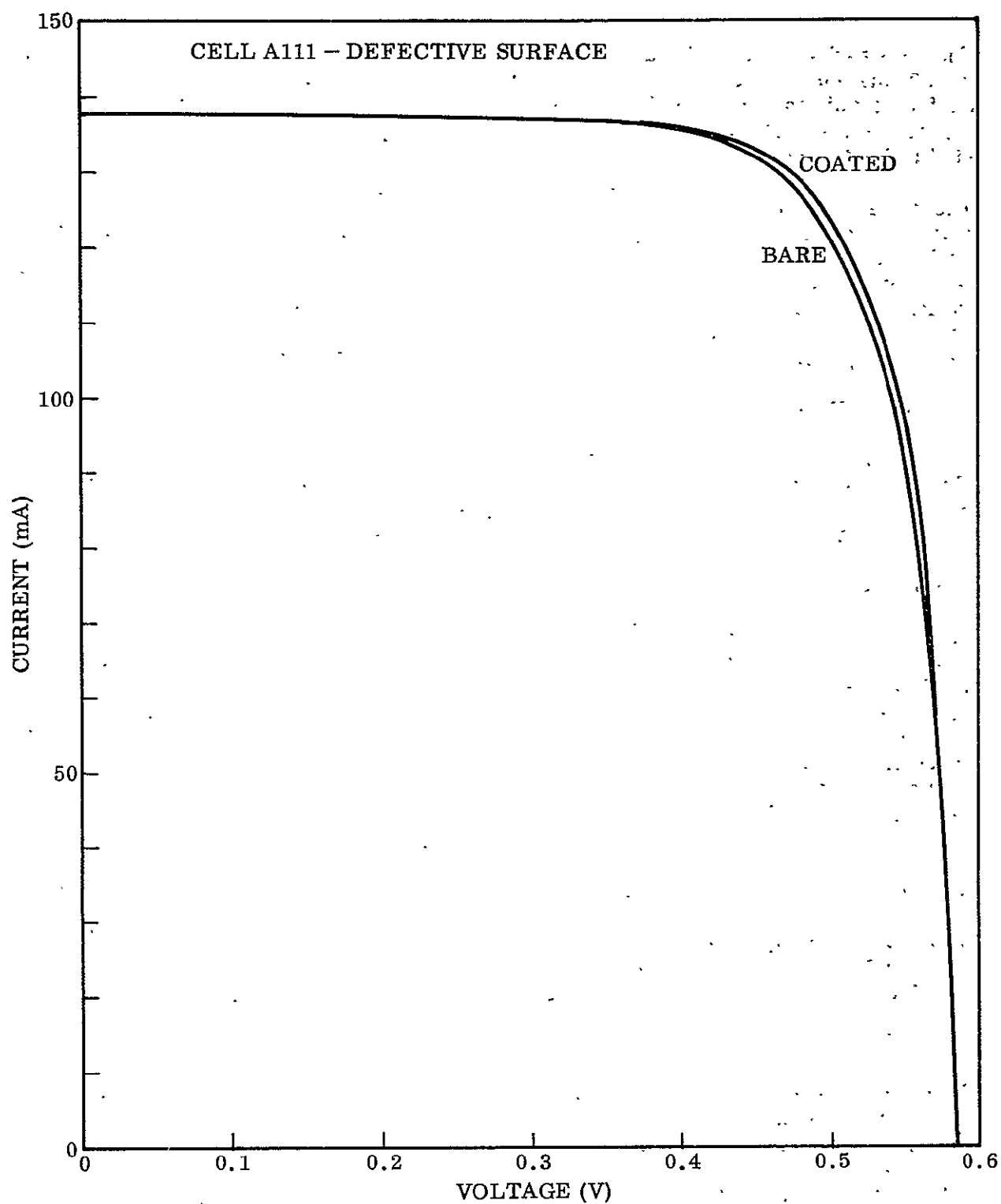


Figure 5. - Effect of surface defects on cell output

The ratios of short-circuit current for the smooth- and matte-finish cells are identical for 30° and 60° incidence of radiation, indicating that transmission is independent of surface condition. Apparently, backscattering is negligible for the particular surface contour studied, although smaller surface defects approximating the wavelength of visible light might result in some attenuation.

The results obtained under the optimization and evaluation phases of this program conclusively demonstrated the reproducibility of the heat-sealing process for bonding FEP Teflon (Type C) to silicon solar cells. The outstanding optical transmission characteristics of the material were exemplified by the fact that the bare and covered solar cells exhibited virtually identical current/voltage curves under simulated sunlight. There was no evidence, in this portion of the study, of any characteristic of the FEP/solar cell package that would cast doubt on the space worthiness of the package.

## 2.5 ABBREVIATED ENVIRONMENTAL TESTS

Silicon solar cells covered with FEP under optimized conditions were subjected to abbreviated environmental tests in order to discern any problem areas requiring process modification. The abbreviated environmental tests included high humidity and temperature, thermal shock, uv radiation, and electron and proton irradiation.

### 2.5.1 High Humidity and Temperature

Three optimized FEP/solar cell packages were subjected to 90% relative humidity at 313°K(40°C) for 72 hr. Simultaneously exposed were three other cells fabricated with FEP overlapping one edge of the cell. The latter were used to measure the effect of the exposure on bond peel strength. The cells were reevaluated after removal from the humidity chamber. No evidence of delamination was noted for any cells. The current/voltage curves of the exposed cells were unchanged from the original traces. The peel strengths of the specially fabricated packages were measured using a 90° and 1 in./min force rate. Comparison of the 25 exposed cells to a control group indicated that the average bond peel strength decreased from 2.14 to 1.25 kg (4.71 to 2.75 lb) upon exposure to the elevated humidity - temperature environment. The high and low values were 1.74 and 0.91 kg (3.83 and 2.0 lb), respectively, with all others in the range 0.91-1.59 kg (2.0-3.5 lb). Unfortunately, the limited number of samples examined cast some doubt upon the statistical validity of the results. In any event, the final bond strength in excess of 0.91 kg (2 lb) is substantial and more than adequate for the anticipated usage.

### 2.5.2 Thermal Shock

Three FEP/solar cell packages were alternately (1) dipped in liquid nitrogen and (2) held at room temperature for 10 such cycles. The cell packages were held in a wire cage so as to impose no mechanical restraints. No evidence of delamination, cracking, or blistering was noted. Following thermal shock exposures, the cells were reevaluated for electrical output and no changes were noted from the pretest values.

### 2.5.3 Ultraviolet Radiation

Three sample FEP/solar cell packages were exposed to ultraviolet radiation in a vacuum of  $7.9 \times 10^{-9}$  N/m<sup>2</sup> ( $6 \times 10^{-7}$  torr). The total exposure was 52 ESH, as determined by the wavelength interval between (0.2 - 0.3  $\mu$ ). From Figure 6, it can be seen that the uv exposure caused a decrease of about 1% in the short circuit current. Figure 7 shows the pre- and post-exposure current/voltage curve for a bare cell simultaneously exposed. Little difference in performance was noted between the covered cells and the bare cells, indicating that the short exposure did not cause measurable degradation of the FEP.

### 2.5.4 Proton Irradiation

Three FEP/solar cell packages and a bare cell were exposed to  $3.2 \times 10^{-16}$  -J (2-keV) protons in a vacuum of  $6.6 \times 10^{-9}$  N/m<sup>2</sup> ( $5 \times 10^{-7}$  torr). The proton flux was measured periodically using Faraday buttons mounted on the rear of a rotatable sample table. The proton flux profile (Fig. 8) was relatively constant and the total dose was integrated to  $2.08 \times 10^{17}$  protons/cm<sup>2</sup>.

Figure 9 shows the effect of the protons on the bare cell. Catastrophic degradation occurred, with a reduction in maximum power of < 65%. Conversely, the FEP-covered cell (Fig. 10) shows only a 5 to 6% loss in short-circuit current and maximum power. It is readily apparent that the FEP cover serves as an excellent radiation barrier for low-energy protons, particularly considering the extreme dose received (in excess of 25 years in the interplanetary solar wind environment).

### 2.5.5 Electron Irradiation

Six FEP-covered cells and three bare cells were subjected to  $3.2 \times 10^{-13}$  -J (2-MeV) electron irradiation in vacuum. The total dose was  $1 \times 10^{16}$  electrons/cm<sup>2</sup> at a flux of  $1.3 \times 10^{12}$  electronics/cm<sup>2</sup>-sec. Following exposure, the samples were removed from the chamber and examined. Three of the six FEP-covered cells exhibited catastrophic failure in which the FEP and silicon oxide coatings on the cells separated, exposing bare silicon patches. The grids remained bonded to the cells, while the SiO<sub>x</sub> coating adhered to the FEP. The other three cells exhibited simple FEP delamination. The separated FEP covers were flexible, but embrittlement increased with time upon exposure to air.

Figures 11, 12, and 13 show, respectively, the current/voltage curves before and after a catastrophic failure; a delaminated cell; and bare cell exposure. There was little difference in performance between the delaminated FEP cell and the bare cell; this was not unexpected, since the range of a  $3.2 \times 10^{-13}$  J (2-MeV) electron is greater than the 5-mil cover thickness.

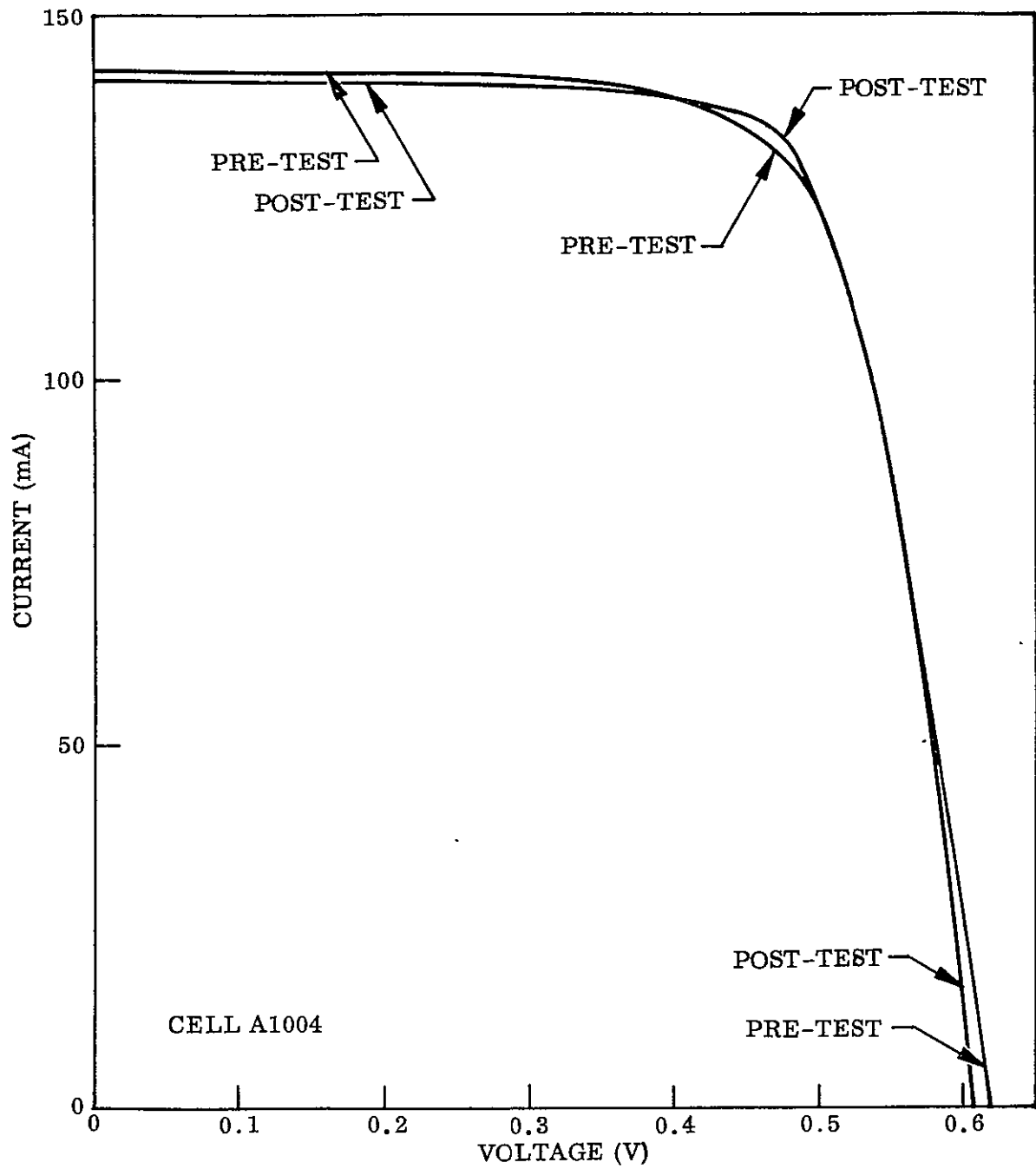


Figure 6. - UV exposure 52 ESH on FEP-covered cell

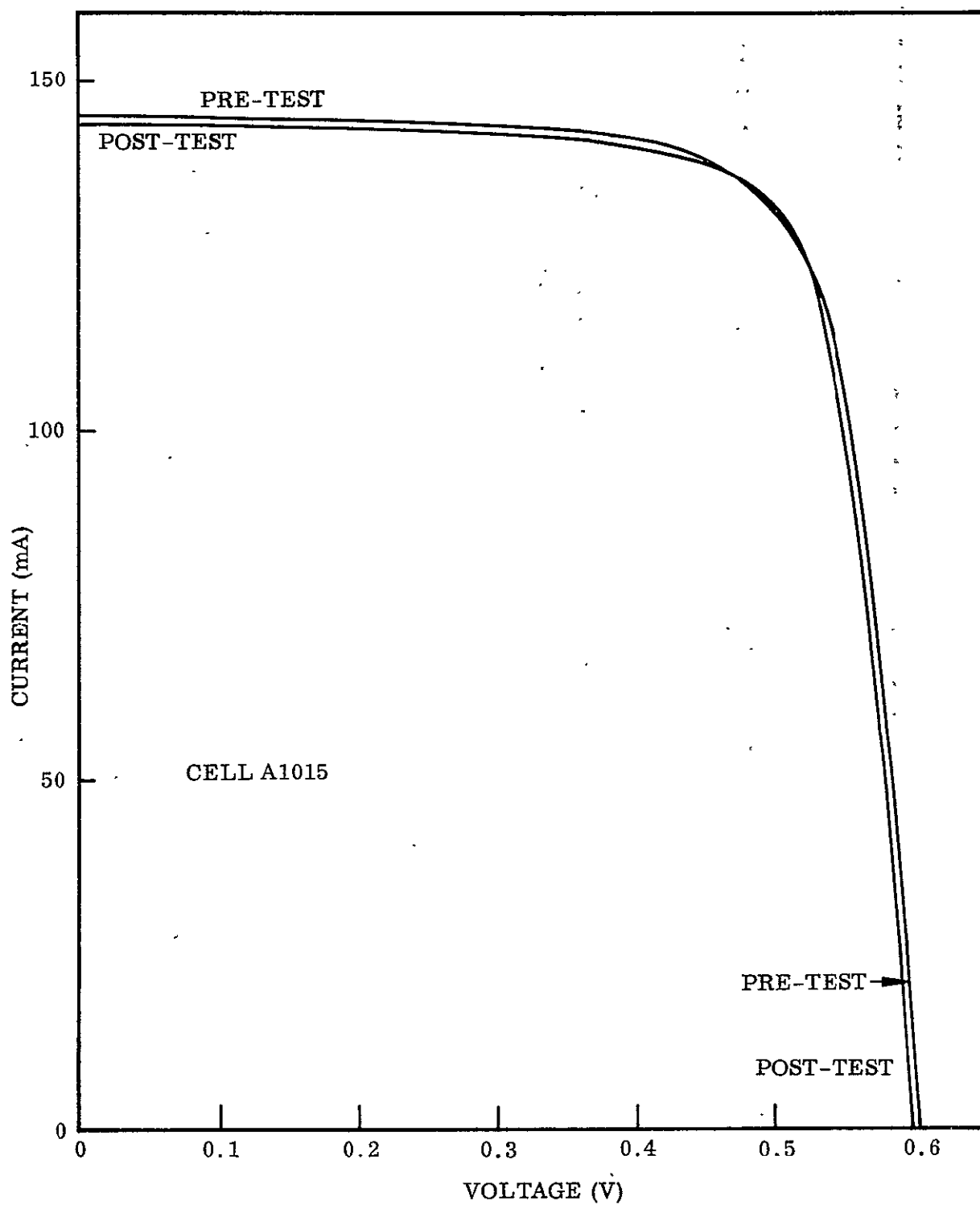


Figure 7. - UV exposure 52 ESH on bare cell

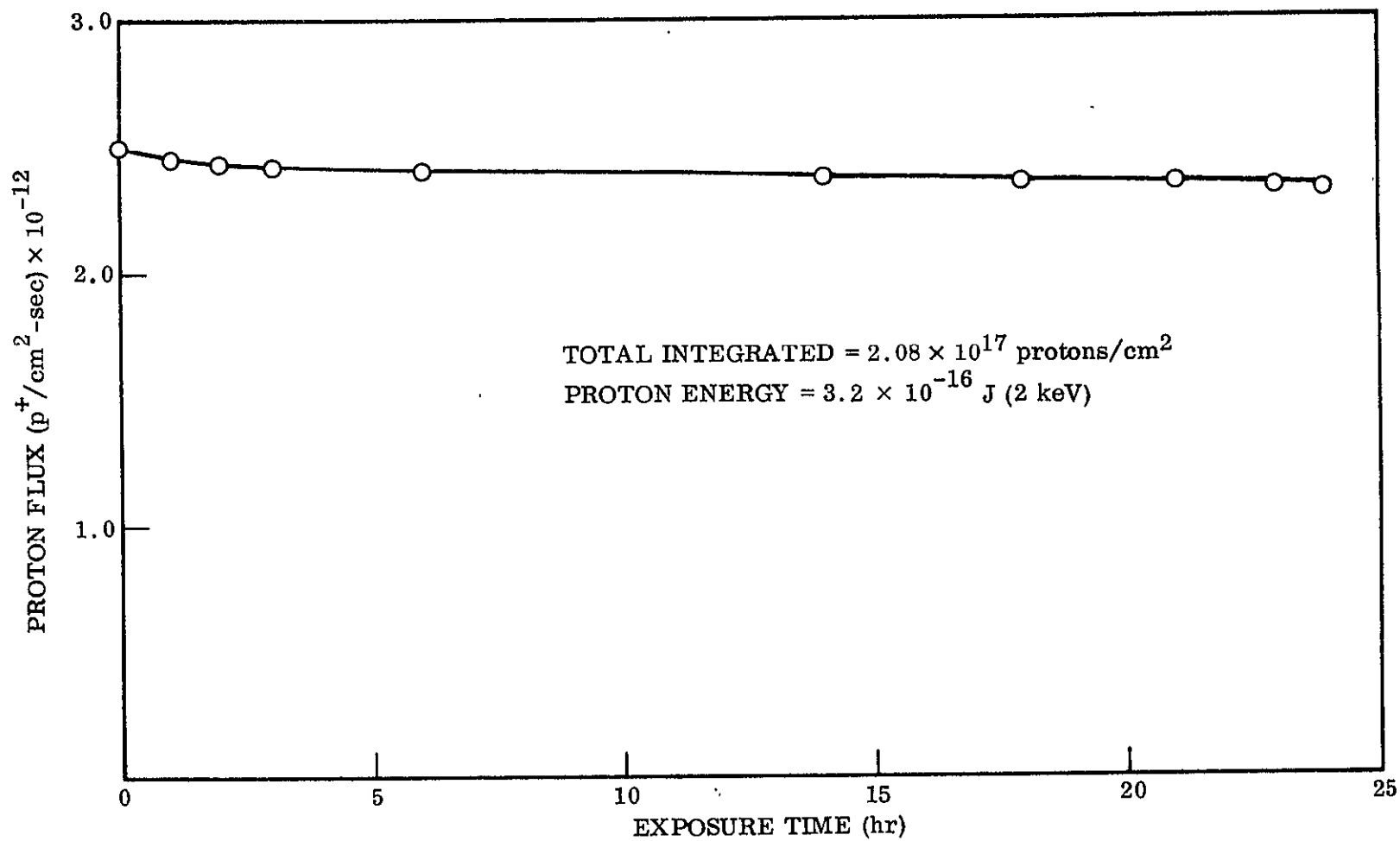


Figure 8. - Proton flux profile



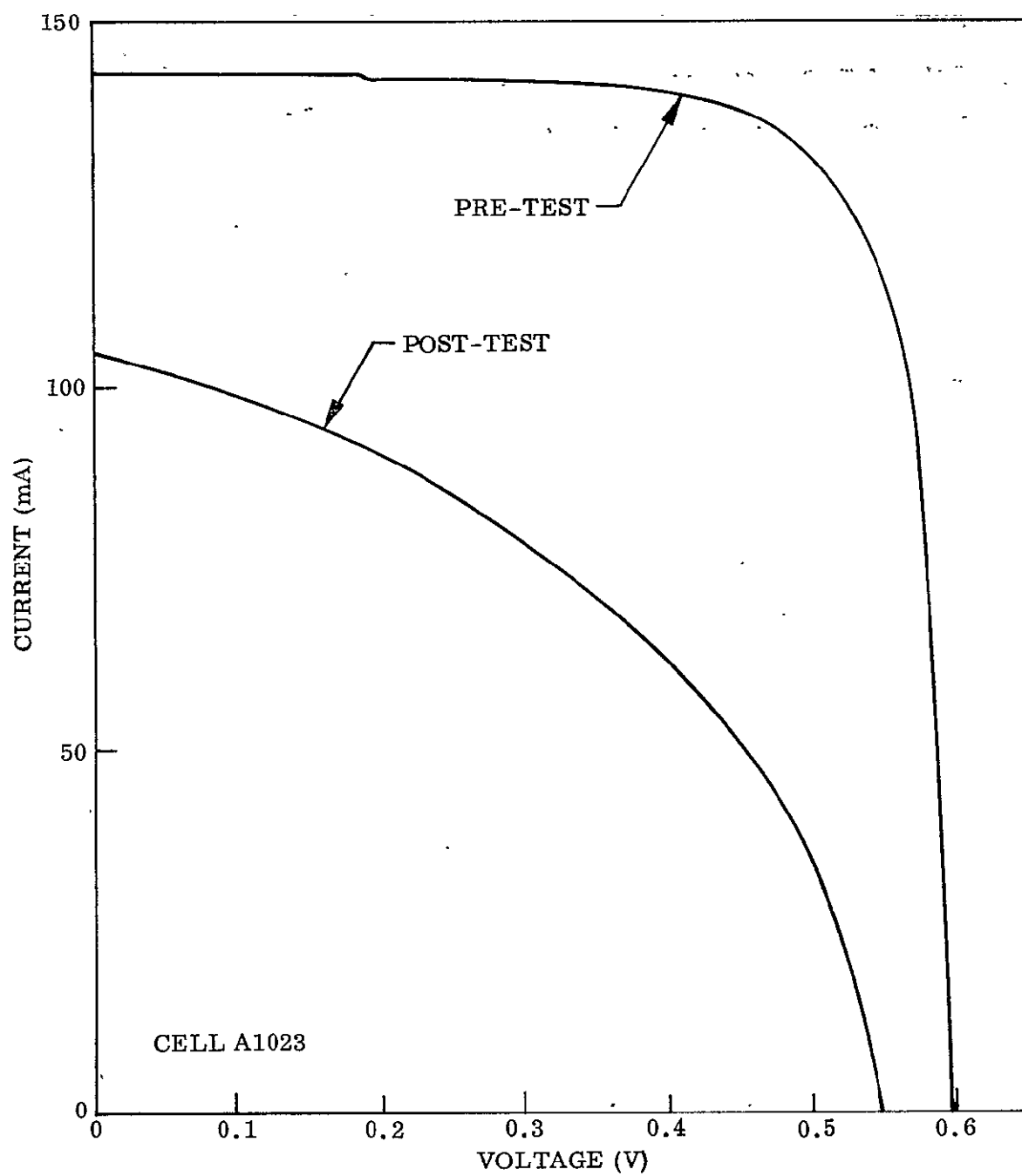


Figure 9. - Proton exposure on bare cell

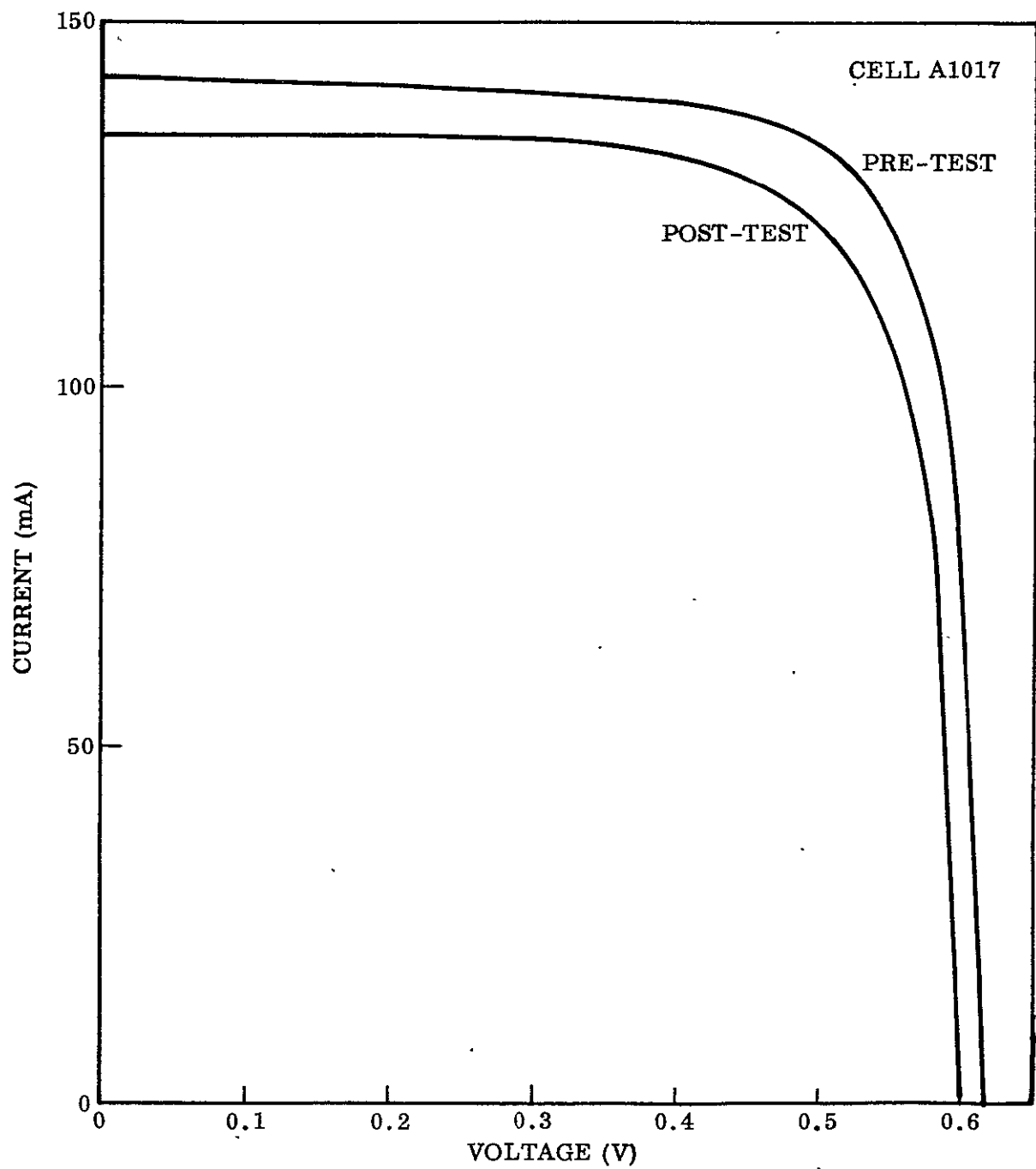


Figure 10.— Proton exposure on FEP-covered cell

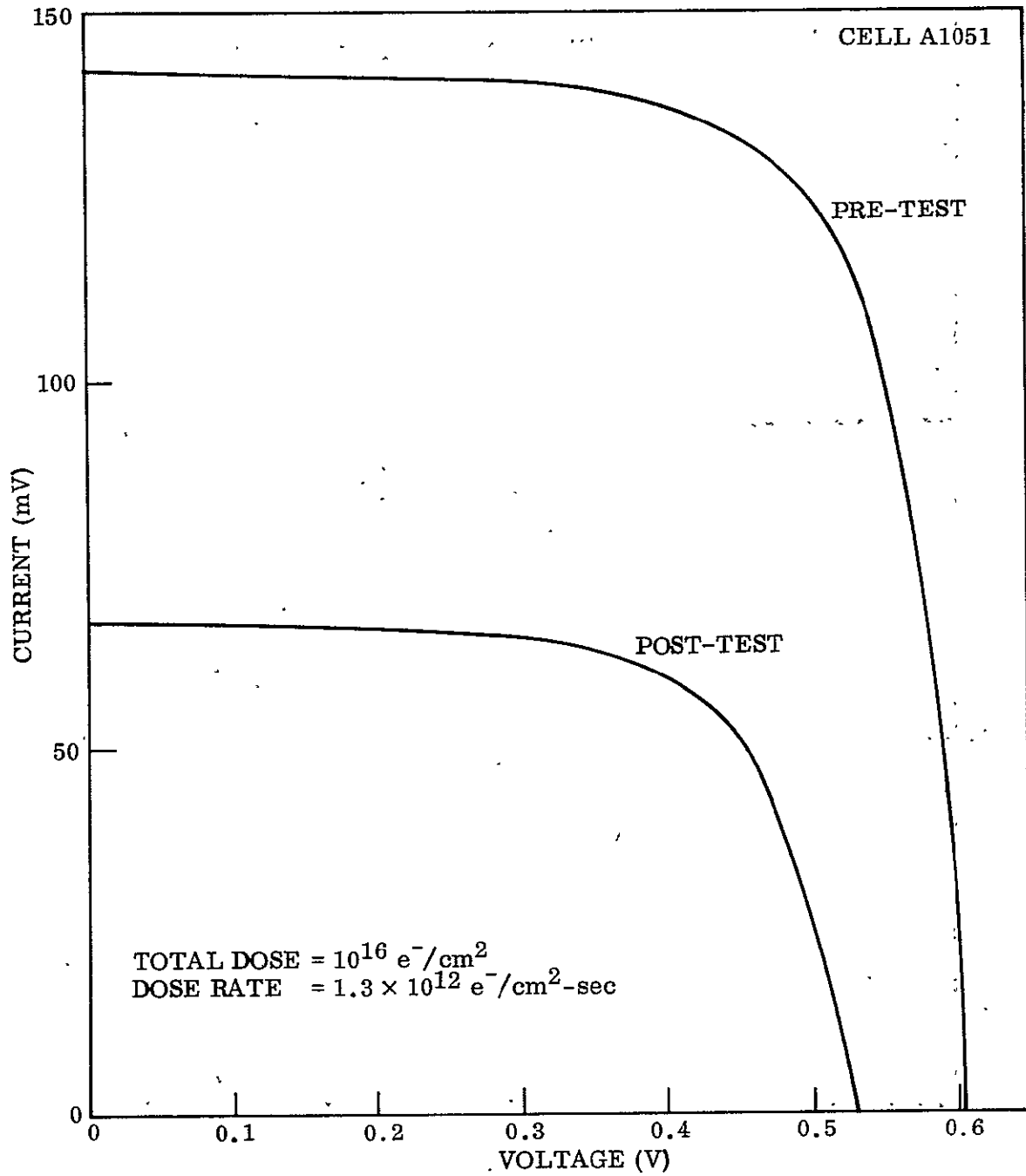


Figure 11. - Effect of  $10^{16} \text{ e}^-/\text{cm}^2$  on FEP-covered cell with catastrophic failure

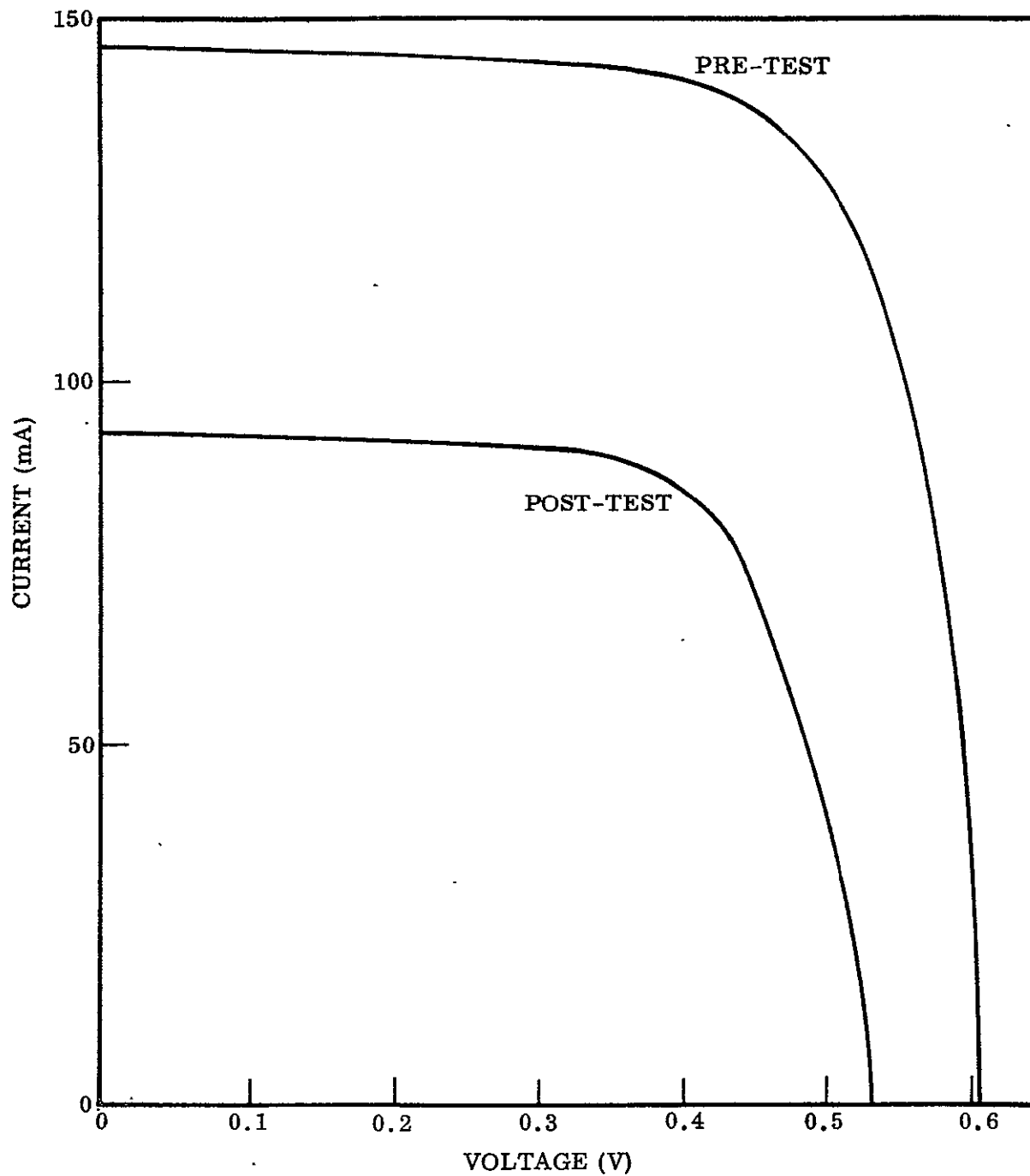


Figure 12. - Effect of  $10^{16} \text{ e}^-/\text{cm}^2$  on FEP-covered cell with delamination

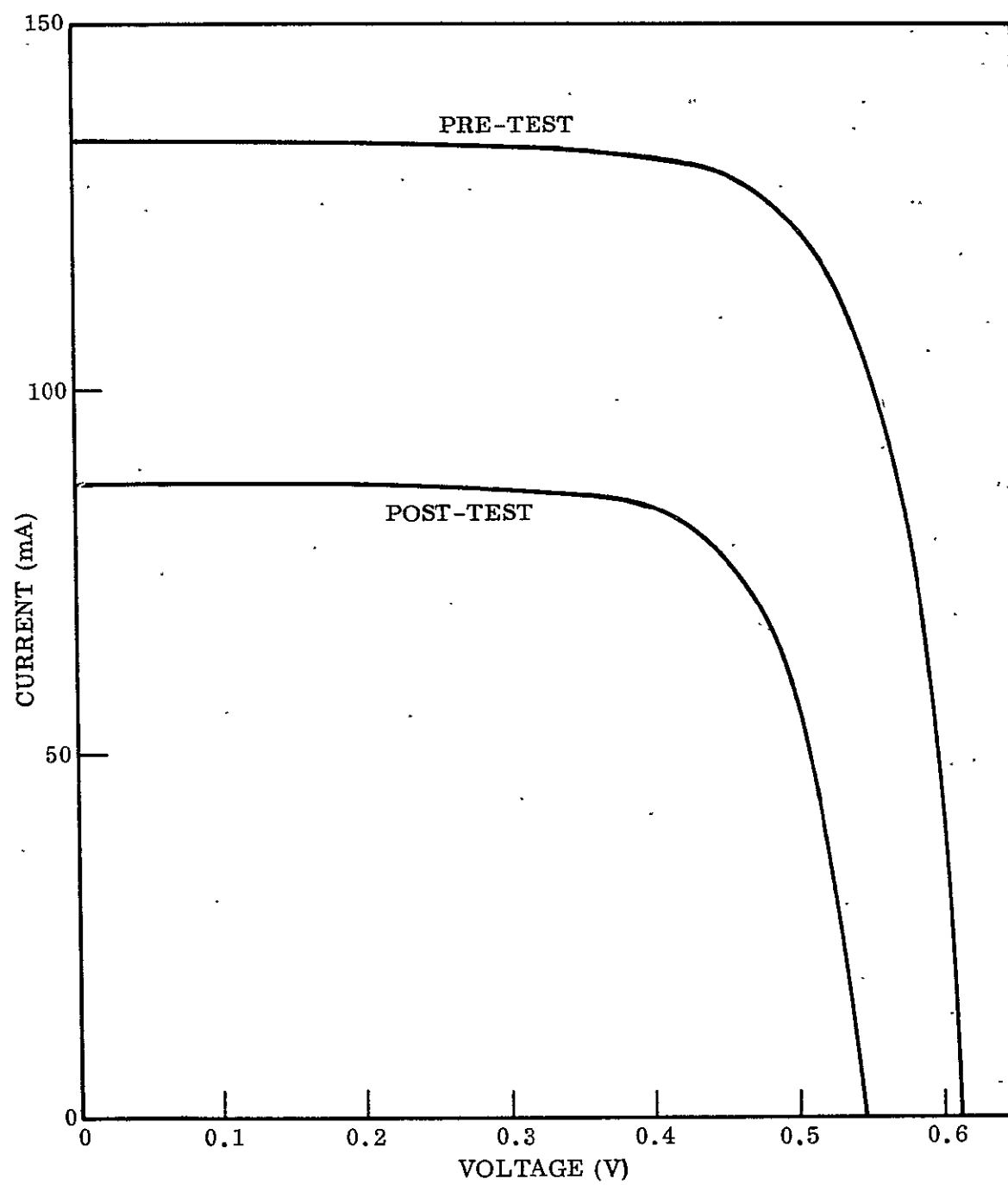


Figure 13. - Effect of  $10^{16} \text{ e}^-/\text{cm}^2$  on bare cell

### 2.5.6 Abbreviated Environmental Test Summary

The single FEP/solar cell packages exhibited excellent performance in the humidity, thermal shock, ultraviolet, and proton irradiation tests. The failures observed in the electron irradiation tests are considered to be related to the extremely high dose rate employed.

Based on the results obtained in the abbreviated environmental tests, cells produced by the optimized process were further evaluated under full environmental test conditions.

## 2.6 FULL ENVIRONMENTAL TESTS

The full environmental tests included the same general conditions as the abbreviated tests but were more extensive in scope and detail.

### 2.6.1 High Humidity and Temperature

Twenty FEP-covered silicon solar cells were subjected to 95% relative humidity at 313°K (40°C) for extended periods. As in the abbreviated test, no evidence of delamination was observed for the first 72 hr. After 110 hr, slight delamination was observed on five of the cells and gross separation was noted on one side of a five-cell string. Evidence of some FEP separation was observed on all cells after 160 hr of exposure. Further exposure for a total of 30 days revealed no further growth of the delamination process, indicating that a limiting condition develops after 160 hr at 313°K (40°C) and 95% relative humidity.

The results obtained appear to be an extension of the abbreviated tests, which indicated a reduction in FEP - solar cell bond strength during exposure to humidity at elevated temperatures. Although the FEP has a relatively low moisture permeability in its virgin state (0.40g/650 cm<sup>2</sup>/24 hr/mil), qualitative tests performed at LMSC indicate at least an order of magnitude increase in room-temperature permeability following the heat-sealing treatment and quench cooling. This effect is considered to be related to a change in crystallinity of the film due to the processing. The humidity-related bond failure occurs at the interface of the treated Type C FEP surface and the solar cell, which suggests that moisture perturbs the proprietary surface layer.

Although this humidity test is probably much more severe than any condition likely to occur in in-flight spacecraft usage, the humidity is not considered to be a satisfactory property. To investigate this effect further, FEP/solar cell packages were processed by heat sealing the Type C FEP at 563°K (290°C) instead of the "optimized" value of 523°K (250°C). All cells prepared in this manner showed no evidence of delamination after 30 days at 313°K (40°C) and 95% relative humidity.

### 2.6.2 Temperature Cycling

Three FEP cell packages were subjected to extended thermal cycling in a vacuum of  $1.3 \times 10^{-8}$  N/m<sup>2</sup> ( $1 \times 10^{-6}$  torr). The thermal cycle profile shown in Figure 14 consisted of the following:

- (1) Cooling the sample table to a nominal temperature of -83°K (-190°C)
- (2) A 5-min soak at -83°K (-190°C)
- (3) Heating the sample table to a nominal temperature of 298°K (25°C)
- (4) A 5-min soak at 298°K (25°C)

The samples were subjected to 150 such cycles.

Both the sample table and one cell were equipped with thermocouples to determine the correlation between sample and table temperature. The maximum deviation observed was 5° at the coldest temperature, presumably due to radiative heat transfer between the bell jar and the sample. Visual observation of the cells was made during cycling. Following completion of the 150 cycles, the cells were removed and examined in detail. No evidence of any deterioration of the bond, fracture of the cells, or any other degradation of the FEP/solar cell packages was noted.

### 2.6.3 Ultraviolet Radiation

Three FEP/solar cell packages and a bare cell were subjected to 2000 equivalent sun hours (ESH) of ultraviolet radiation in a vacuum of  $6.6 \times 10^{-9}$  N/m<sup>2</sup> ( $5 \times 10^{-7}$  torr). The intensity of the uv at the sample positions was 10 equivalent suns, based upon the 0.2–0.3  $\mu$  wavelength range. Current voltage curves of the cells were determined before irradiation and at 500-ESH nominal increments. The results of this test are shown in Figure 15 for a typical cell. The majority of the degradation occurs in the first 1000 ESH and tends to saturate near a value of 3% reduction in transmittance of the 5-mil FEP in the near-visible and ultraviolet regions. The bare cell exposed simultaneously showed no change in output as a result of the uv exposure. The small uv-induced degradation is not considered significant enough to compromise the utility of the FEP covers, which more than compensate for this loss by eliminating the requirement for the blue filter used with conventional adhesive-bonded covers (ref. 2).

### 2.6.4 Proton Irradiation

Four sets of FEP/solar cell packages and bare cells were subjected to  $3.2 \times 10^{-16}$  J(2 keV) protons in a vacuum of  $7.9 \times 10^{-9}$  N/m<sup>2</sup> ( $6 \times 10^{-7}$  torr) at an average dose rate of  $1.3 \times 10^{12}$  p/cm<sup>2</sup> sec. Using a rotating sample table, total exposures of  $1 \times 10^{13}$  p/cm<sup>2</sup>,  $1 \times 10^{15}$  p/cm<sup>2</sup>,  $1 \times 10^{17}$  p/cm<sup>2</sup>, and  $2 \times 10^{17}$  p/cm<sup>2</sup> were performed. Little effect was noted on the open-circuit voltage for the FEP-covered cells. The bare cells degraded significantly more than the FEP-coated cells, as shown in Figure 16.

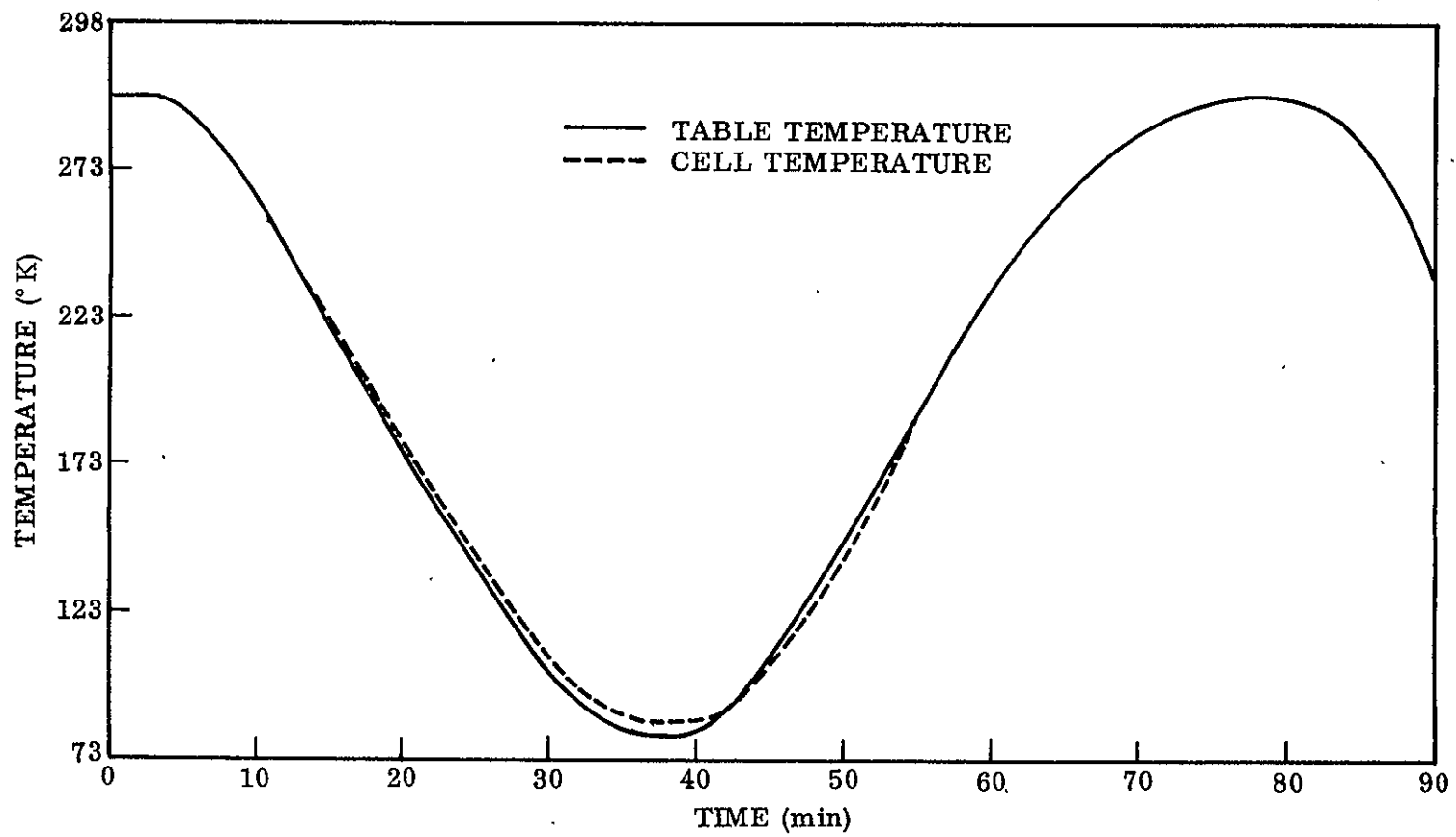


Figure 14. — Thermal cycling profile



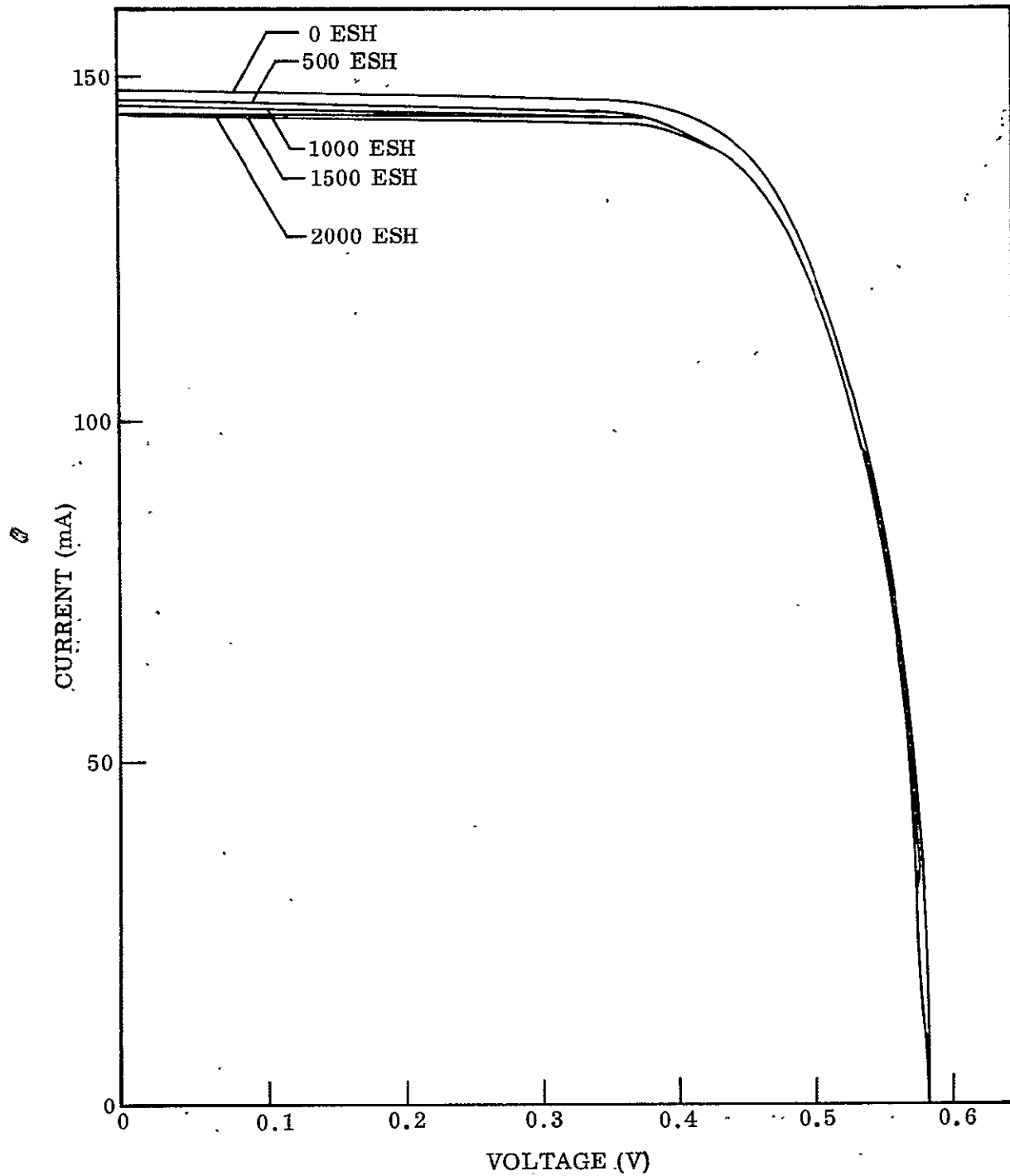


Figure 15. — Effect of uv exposure on output of FEP-covered cell

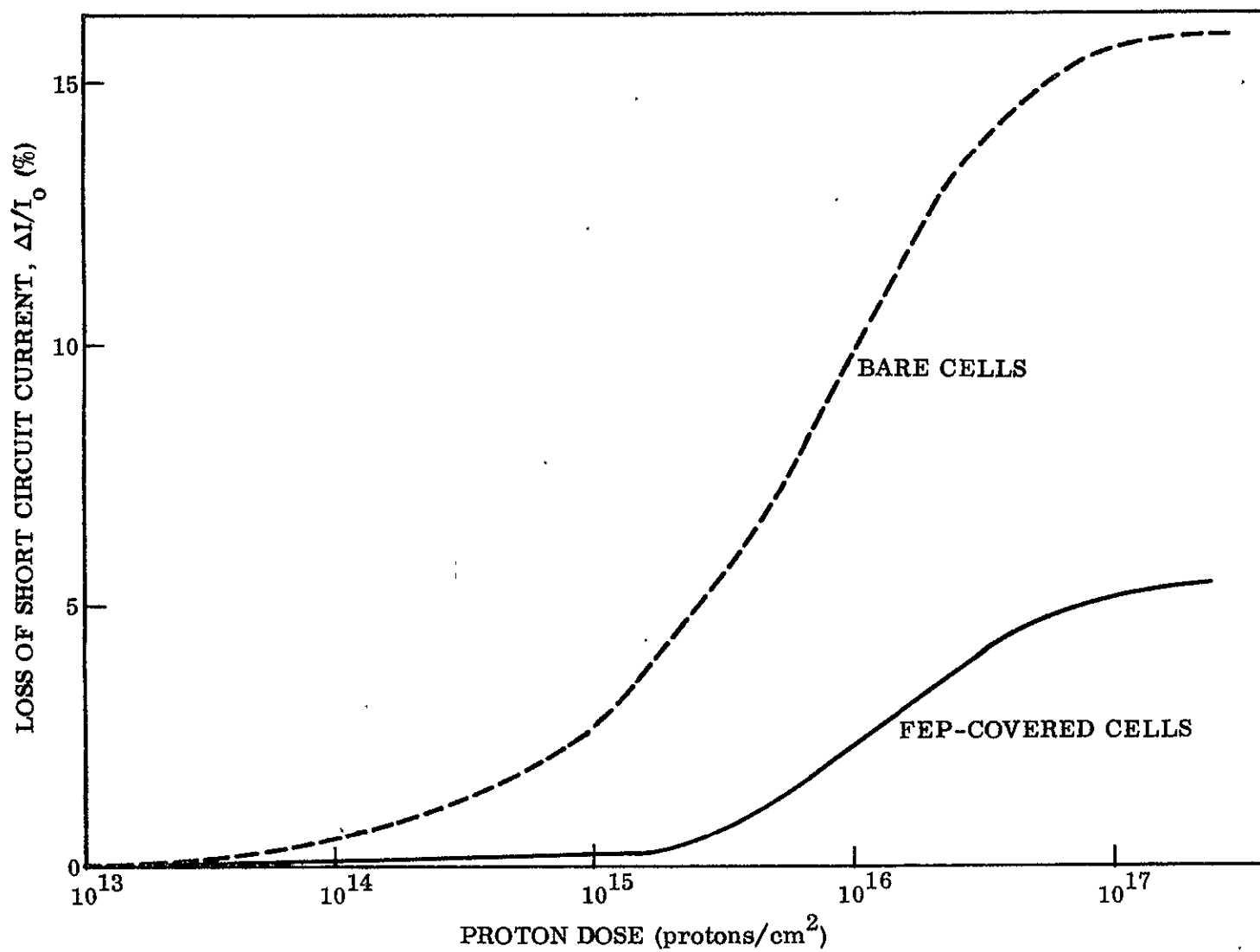


Figure 16. - Effect of protons on short-circuit current

Degradation of both bare and FEP-covered cells appears to saturate at doses in the  $1 \times 10^{17} \text{ p}^+/\text{cm}^2$  region. It is not surprising that the FEP affords significant protection from low-energy protons, since the range of a  $3.2 \times 10^{-16}\text{-J}$  (2-keV) proton in FEP is on the order of 1500 Å. The loss in short-circuit current is due to slight discoloration of the FEP as the result of proton damage. However, for reasonable doses in the  $10^{16} \text{ p}/\text{cm}^2$  region ( $\sim 5$  years in interplanetary space), a reduction of only a few percent in current is noted. Conversely, unprotected cells degrade 10 to 15% for the same proton dose. Thus, the FEP is considered to provide excellent protection from low-energy protons for extended exposures.

Examination of exposed cells showed no evidence of bond failure or any other detrimental effects due to proton exposure.

### 2.6.5 Electron Irradiation

Exposures of individual Teflon/solar cell packages were performed at Gulf Radiation Technology. Three Teflon-covered cells and one bare cell were subjected to electron irradiation using the Gulf  $4 \times 10^{-12} \text{ J}$  (25-MeV) L-band linear accelerator operating in pulsed mode at  $3.2 \times 10^{-13}\text{-J}$  (2 MeV). Dosimetry was performed using a series of graphite Faraday buttons distributed over the geometrical position of the samples. The flux was measured at  $1.30 \times 10^{12} \text{ electrons}/\text{cm}^2\text{-sec}$  and was within  $\pm 5\%$  over the total sample area. Samples were mounted on an aluminum plate equipped with water cooling. The temperature of the fixture was maintained at 294°K (21°C) prior to exposure and rose to a maximum value of 296°K (23°C) during irradiation. The sample chamber was maintained at a vacuum of  $8 \times 10^{-19} \text{ N}/\text{m}^2$  (6 to  $8 \times 10^{-7}$  torr) during irradiation using an oil diffusion pump in conjunction with a liquid nitrogen cooled baffle. At the flux employed, the time required to achieve an integrated dose of  $1 \times 10^{16} \text{ e}^-/\text{cm}^2$  at the solar cell surfaces was  $7.7 \times 10^3 \text{ sec}$ .

Following exposure of the samples in vacuum, the chamber was opened and the samples were observed. Two of the three Teflon-covered cells exhibited catastrophic failure, in which the Teflon and silicon oxide coatings on the cells separated, exposing bare silicon surfaces. The grids remained bonded to the front surfaces of the cells, while the silicon oxide remained on the Teflon. The other cell showed simple delamination of the Teflon - solar cell bond. The bare cells appeared unchanged. The separated Teflon covers did not substantially embrittle and were capable of repeated 90° flexing.

The tests were repeated for groups of four cells (three covered and one bare) to fluences of  $1 \times 10^{15} \text{ e}^-/\text{cm}^2$  and  $1 \times 10^{14} \text{ e}^-/\text{cm}^2$ . For the  $1 \times 10^{15} \text{ e}^-/\text{cm}^2$  test, initial removal from the vacuum chamber indicated no delamination. However, over a period of 30 min, delamination became increasingly severe under laboratory ambient conditions. After 24 hr, complete delamination of all covered cells resulted. For the  $1 \times 10^{14} \text{ e}^-/\text{cm}^2$  dose, initial observations indicated no delamination. After 24 hr in air, however, bond strength (tested by means of a probing technique) appeared to be negligible.

A typical pre- and post-exposure current/voltage curve for the  $10^{16}$  e-/cm<sup>2</sup> exposure with failure is shown in Figure 17, where the severe power loss is indicative of substantial damage to the cell integrity. Figure 18 shows the results for a cell suffering simple delamination following exposure to  $10^{16}$  e-/cm<sup>2</sup>. The post-test measurements were made with the separated cover overlaying the cell and held in place by the screws used for mounting to the sample plate. Comparison of a bare cell under the same exposure conditions (Figure 19) shows that the Teflon did not appreciably suffer a loss in transmittance. The small reduction in the ratio of short-circuit currents pre- and post-exposure for the covered cell compared with that for the bare cell may be due to reflection losses related to the incomplete Teflon/solar cell bond.

Figures 20 and 21 show input/voltage curves pre- and post-exposure for covered and bare cells, respectively, for an electron dose of  $1 \times 10^{15}$  e-/cm<sup>2</sup>. Similarly, Figures 22 and 23 show the effects of  $1 \times 10^{14}$  e-/cm<sup>2</sup> on a Teflon-covered and a bare cell.

#### 2.6.6 Full Environmental Test Summary

Single FEP/solar cell packages as prepared under the nominally optimum processing conditions (section 2.4.6) were subjected to the full environmental testing sequence. As was the case with the abbreviated tests, the packages exhibited excellent performance in the thermal cycling, ultraviolet, and proton irradiation tests. The electron irradiation test results indicated that a problem exists relative to electron irradiation induced bond failure. However, the scope of the problem was such as to preclude a more detailed experimental analysis of the parameters associated with this failure mode. The delamination observed for cells processed under the nominally "optimum" conditions in the high temperature and humidity test was rectified by heat sealing at 563°K (290°C) with the FEP directly fused to the solar cells. This finding requires a modification of the process parameter specification.

The overall results of the single cell tests were encouraging in that they demonstrated the feasibility of the use of FEP Teflon as a replacement for conventional covers. Based on the results obtained with individual FEP/solar cell packages, the technique was extended to multicell (15) modules in an attempt to verify the utility of the approach for large-area solar arrays.

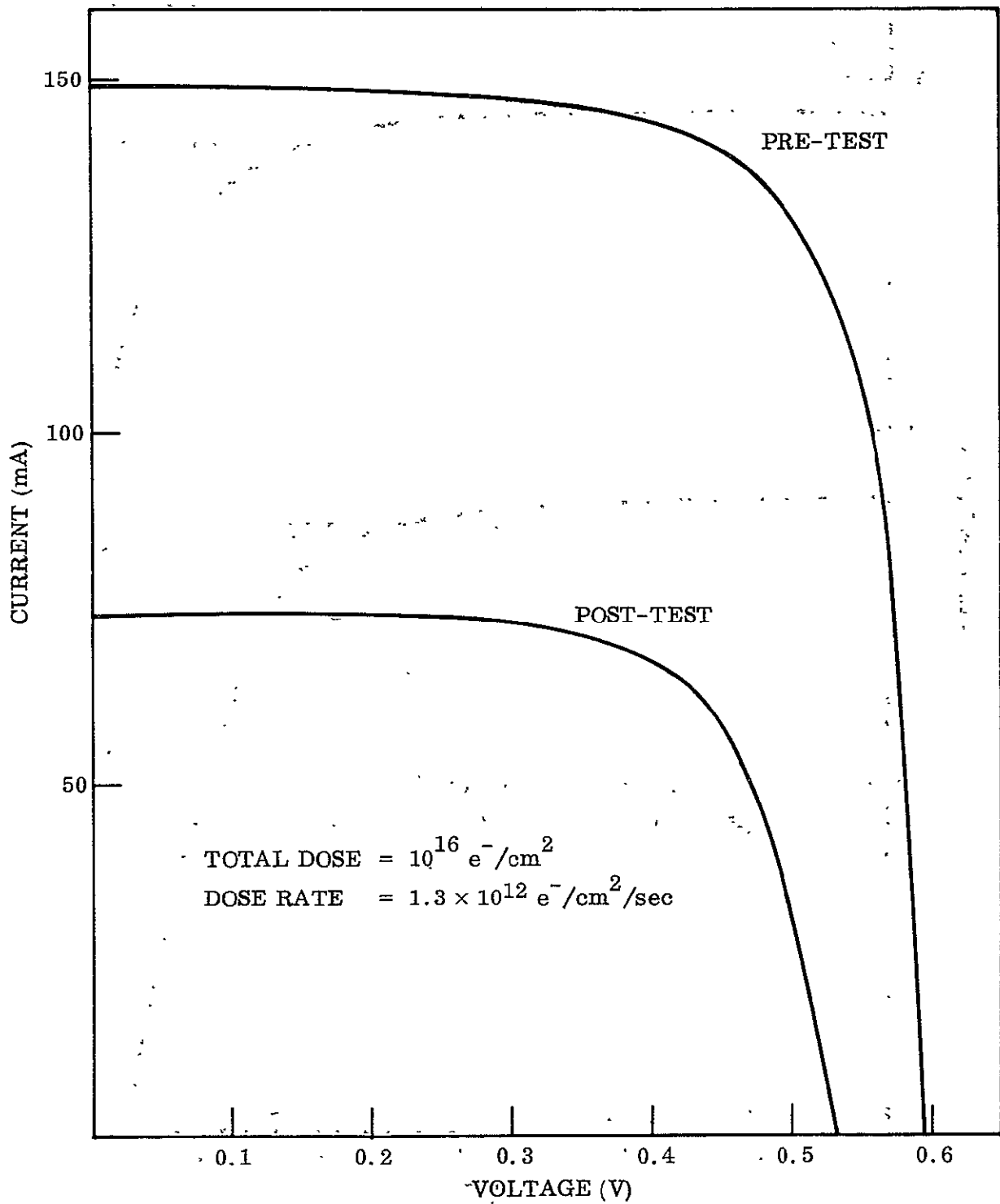


Figure 17. — Effect of  $10^{16} \text{ e}^-/\text{cm}^2$  on FEP-covered cell with silicon oxide removal

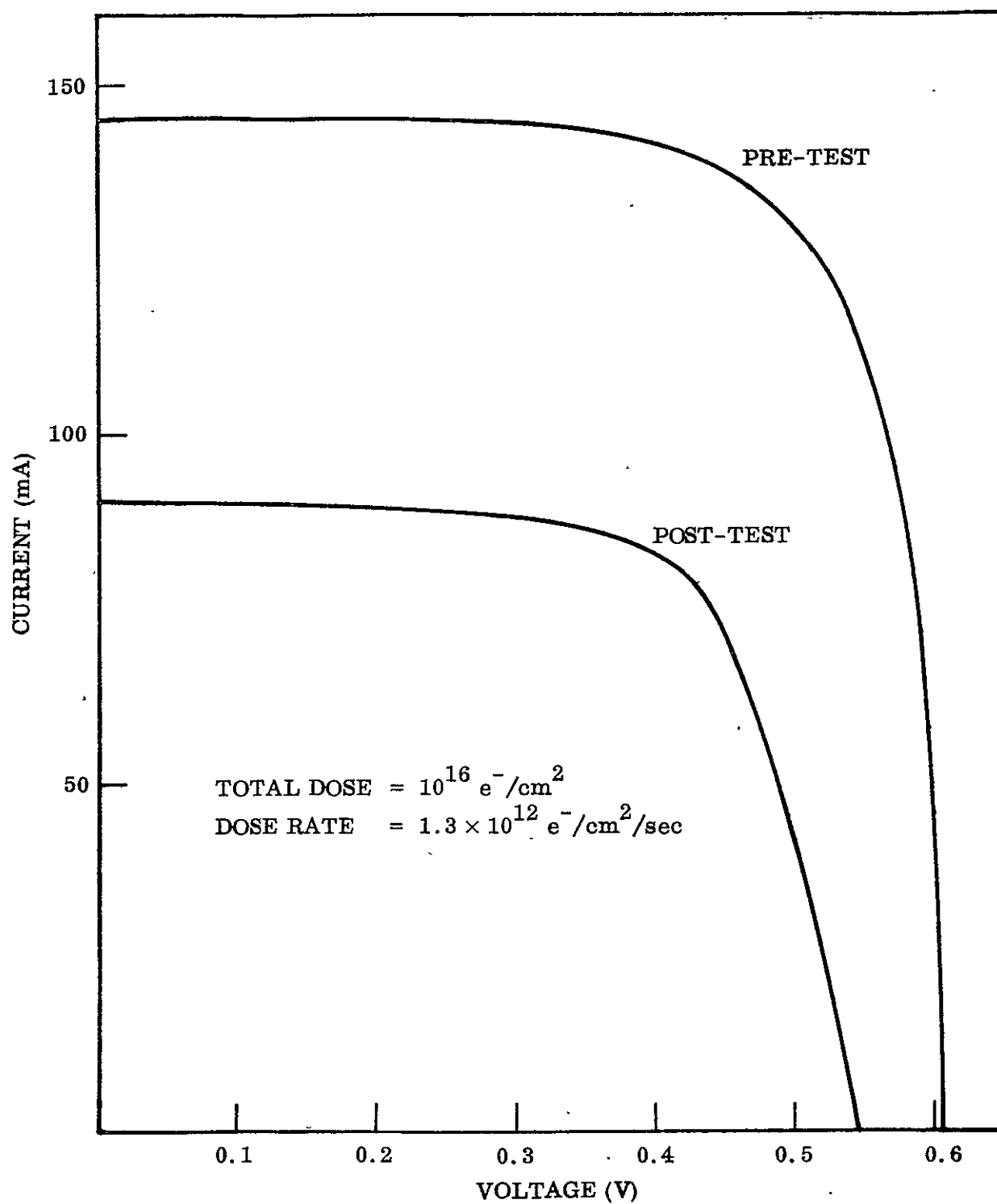


Figure 18. - Effect of  $10^{16} \text{ e}^-/\text{cm}^2$  on FEP-covered cell with delamination

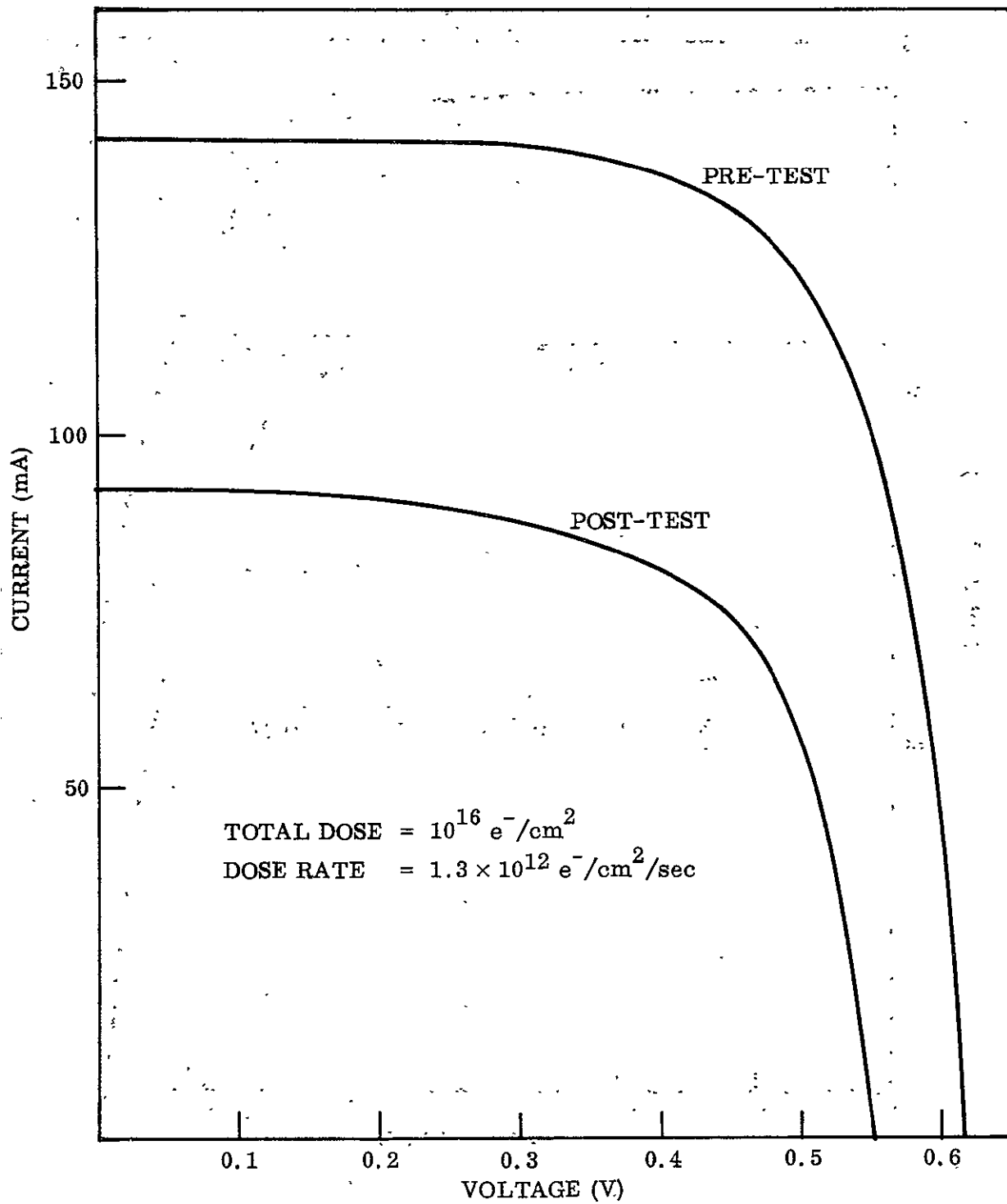


Figure 19. - Effect of  $10^{16} \text{ e}^-/\text{cm}^2$  on bare cell.

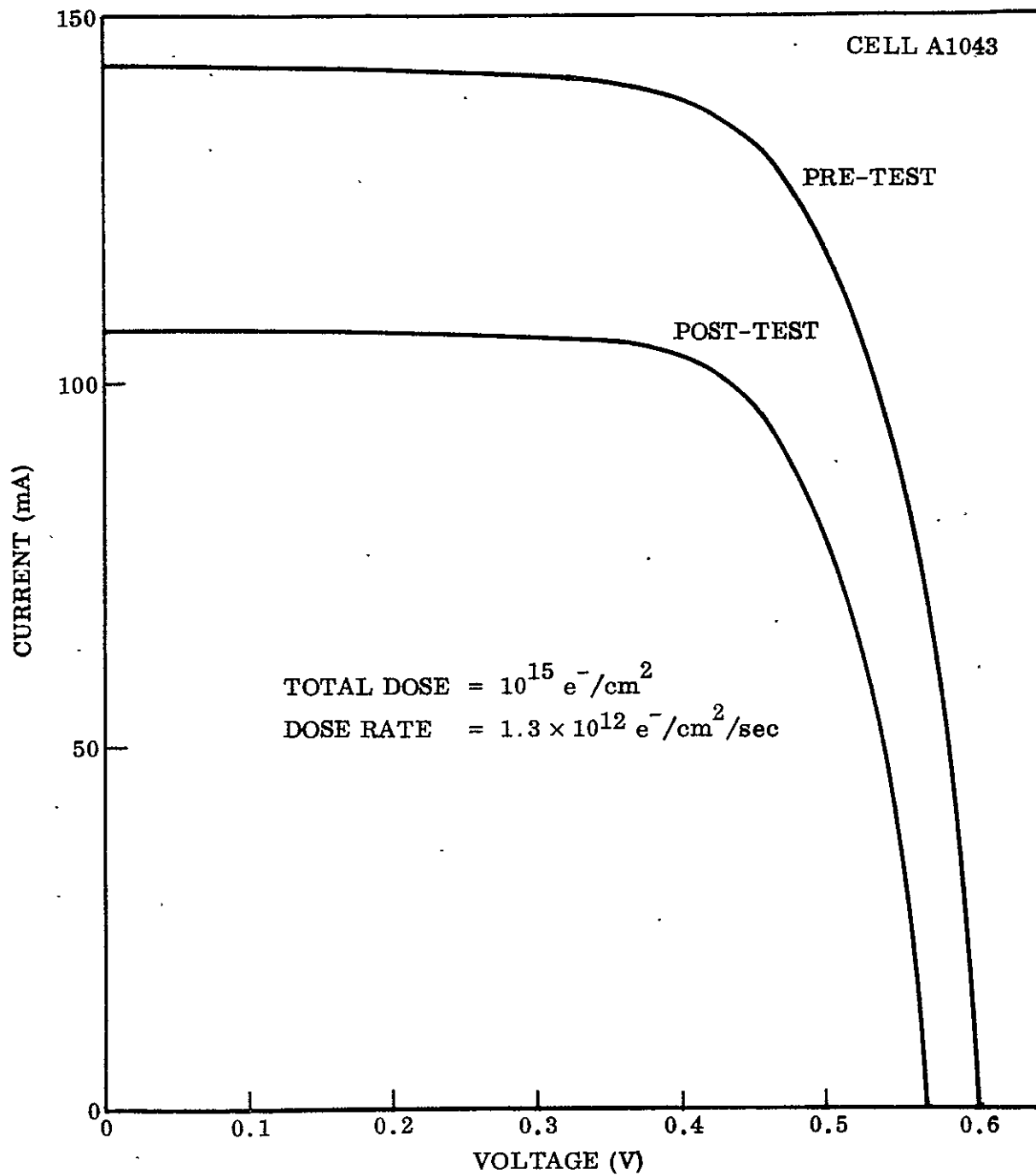


Figure 20. - Effect of  $10^{15} \text{ e}^-/\text{cm}^2$  on FEP-covered cell



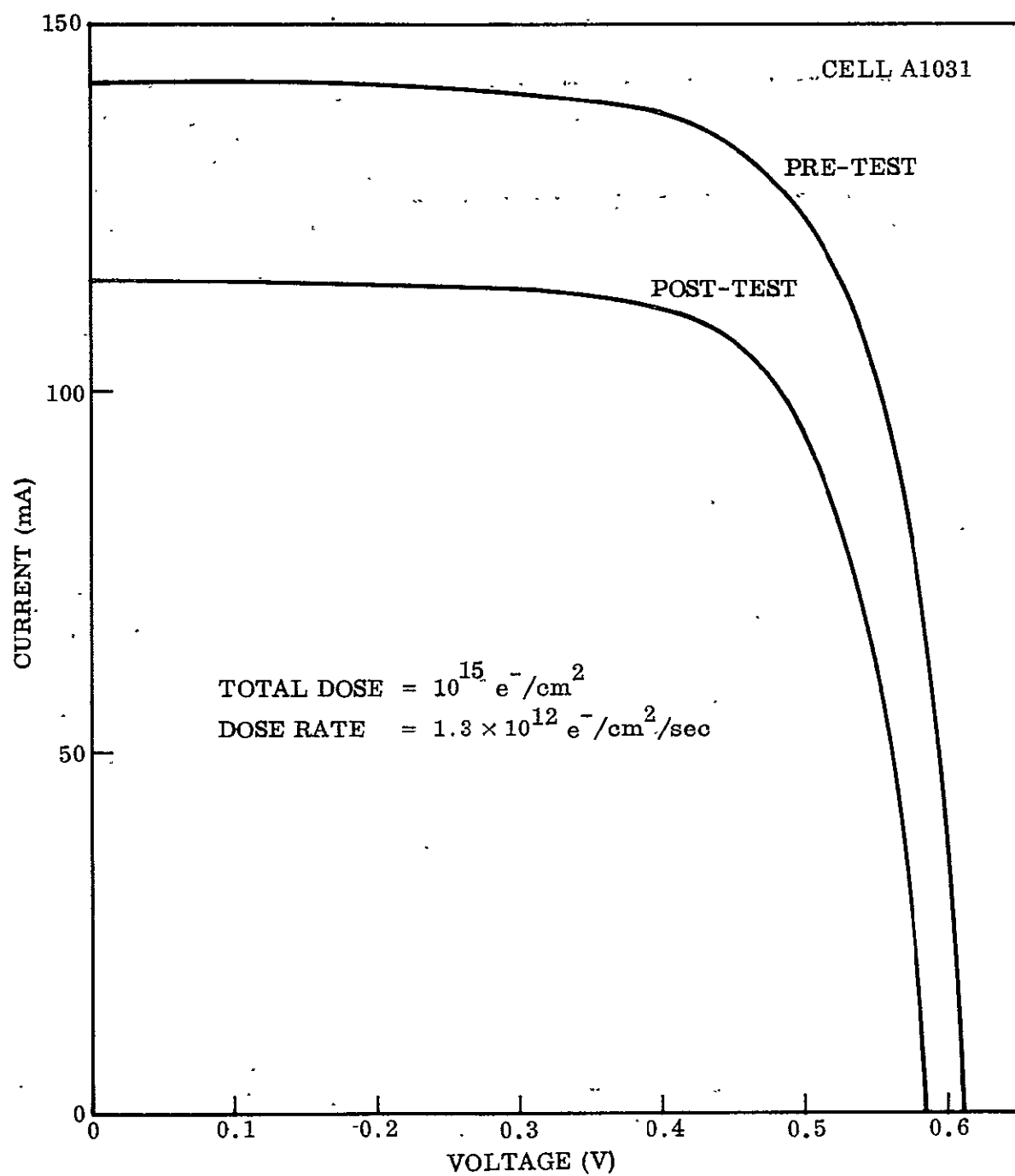


Figure 21. - Effect of  $10^{15} \text{ e}^-/\text{cm}^2$  on bare cell.

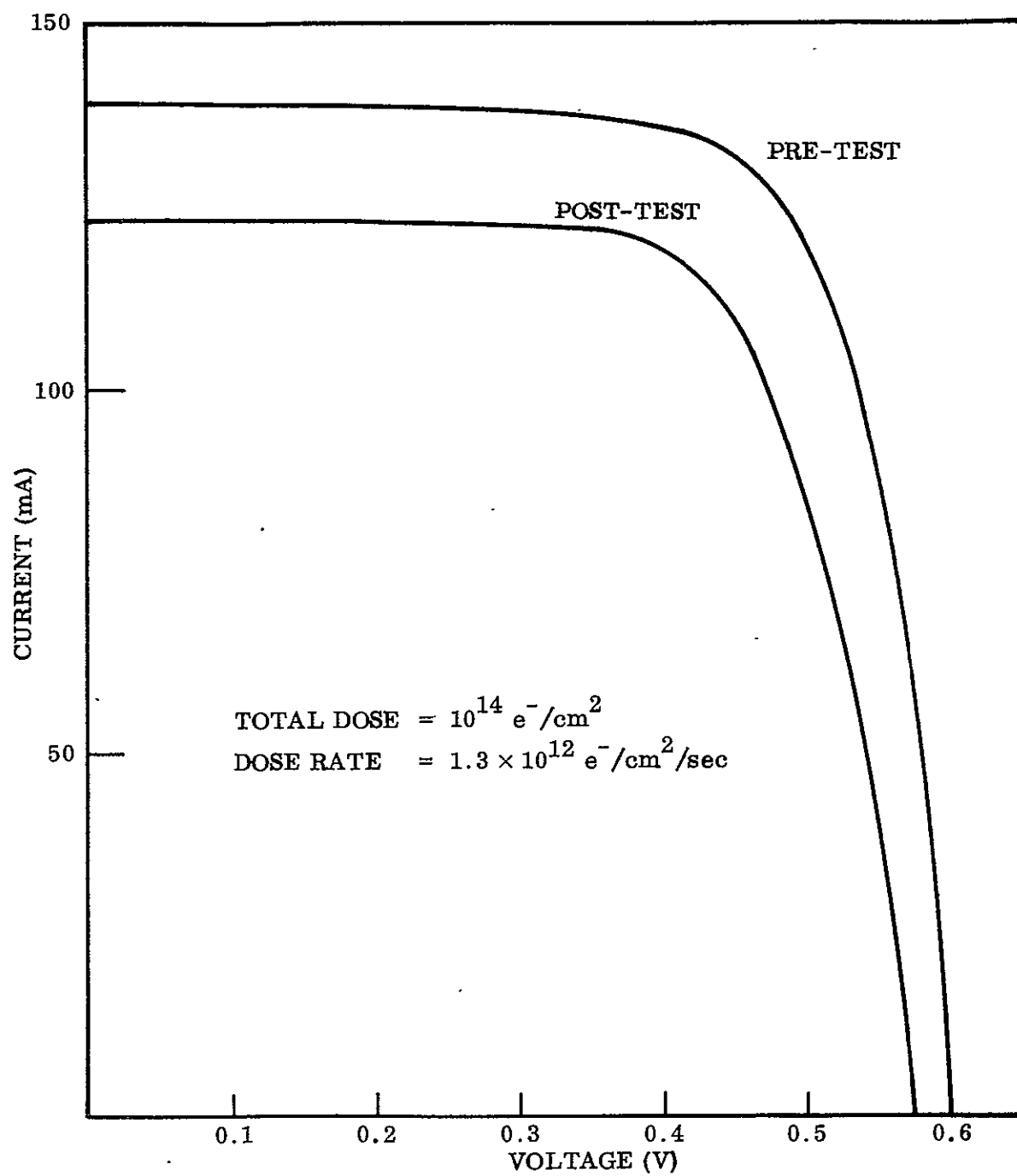


Figure 22. - Effect of  $10^{14} \text{ e}^-/\text{cm}^2$  on FEP-covered cell

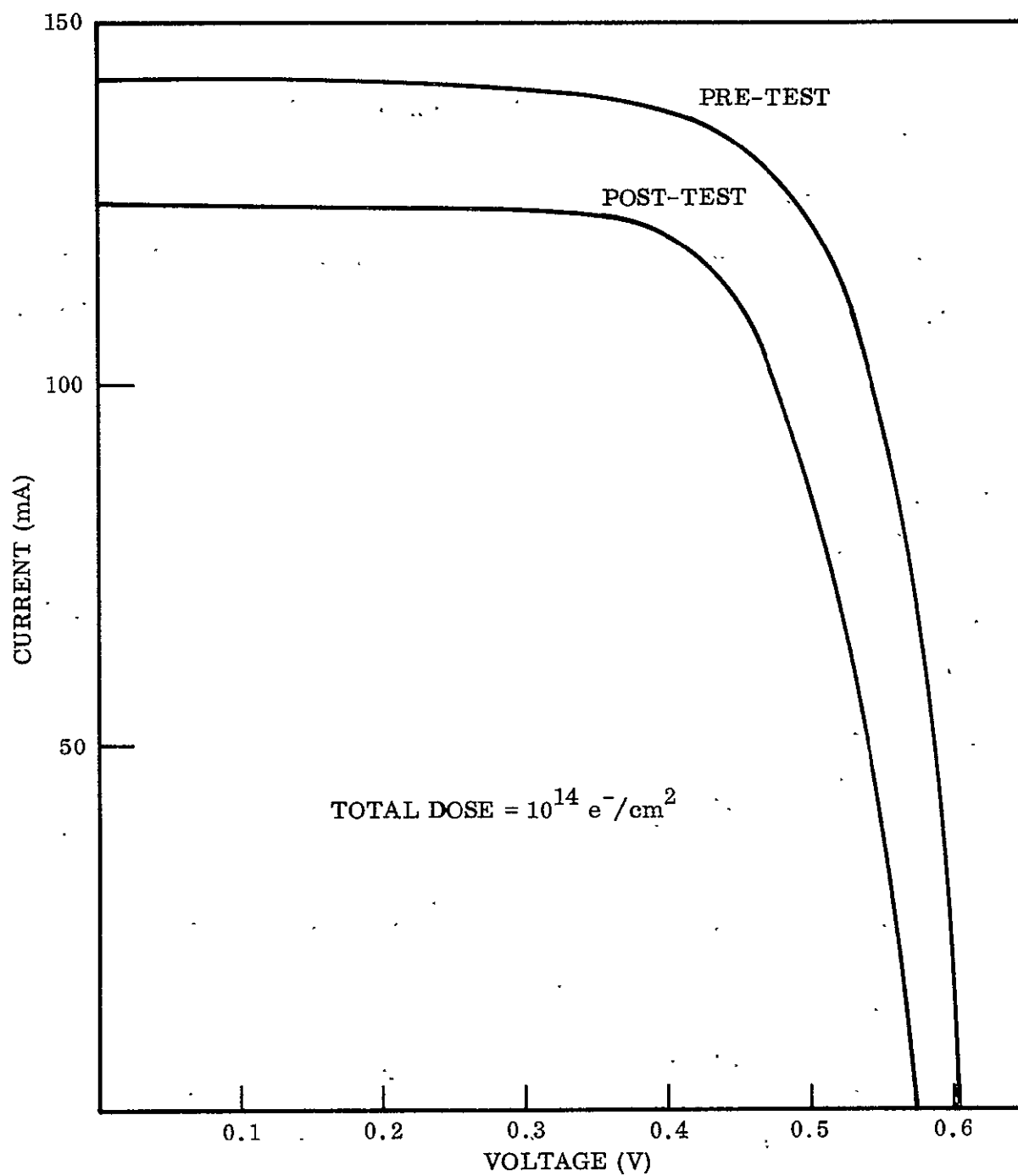


Figure 23. - Effect of  $10^{14} \text{ e}^-/\text{cm}^2$  on bare cell

## Section 3

### STUDIES ON MULTICELL MODULES

#### 3.1 OBJECTIVES

Based on the results described in Section 2 for optimization of the FEP heat-sealing process for individual solar cells, the technique was extended to 15-cell modules having 5 cells in each parallel string and 3 such strings in series. The modules were fabricated on flexible substrates with interconnects of an LMSC design.

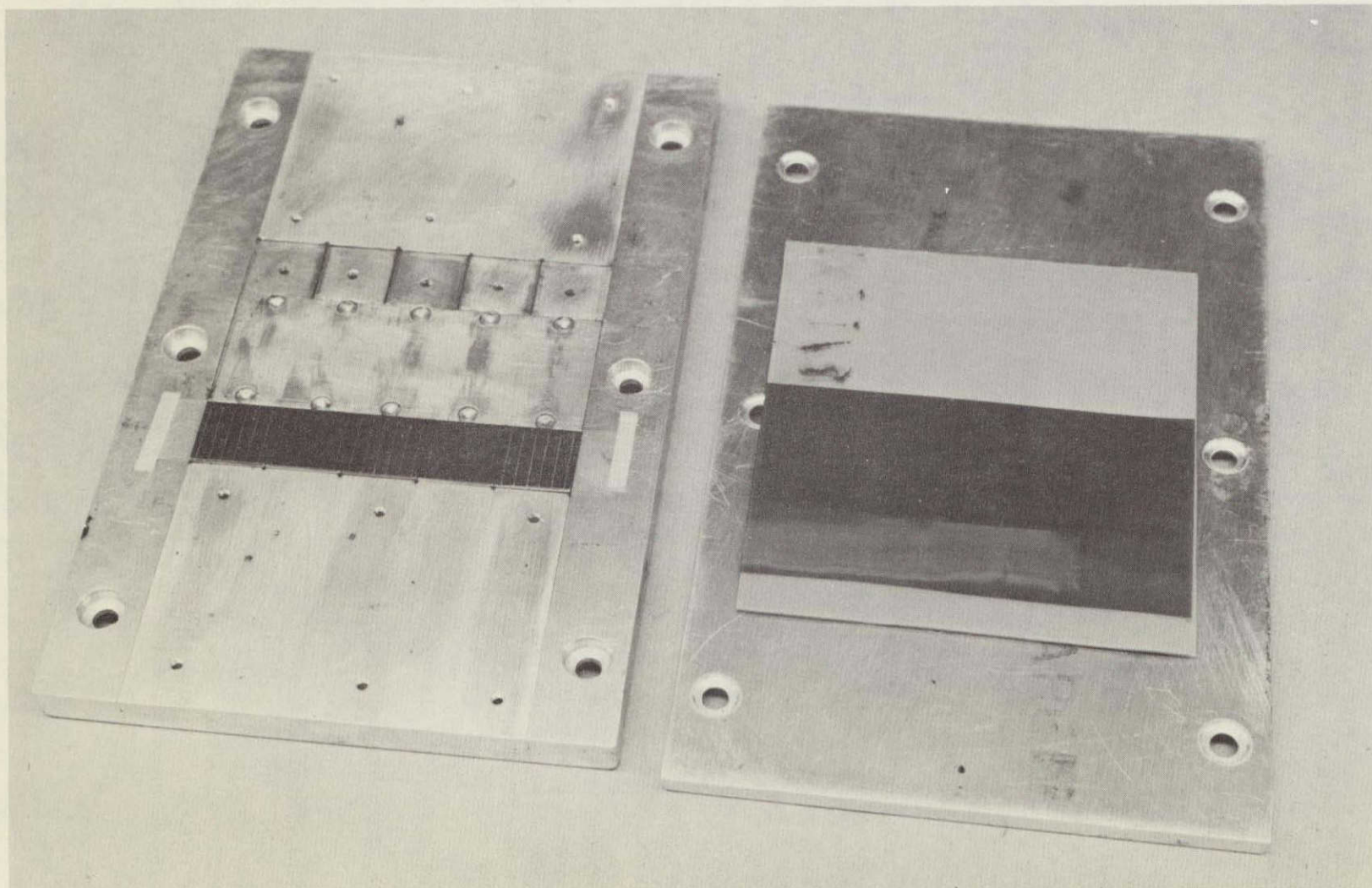
#### 3.2 MODULE FABRICATION

##### 3.2.1 FEP Installation on Five-Cell Submodule Groups

Tooling. A special tool was designed and built for simultaneously bonding FEP to two precision-aligned five-cell submodules. (See Figure 24.) The tool is made of aluminum and consists of two rows of 0.018 cm (0.007-in.) depressions, sized to accommodate 2 cm by 2 cm cells at the high end of their tolerance [2.01 cm (0.793 in.) square]. Depressions are separated by 0.013-cm (0.005-in.) shim stock. A 0.32 cm (1/8 in.) thick aluminum coverplate and six bolts, springs, washers, and wingnuts complete the tool.

Loading the Tool. Cells were laid top up in the depressions and oriented so that N-strips were always along the same edge. Cells were then pushed against this edge to provide uniform N-strip edges on the FEP-covered solar cell submodule. A straight line of cell edges along the N-strips made it easier to position the five-cell submodule accurately when it was later installed on a substrate. Loading was accomplished as follows:

- FEP strips, 1.9 by 15 cm (3/4 by 6 in.), were cut from 0.013-cm (0.005-in.)-thick, Type C material. Strips were cleaned with an alcohol-dampened Kimwipe and, after drying, laid treated-side down over the cells.
- Leading FEP edges were aligned with the inside edges of the cell N-strips, then secured at both ends with glass tape.
- Alignments were carefully rechecked at this point.
- A layer of 0.0076-cm (0.003-in.)-thick Kapton film was placed over the cell areas; this was followed by a sheet of 0.16-cm (1/16-in.)-thick, high-temperature silicone rubber.
- A top pressure plate was carefully laid over the rubber pad and secured with bolts, springs, washers, and wingnuts; the springs assured that constant pressure was maintained by the top cover plate on the FEP and cells during subsequent operations.



NOT REPRODUCIBLE

Figure 24. - Tooling for five-cell submodules



Pressing Operations. A 46 by 61 cm (18 by 24-in.) platen press was used to heat the cell-holding tool. However, only the bottom platen plate was heated to 548°K (275°C). In effect, therefore, the platen was a high-heat-capacity "hot plate," upon which the tool was placed.

Eleven minutes was established as an optimum heating time for the particular tool used. In that period, the temperature at the cell/FEP interface reached 503°–523°K (230–250°C). After the 11 min, the tool was placed on a water-cooled heat sink (Figure 25). The tool temperature was thus rapidly lowered to below 463°K (190°C) to "set" the Type C FEP. After 10 to 12 min of cooling, an operator was able to undo the wingnuts, remove the top plate, rubber pad, and Kapton, and lift the two FEP-covered five-cell submodules from the tool. Excess FEP at the cell edges was removed with an X-Acto knife. Figure 26 shows two FEP-covered five-cell submodules ready for installation on a flexible substrate.

### 3.2.2 Flexible Substrate Fabrication

Base substrate polyimide/FEP laminates were prepunched with rectangular holes. These were located at each cell N-strip tab point. Prepunched substrates were fusion bonded with FEP adhesive to layers of 0.005 cm (2-mil), soft annealed copper foil. The copper was cleaned and a 0.002 cm (3/4-mil) photopolymer dry film layer (Riston) was installed on their surfaces. The prepunched base substrate holes were aligned with a negative phototemplate by means of tooling holes, permitting proper location of images on the copper.

Foils were then photoexposed and chemically etched to form circuitry interconnect patterns, contact points, and soldering tabs. Figure 27 shows this pattern.

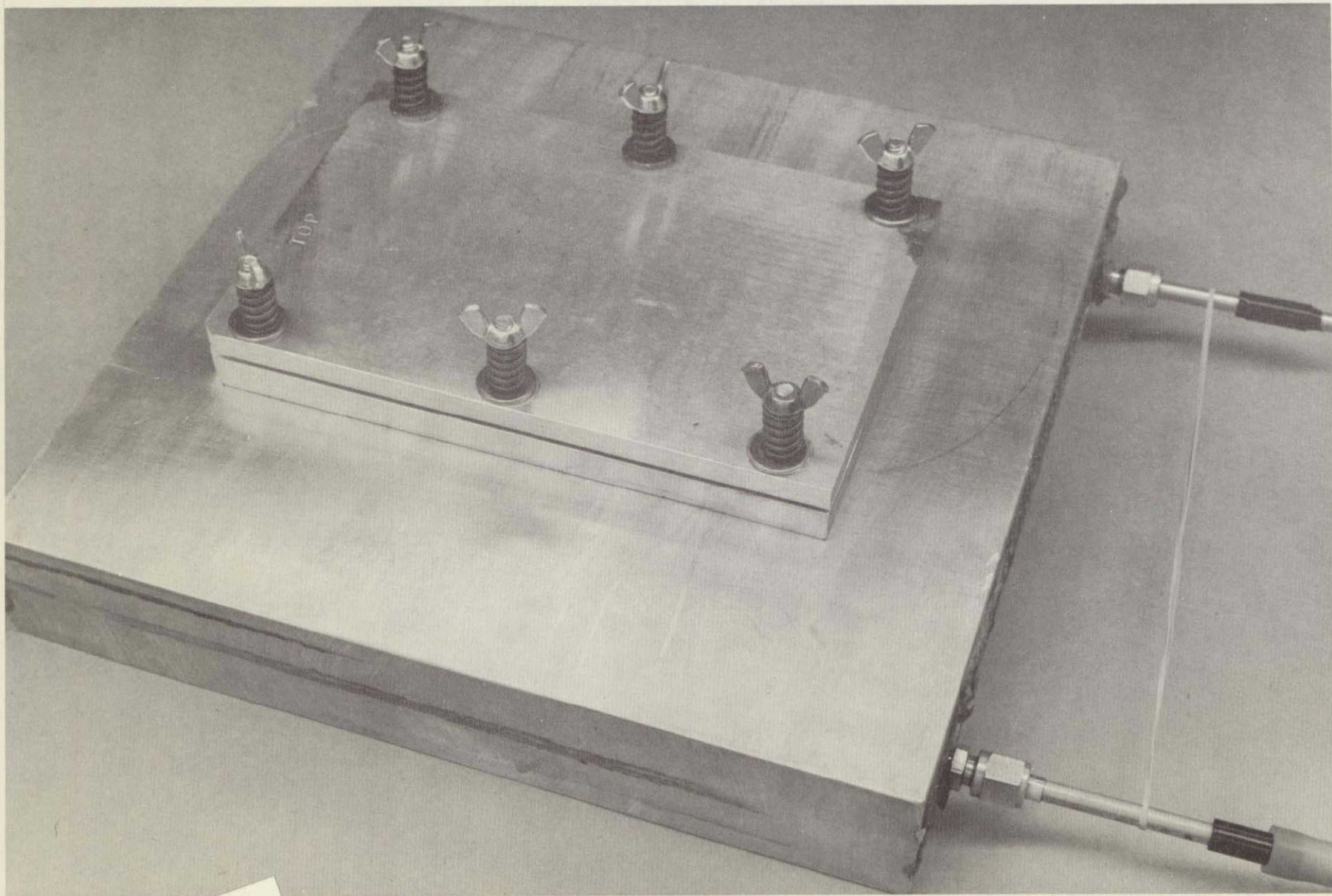
A second group of 0.0025-cm (1-mil)-thick layers of polyimide was prepunched to expose the P-contact soldering points and the cell interconnect tabs. A layer of this was laminated over each etched copper pattern, again using FEP as the adhesive. Finally, soldering points and tabs were electroless tin coated to a nominal  $7.6 \times 10^{-5}$  cm ( $30 \times 10^{-6}$  in.) thickness.

These operations produced the flexible substrates with integral interconnects.

### 3.2.3 Induction Soldering of P-Cell Contacts

Sn 62 solder was added to each substrate cell contact in controlled amounts. The module substrate was then positioned so that a row of P-contact points was over the respective electromagnetic flux concentrators on an induction heater tool. A submodule string of five FEP-covered solar cells was first coated on the backsides with flux per MIL-F-14256, Type A, then positioned on the substrate, over the P-contact pads. The cells were aligned along the cell N-strip edges with the copper interconnect traces, and induction reflow soldered into position. These operations were repeated for each of the other two five-cell submodules.





NOT REPRODUCIBLE

Figure 25. — Water-cooled heat sink

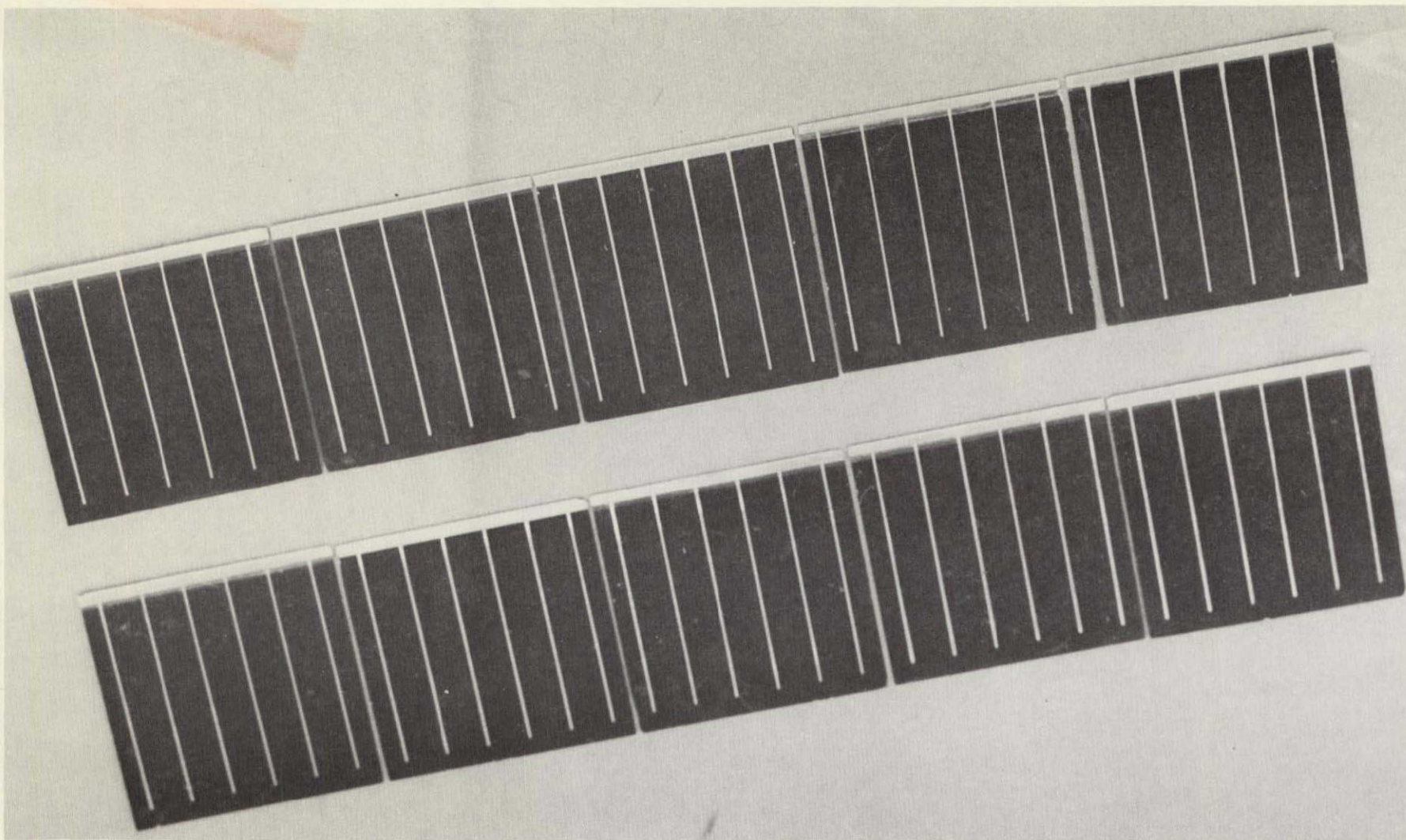


Figure 26. - FEP-covered submodules



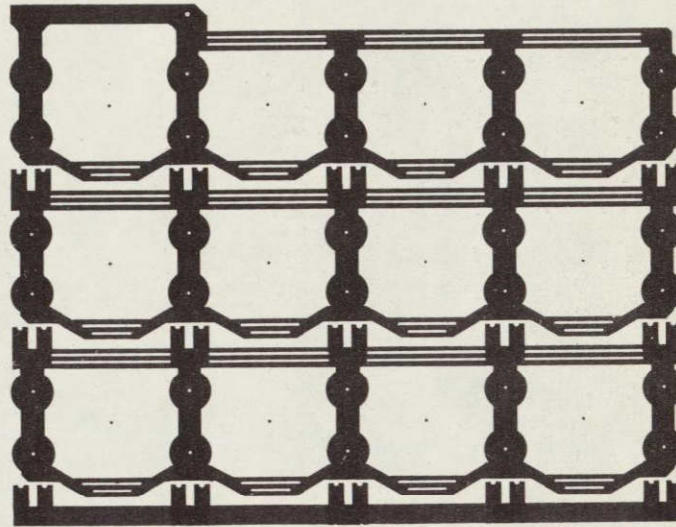


Figure 27. - Circuitry interconnect pattern

NOT REPRODUCIBLE

LMSC-D243070

44

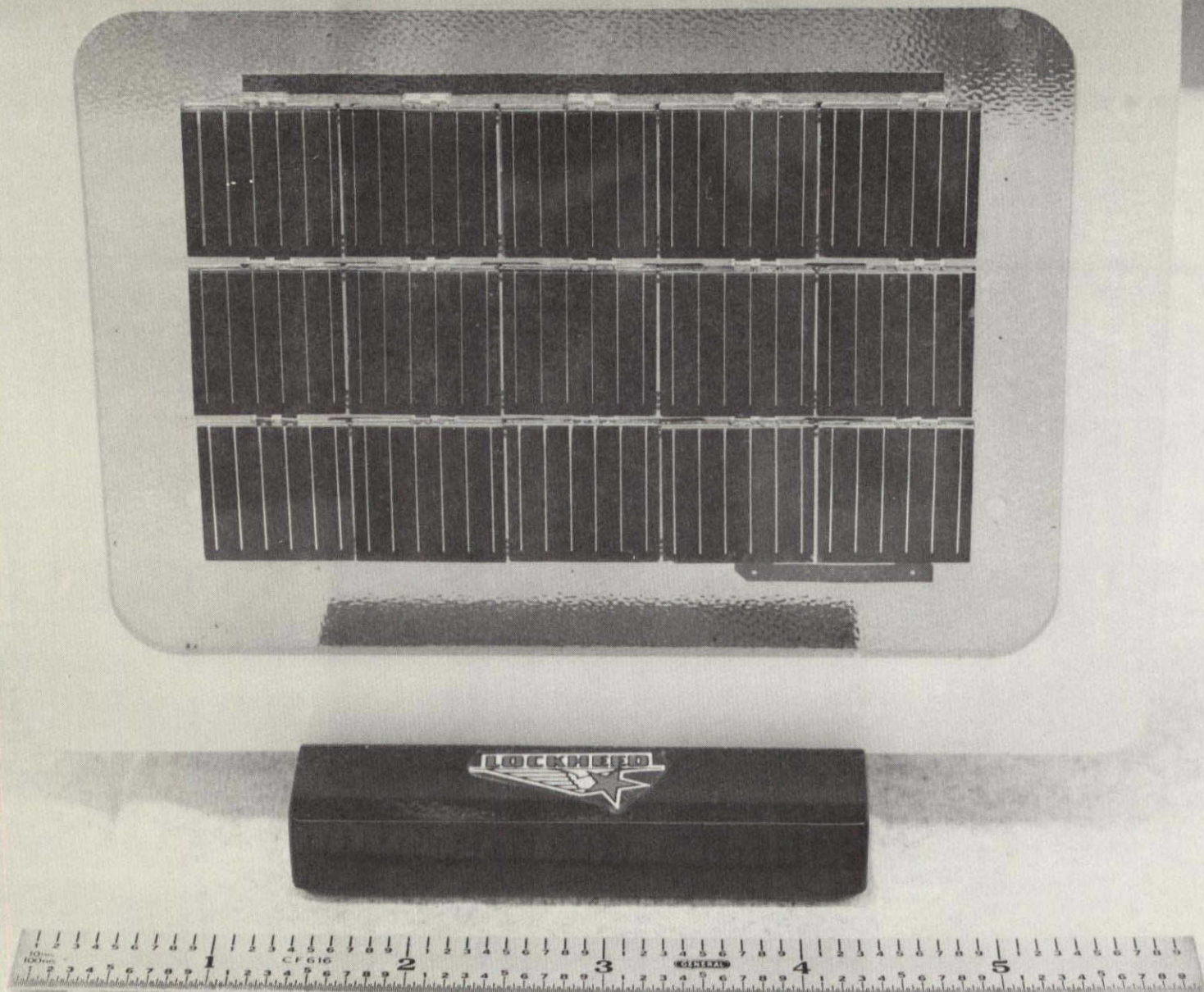


Figure 28. - FEP-covered module

### 3.2.4 Series Tab Interconnections

Two series interconnection tabs were provided for each cell. (These tabs were bent 90° up from the substrate during solar cell submodule installation.) With the cells in position on the substrate, each tab was bent around a No. 71 drill rod to provide a uniform radius, and placed on its corresponding cell N-strip. Solderless cells were used, so an Sn-62 solder preform [0.005 cm (0.002 in.) thick] had to be placed under each tab. Flux was added; then each tab was soldered in position with a time- and current-controlled soldering head and adjusted to provide less than 0.34 kg (3/4 lb) of electrode pressure on the cells. This completed fabrication of the solar modules configured with five cells in a parallel string and three strings in series. (Figure 28.)

### 3.3 FULL ENVIRONMENTAL TESTS

Fifteen cell modules fabricated as described in section 3.2 were subjected to the same full environmental test program as the single-cell packages.

#### 3.3.1 Thermal Cycling

A 15-cell FEP/solar cell module was mounted on the sample table in vacuum [ $1.3 \times 10^{-8}$  N/m<sup>2</sup> ( $1 \times 10^{-6}$  torr)] and observed during cooldown through the glass belljar. As the sample reached a temperature of approximately 153°K (-120°C), a sudden cracking appeared in three cells. As the temperature decreased to 143°K (-130°C), cells continued to crack until at 133°K (-140°C) 14 of the 15 cells were destroyed. Removal of the module and subsequent examination revealed simple cell fracture in six cells without delamination. The other eight damaged cells had suffered a cleavage within the silicon, resulting in a partial internal peeling effect in which the cleaved segment remained adhered to the FEP. The process was repeated with small sections (five cells) cut from a new module. The same dramatic failure mode was observed. Immersion of a module section in liquid nitrogen produced the same results.

This peculiar failure is suspected to be due to the mismatch of thermal expansion coefficients between the FEP on the front and the solder on the rear face of the cells. Perceptible bowing of single cells covered with FEP can be noted upon cooling to liquid nitrogen temperatures. However, no cracking or delamination was noted for single cells, which had no backface restraint. The internal cleavage observed with the module cells that were zone soldered provides an indication of the extreme strength of the FEP/solar cell bond at low temperatures.

To circumvent the thermal shock failure, a module was fabricated in which the FEP/solar cell packages were solder coated on the backfaces before attachment to the flexible substrate. Some difficulty was experienced in obtaining uniform backface solder coverage due to silver depletion of the solder pot; however, it was possible to obtain complete coverage on a reasonable number of cells.



This module, with fully soldered cells, was replaced in the thermal cycling apparatus. Observation of the module during cooling indicated that one cell suffered a simple fracture at approximately 123°K (-150°C) on the first cooldown. The module was exposed for 150 cycles between 298° and -436°K (25°C and -190°C) in a vacuum of  $1.3 \times 10^{-6}$  N/m<sup>2</sup> ( $1 \times 10^{-6}$  torr). Examination of the module subsequent to the test indicated that the initial crack was the total extent of module damage. Further examination of the cracked cell indicated that the backface had a nonuniform solder layer that is likely to have caused the failure.

### 3.3.2 Ultraviolet Exposure

A single 15-cell module was exposed to 2000 ESH of ultraviolet radiation in a vacuum of  $6.6 \times 10^{-7}$  N/m<sup>2</sup> ( $5 \times 10^{-7}$  torr), at an intensity of 10 equivalent suns, based on the 0.2-0.3  $\mu$  wavelength region. Measurements of the module output were made prior to exposure and after 500-ESH exposure increments. Figure 29 shows the results of the uv exposure. The open-circuit voltage was unaffected by the uv. The short-circuit current decreased by less than 3% in a manner similar to that experienced by the single cells under identical exposure conditions. The damage appears to have saturated near 1500 ESH, indicating that more prolonged exposure would not substantially change the module output.

### 3.3.3 Proton Exposures

Fifteen cell modules were exposed to  $3.2 \times 10^{-16}$  J (2-keV) protons in vacuum [ $7.9 \times 10^{-9}$  N/m<sup>2</sup> ( $6 \times 10^{-7}$  torr)]. Doses of  $1 \times 10^{13}$ ,  $1 \times 10^{15}$ ,  $1 \times 10^{17}$  and  $2 \times 10^{17}$  p<sup>+</sup>/cm<sup>2</sup> were received on four separate modules. Figures 30, 31, 32, and 33, respectively, show pre- and post-exposure current/voltage curves for those proton doses. The proton flux for these tests was  $1.94 \times 10^{13}$  p/cm<sup>2</sup>-sec. Comparison of Figures 30, 31, and 32 with the results from single-cell packages similarly exposed (Figure 16) reveals a strong correlation. For the modules, the extent of short-circuit current reduction varied from 0 for the  $1 \times 10^{13}$  p/cm<sup>2</sup> dose to approximately a 5% reduction for the  $1 \times 10^{17}$  p/cm<sup>2</sup> and  $2 \times 10^{17}$  p/cm<sup>2</sup> doses, the  $1 \times 10^{15}$  p/cm<sup>2</sup> dose causing a 2% decrease.

### 3.3.4 High Humidity and Temperature Test

Based on the experience gained with humidity testing of single cells, the module fabricated for such exposure was assembled from solar cells that had FEP covers heat sealed at 563°K (290°C), rather than 523°K (250°C). Exposure of this module to 95% relative humidity at 313°K (40°C) for 30 days resulted in no observable delamination or bubble formation. Attempts to separate the FEP after exposure using a sharp scalpel to probe the edges demonstrated adhesion of the same quality as the original module. It must be concluded that the FEP fusion bond provides superior resistance to high temperature and humidity exposures of the most extreme type likely to be encountered by solar panels under normal use.

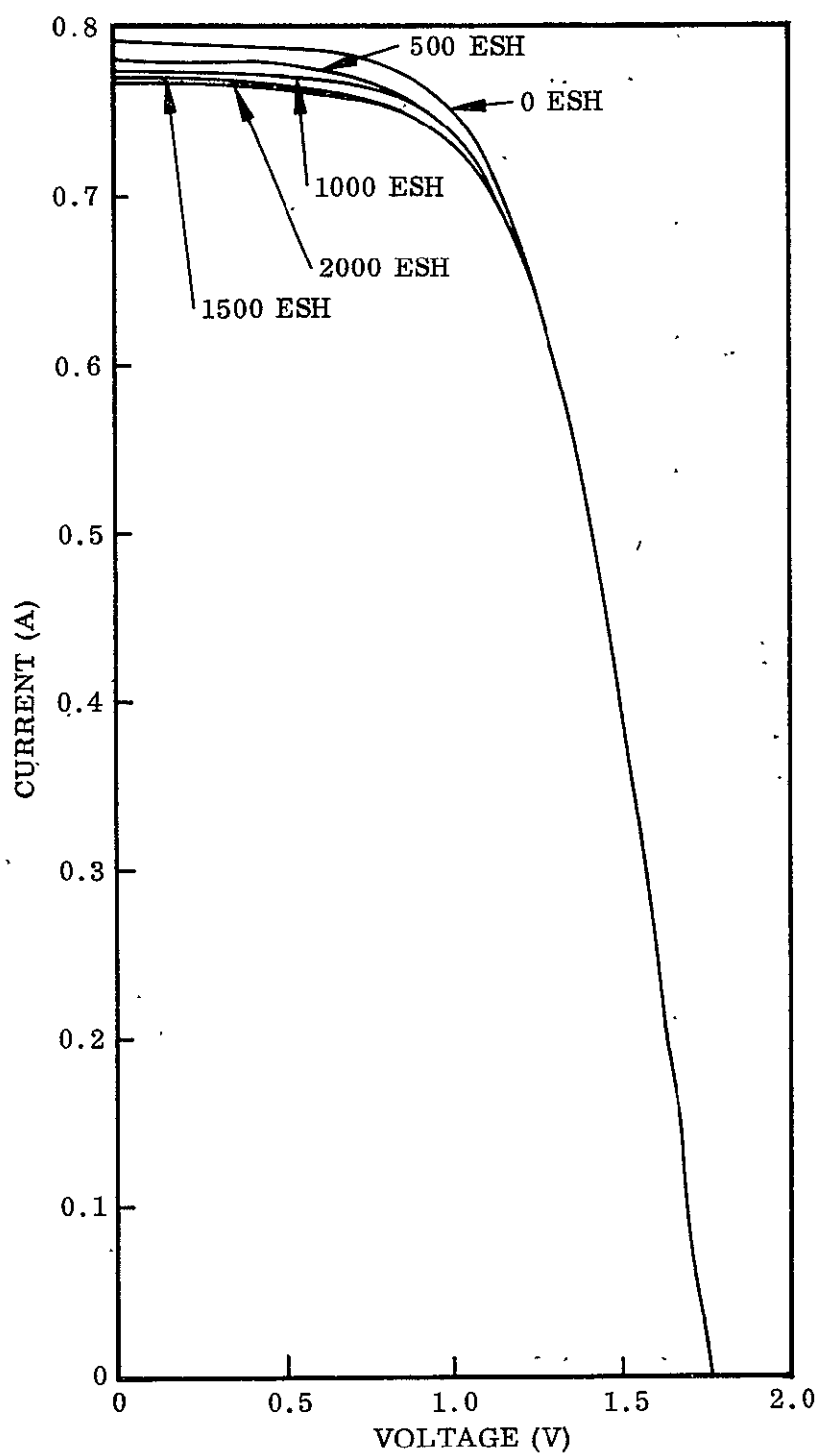


Figure 29. — Effect of uv on FEP-covered module

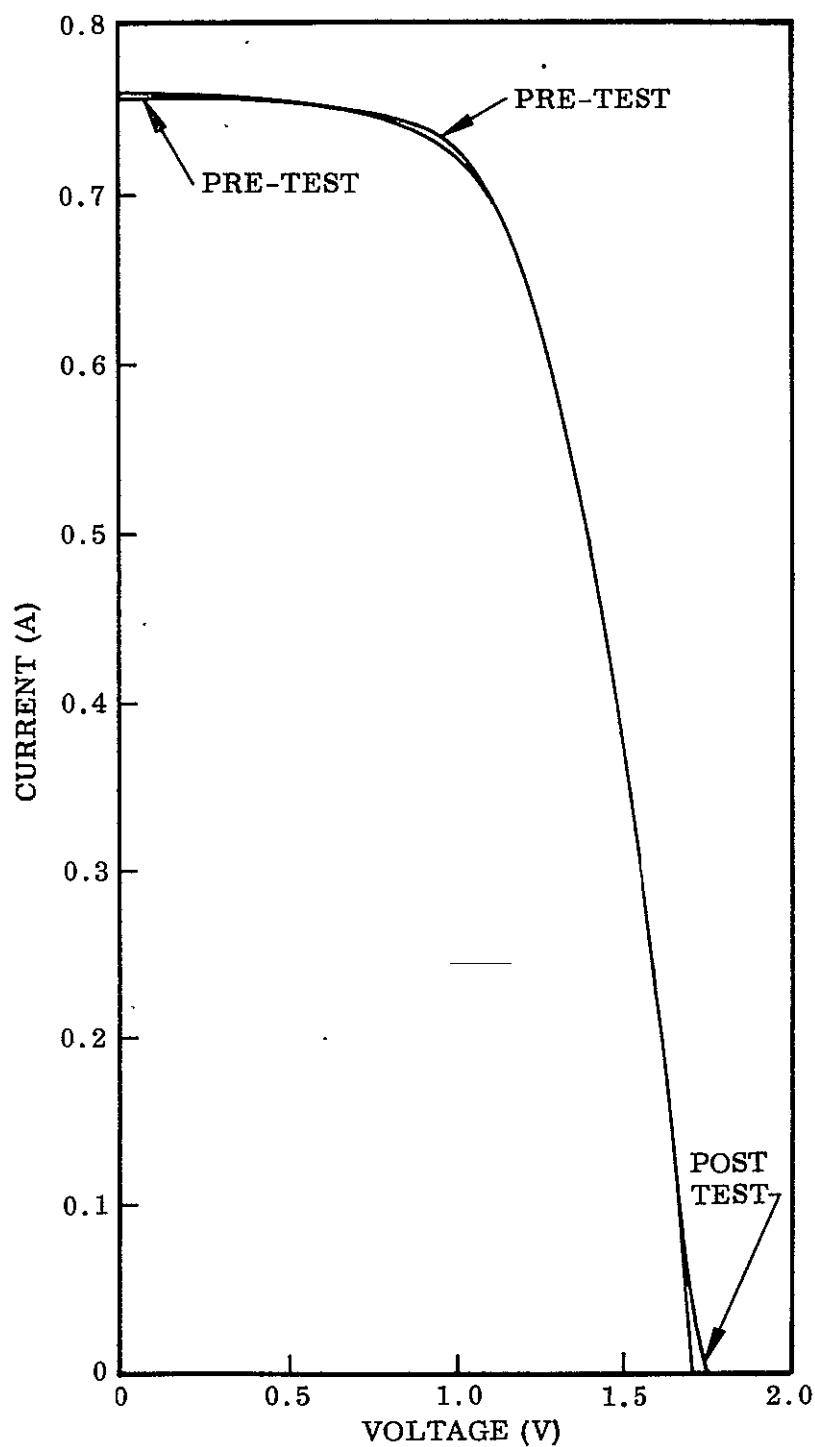


Figure 30. - Effect of  $1 \times 10^{13} \text{ p}^+/\text{cm}^2$  on FEP-covered module

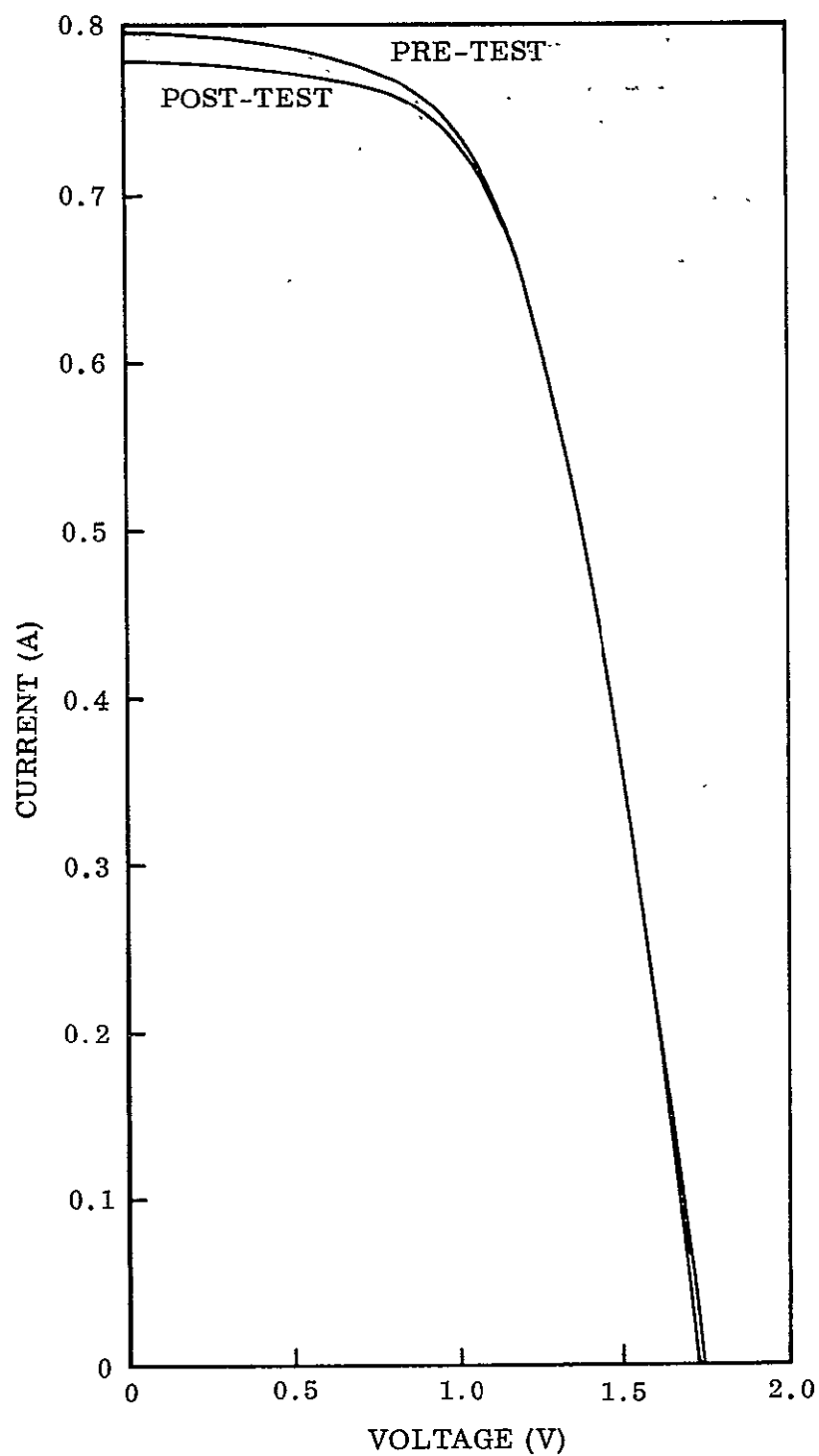


Figure 31. - Effect of  $1 \times 10^{15} \text{ p}^+/\text{cm}^2$  on FEP-covered module

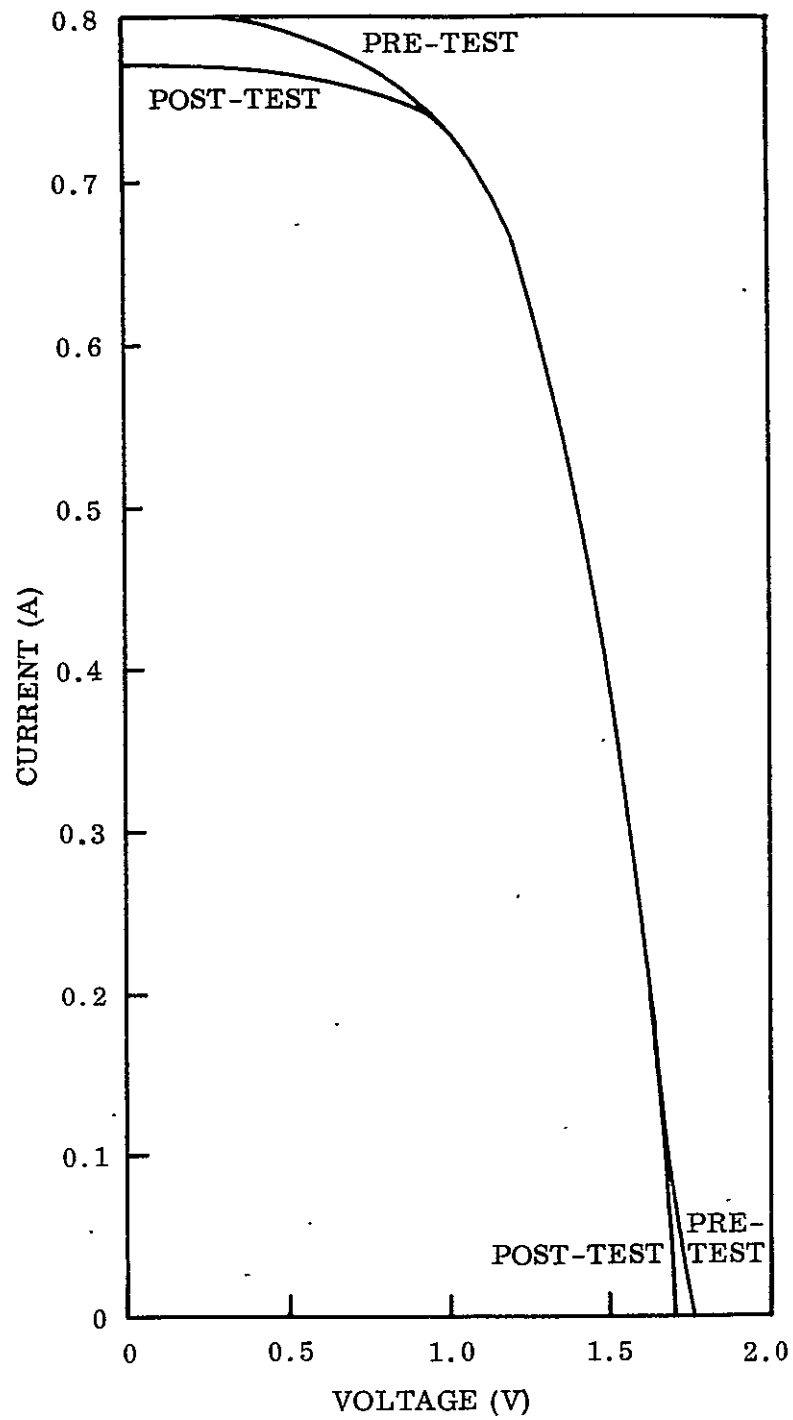


Figure 32. - Effect of  $1 \times 10^{17} \text{ p}^+/\text{cm}^2$  on FEP-covered module



### 3.3.5 Electron Irradiation

Modules were exposed to  $3.2 \times 10^{-13}$  J (2-MeV) electrons at the Gulf Radiation Technology  $4 \times 10^{-12}$  J (25-MeV) L-Band Linear Accelerator facility. The modules were held in vacuum [ $1.1 \times 10^{-9}$  N/m<sup>2</sup> ( $8 \times 10^{-7}$  torr)] and irradiated through an aluminum foil window. They were fastened to an aluminum water-cooled block to prevent excessive temperature rise. Total exposures of  $1 \times 10^{15}$  and  $1 \times 10^{14}$  e<sup>-</sup>/cm<sup>2</sup> were conducted at an electron flux of  $9.2 \times 10^{11}$  e<sup>-</sup>/cm<sup>2</sup> sec. The irradiated modules were removed from the chamber and immediately placed in an evacuated dessicator. Separation of the silicon oxide coating on the solar cell occurred for both modules, but to a greater extent for the higher dose. No gross delamination of the FEP occurred, but buffles were visible, particularly in the region of antireflection coating separation. These modules were retained under vacuum and current/voltage measurements were made within 24 hr. Subsequently, they were maintained in vacuum for 30 days with no noticeable change in appearance.

In order to establish a dose rate effect, an additional module was exposed for a total dose of  $4 \times 10^{14}$  e<sup>-</sup>/cm<sup>2</sup> but at a lower flux of electrons ( $5.7 \times 10^{10}$  e<sup>-</sup>/cm<sup>2</sup>-sec. At this dose rate, only a single small area (1 cm<sup>2</sup>) showed evidence of loss of antireflection coating and the FEP remained intact. Figures 34, 35, and 36 show the pre- and post-exposure module outputs for  $1 \times 10^{15}$ ,  $1 \times 10^{14}$ , and  $4 \times 10^{14}$  e<sup>-</sup>/cm<sup>2</sup>, respectively. It should be noted that the module that received  $4 \times 10^{14}$  e<sup>-</sup>/cm<sup>2</sup> was less damaged than the one that received  $1 \times 10^{14}$  at the higher flux. The difference may be due to the fate of the antireflection coating, which influences the solar absorptance of the module surface. The results tend to substantiate the premise that the catastrophic electron-induced failure of the FEP/solar cell bond is a result of the excessively high electron flux used in these tests.

### 3.3.6 Full Environmental Test Summary

The testing of the 15-cell modules conclusively demonstrated the feasibility of extending the process for single FEP/solar cell packages to multicell modules. No significant differences were noted for the performance of the modules in comparison with the FEP-covered single cells.

No special manufacturing problems were encountered in fabrication of the modules. The procedures developed appear to be amenable to large-scale production; however, it was not the intent of the research program to develop manufacturing procedures, but rather to establish the feasibility of the concept.

### 3.3.7 Optical Properties of FEP-Covered Solar Cells

In addition to providing environmental protection of solar cell assemblies, the function of cell covers is to provide temperature control through radiative heat transfer in the space environment. The equilibrium heat temperature of a surface in space with no internal heat load is governed by the ratio of solar absorptance  $\alpha_s$  and infrared

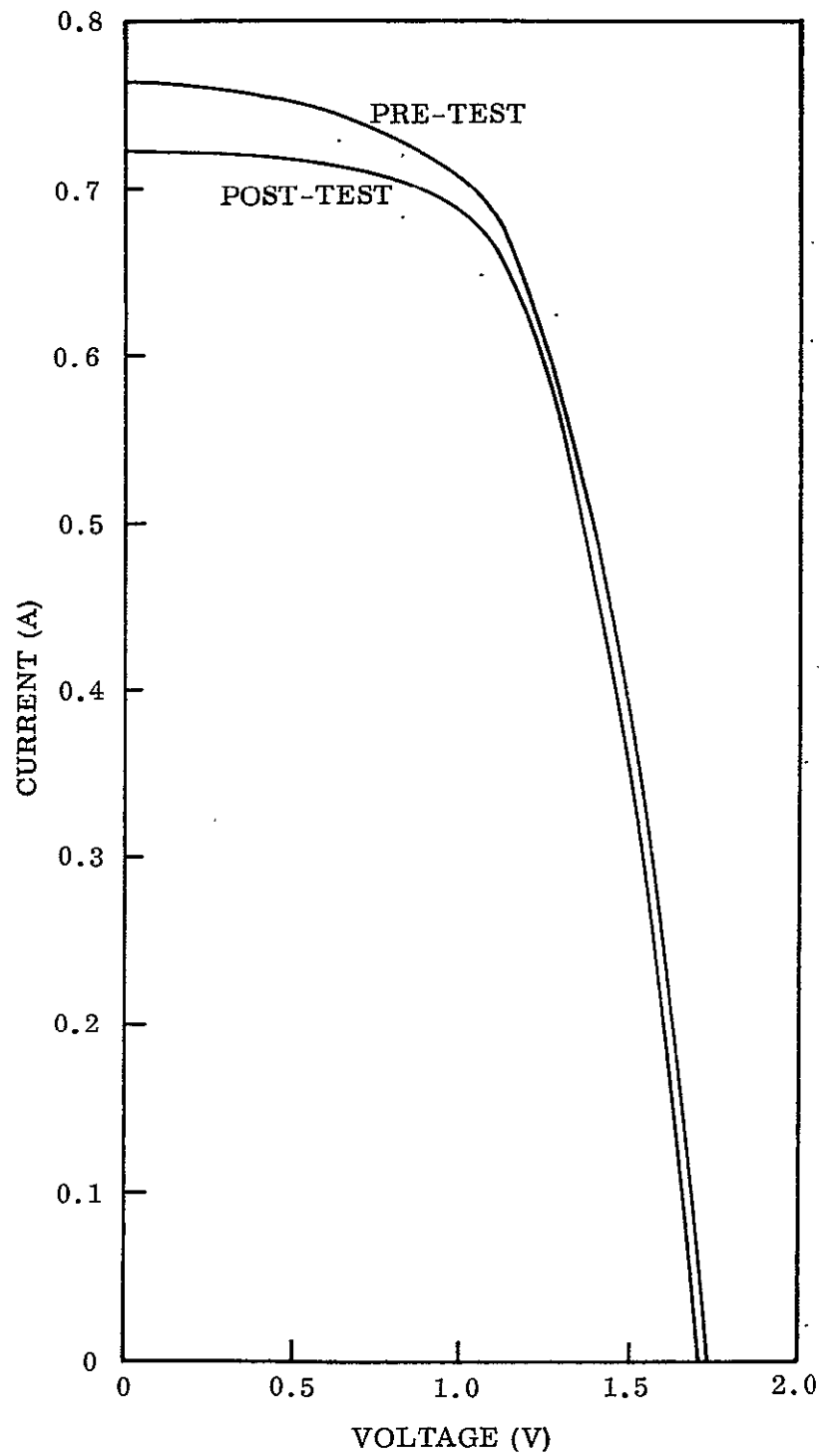


Figure 33. — Effect of  $2 \times 10^{17} \text{ p}^+/\text{cm}^2$  on FEP-covered module

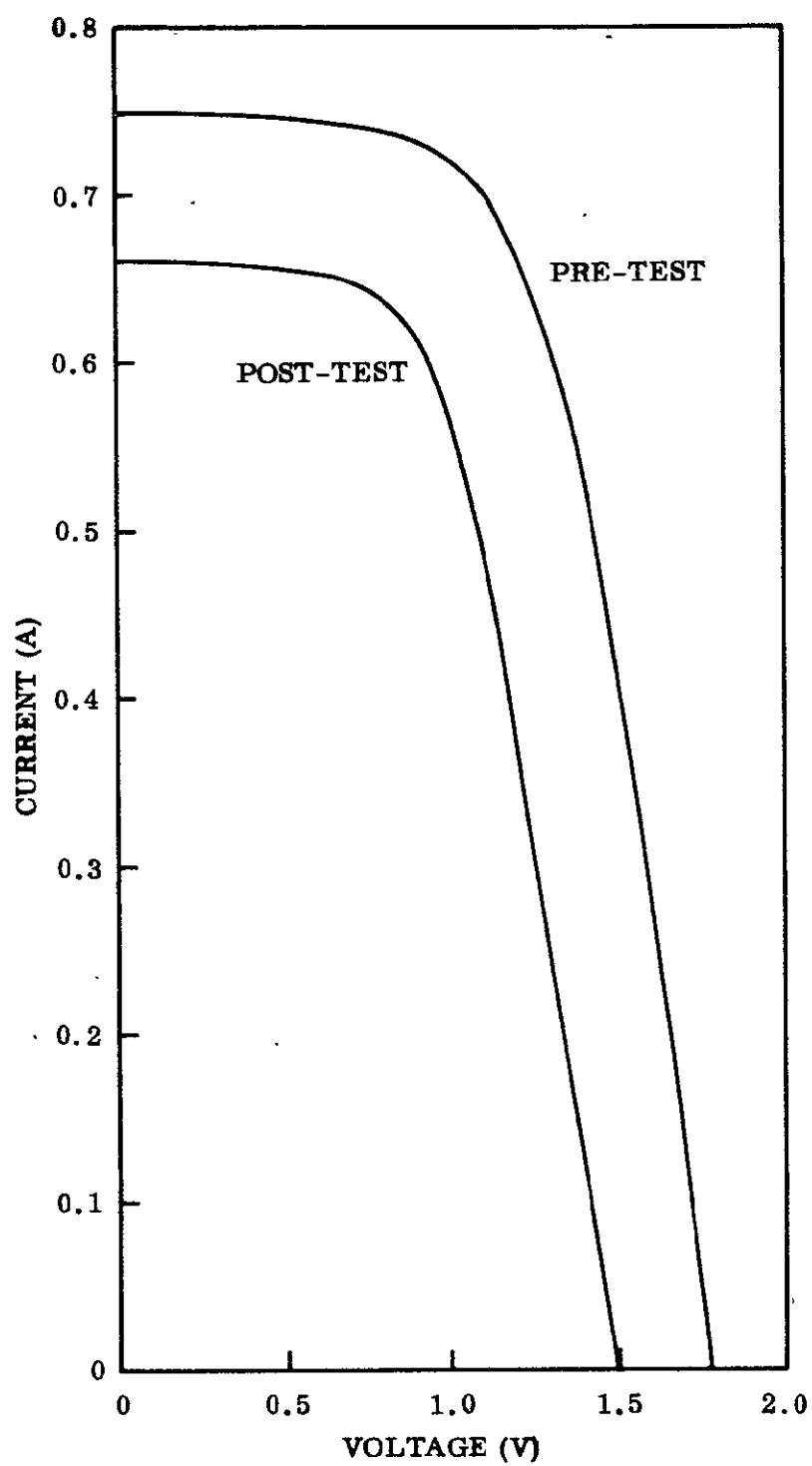


Figure 35. - Effect of  $1 \times 10^{14} \text{ e}^-/\text{cm}^2$  on FEP-covered module

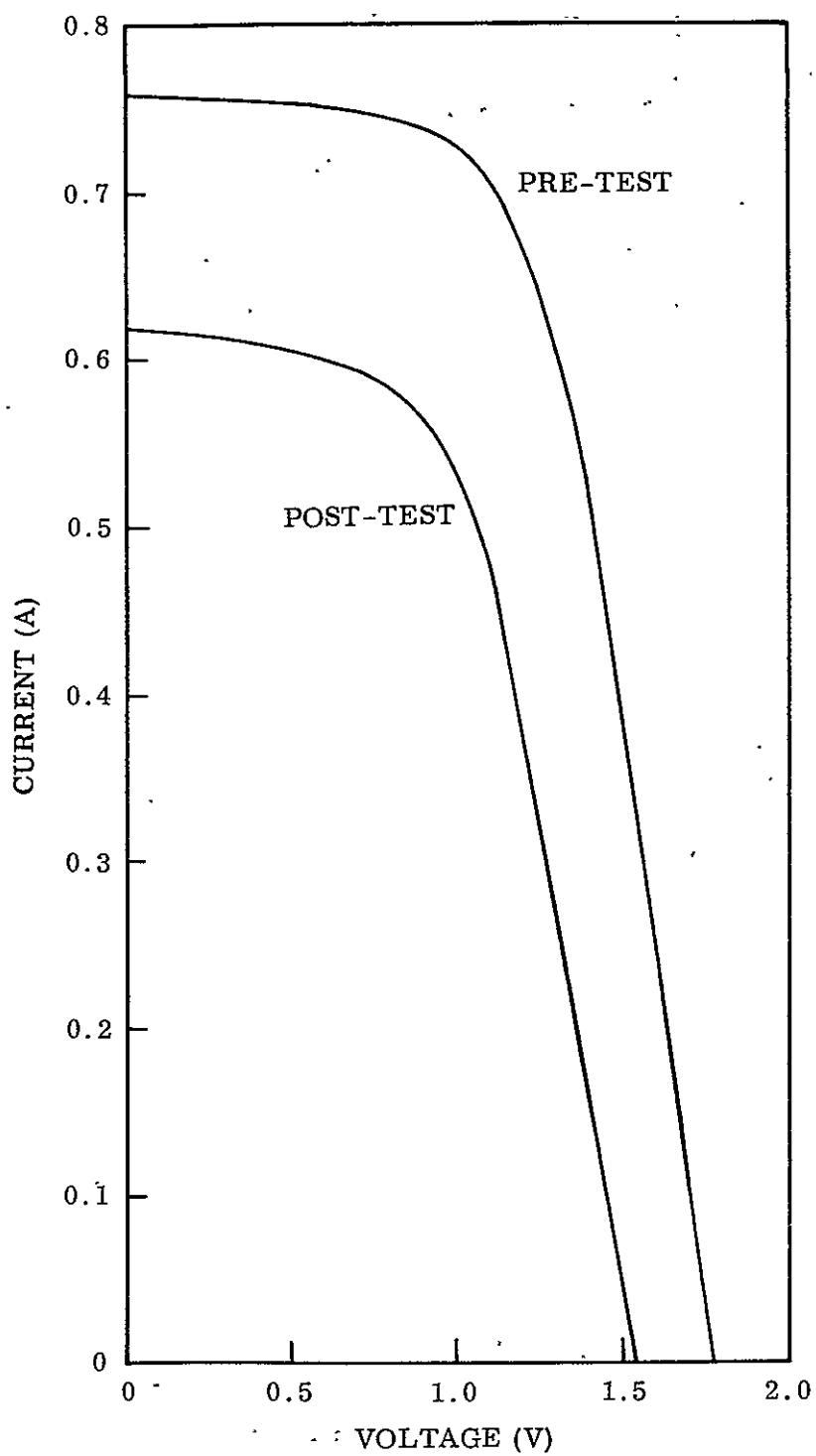


Figure 34. - Effect of  $1 \times 10^{15} \text{ e}^-/\text{cm}^2$  on FEP-covered module

emittance  $\epsilon$ . The lower the ratio  $\alpha_s/\epsilon$ , the lower the surface temperature will be. Since for a solar array, the efficiency increases inversely as the temperature, it is advantageous for the emittance to be as high as possible.

Figure 37 shows a comparison of emittance versus temperature for 5-mil FEP and 6-mil fused silica. Over the temperature range 173° to 423°K (-100° to +150°C), the FEP emittance is significantly greater than that of the fused silica.

A direct comparison can be made between the  $\alpha_s/\epsilon$  values for conventional modules and FEP-covered modules. Table 4 provides such a comparison for 15-cell modules fabricated from the same type of solar cell.

It can be seen that the emittance of the FEP-covered module is nearly 10% greater than the conventionally covered sample. In addition, because of the favorable refractive index match between the FEP and the silicon oxide cell coating, as well as the solderless condition of the FEP-covered cells, the solar absorptance of the FEP module is much greater. This should result in significantly greater power output (efficiency) for the FEP-covered cells, provided the temperature is the same for both types. However, calculations show that the FEP-covered cells will run as much as 13° hotter.

TABLE 4. COMPARISON OF OPTICAL PROPERTIES OF  
CONVENTIONAL AND FEP-COVERED MODULES

Type of cell	Cover	$\alpha_s$	$\epsilon$	$\alpha_s/\epsilon$
Centralab 12 mil, soldered	12-mil fused silica-silicone adhesive; blue filter and AR Coating	0.69	0.81	0.85
Centralab 12 mil, solderless	FEP-Type C, 5 mils, heat sealed	0.83	0.88	0.94

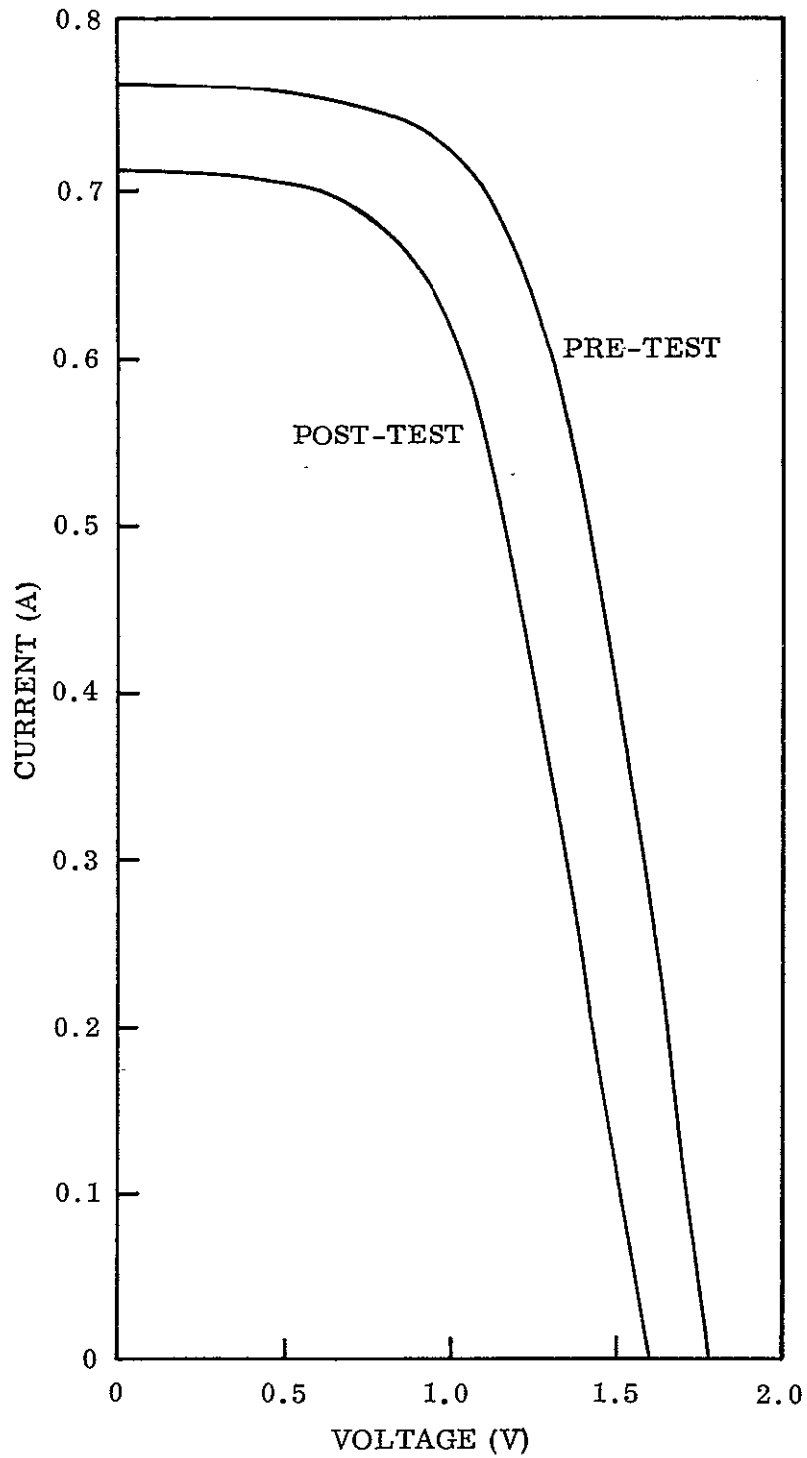


Figure 36. - Effect of  $4 \times 10^{14} \text{ e}^-/\text{cm}^2$  on FEP-covered module

## Section 4

## DISCUSSION AND CONCLUSIONS

The primary purposes of solar cell covers are to provide protection from penetrating radiation and to lower the operating temperature of the cells via high infrared emittance. Although conventionally protected solar arrays have been successful in providing reliable power for numerous spacecraft missions, many limitations exist. For many missions, the use of 0.005 to 0.01 cm (2 to 4 mil) covers would be adequate for both thermal control and radiation protection. Although this would result in a significant weight savings, especially for large arrays, it is not feasible because such thin fused silica is not currently available on a production basis at a reasonable cost. Even 0.075 cm (3-mil)-thick cover glasses provide a significant price penalty compared with 0.150 cm (6-mil) fused silica. An additional factor is the tendency of conventional solar cell cover application procedures to add a sizable amount to solar array fabrication costs.

Many of these problems can be overcome by the use of FEP as the solar cell cover material. In addition to providing equivalent radiation and temperature control properties, significant savings in cost, weight, and manufacturing operations can be effected.

Availability of the FEP film in thicknesses ranging from 0.0013 to 0.051 cm (0.5 to 20 mils) offers a wide range of temperature control, radiation protection, and array weight, so that suitable tradeoffs can be made within the current state-of-the-art. The direct heat sealing eliminates the need for adhesives, which add weight and fabrication complexity and require uv radiation protection. The low refractive index ( $n = 1.34$ ) ensures low front surface reflection losses without the need for antireflection coatings.

Material and installation costs provide a major advantage over conventional cover glasses. FEP is commercially available in large area rolls at a cost of \$0.008/m<sup>2</sup> (0.5 mil) to \$0.053/cm<sup>2</sup> (5 mils). The cost of coated fused silica cover glasses is about \$2500/m<sup>2</sup>. Installation costs add another \$2000 - 3000/m<sup>2</sup>. Since current production solar arrays provide approximately 100 W/m<sup>2</sup>, a 10-kW array would cost in the vicinity of \$500,000 more for adhesive-bonded 0.015 cm (6-mil) silica cover glasses than for 0.013 cm (5-mil) FEP film covering. Requirements for thinner cover slide application would result in even greater economies using FEP covers.

A comparison of FEP and fused silica cover material is presented in Table 5.

The results of this research program indicate that the Lockheed-developed concept for heat sealing of FEP to solar cells appears to provide a feasible alternative to conventional fused silica cover glasses. The handling, processing, and economic and

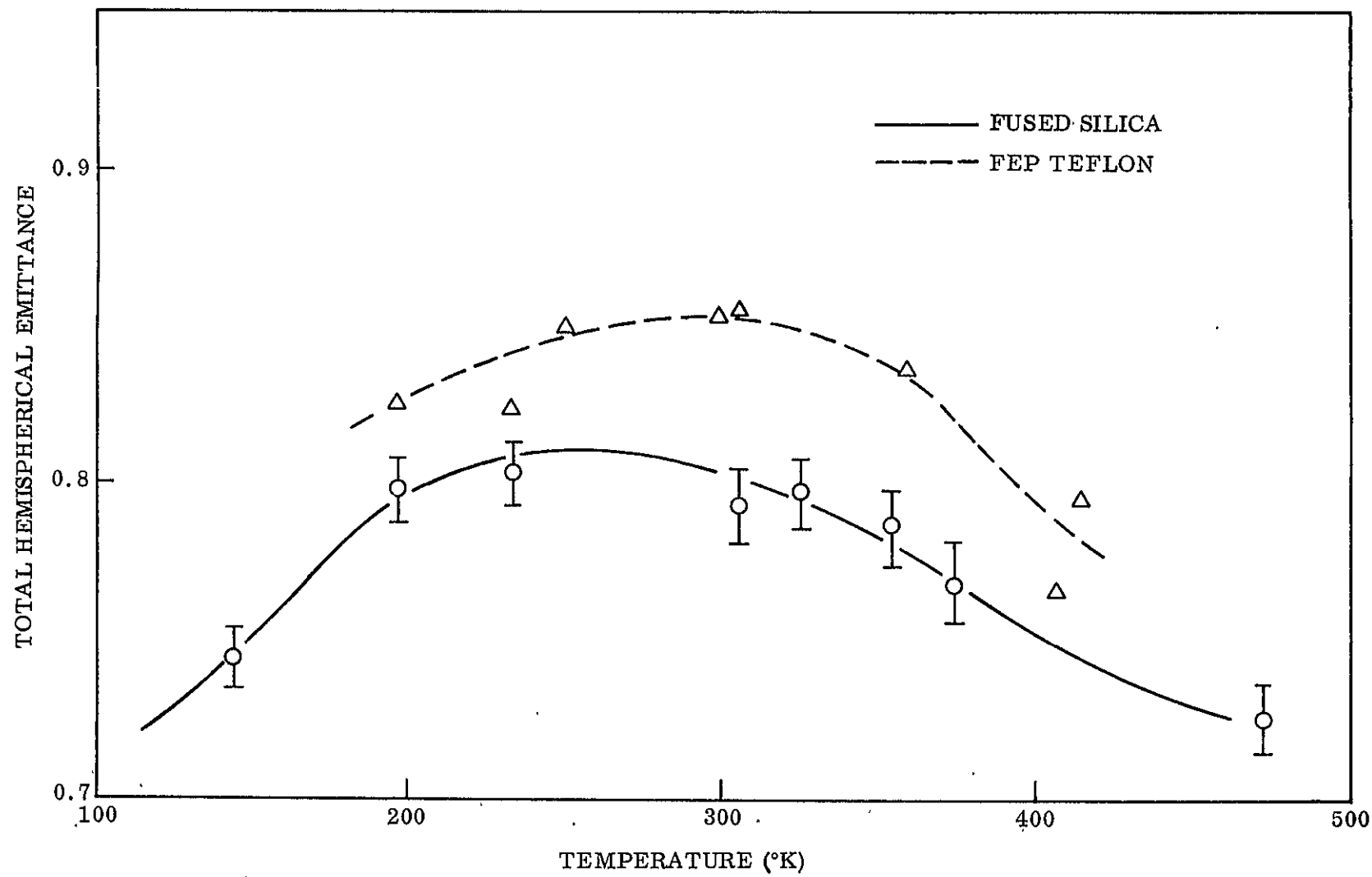


Figure 37. - Total hemispherical emittance of FEP compared with fused silica



## Section 5

### RECOMMENDATIONS FOR FUTURE STUDIES

The results obtained under this program have demonstrated the feasibility of using FEP heat sealed to silicon solar cells as a replacement for conventional adhesive-bonded fused silica. However, some areas require extensive research and development before large-scale production can be attempted. Some of these are listed below.

- Investigation of electron irradiation rate effects
- Alternate procedures for thermal cycling compatibility
- Techniques for covering large areas
- Comparison of Type A FEP with Type C FEP
- Analysis of FEP performance as a function of film thickness
- Application of the technique to silicon solar cells with wrap-around contacts
- Development of manufacturing and large-scale processing techniques
- Investigation of cell replacement procedures
- Studies of alternate materials and application techniques
- Investigations of adhesive-bonded FEP covers for large areas
- Flight testing of modules

The great promise of the FEP solar cell cover concept surely warrants continued effort, and a substantial amount of data must be generated if widespread confidence in the approach is to be achieved.

TABLE 5. — COMPARISON OF FEP AND FUSED SILICA COVERS

Property	Fused silica	FEP
Density (g/cm <sup>3</sup> )	2.20	2.15
Refractive Index	1.54	1.34
Front Surface Reflectance (%)	4.2	2.1
Handling	Fragile	Flexible
Bonding	Adhesive required	Heat sealing; no adhesive
Available thickness	0.015–0.10 cm (6–40 mils)	0.013–0.051 cm (0.5–20 mils)
Relative Cost	500	1
Antireflection Coating	Required	Unnecessary
Ultraviolet Filter	Required	Unnecessary
Radiation Protection	Equivalent for equal mass per unit area	Equivalent for equal mass per unit area
Radiation Stability	Good	Appears adequate but further testing required
Emittance	Equivalent	Equivalent
Area	Limited to single cells or small modules	Applicable to large areas; also protects cell edges
Application Cost	High	Low
Solar Transmittance	Equivalent	Equivalent

environmental characteristics of the heat-sealed FEP covers have been shown to be equivalent or superior to those of conventional adhesive-bonded cover glasses for silicon solar cells. The environmental test conditions employed in this study were, in many cases, much more severe than are anticipated for normal use. They do, however, in this early state of development of this concept, tend to accentuate the areas that require further development.

Since this program was designed to establish the feasibility of the Lockheed concept, rather than to serve as a flight qualification program, the limitations encountered do not diminish the potential utility of this system. On the contrary, the encouraging results obtained, to date, conclusively justify substantial continued research and development of the FEP heat-sealing techniques. It is anticipated that the use of FEP solar cell covers will provide a major milestone in solar cell technology.

## Appendix A

### EXPERIMENTAL APPARATUS

#### A.1 STATIC ULTRAVIOLET EXPOSURE APPARATUS

The static ultraviolet exposure chamber is a water-cooled stainless steel bell jar 35 cm (14 in.) tall and 35 cm (14 in.) in diameter. The solar cells are mounted on a water-cooled, semicylinder copper sample holder concentric with the ultraviolet source and at a distance of 10 cm (3.9 in.), which results in nominal irradiances of 10 suns of ultraviolet energy. A flux density of 1 sun of ultraviolet energy is defined as the flux density of extraterrestrial radiation at 1 AU from the sun, in the wavelength interval of 0.2 to 0.3  $\mu$  (2000 to 3000 Å). At these flux densities, the sample temperatures are maintained between 311° and 325°K for all ultraviolet tests in this chamber. Thermal contact conductance between the sample and the water-cooled copper sample holder is controlled with individual mounting frames which pressed the backface of the sample against the copper. Vacuums are established prior to initiation of ultraviolet exposure with cryogenic sorption roughing pumps and an electronic high-vacuum pump to avoid potential oil contamination problems. The chamber pressure is typically  $2.7 \times 10^{-9}$  N/cm<sup>2</sup> ( $2 \times 10^{-7}$  torr).

The source of ultraviolet energy is a 1-kW A-H6 (PEK Labs Type C) high-pressure mercury-argon capillary arc lamp. Approximately 35% of the lamp's radiant output is in the interval 0.2  $\mu$  to 0.4  $\mu$  (2000 to 4000 Å). The total output of the lamp is in the interval 0.2 to 2.6  $\mu$  (2000 to 26,000 Å). The lamp is water cooled and has a quartz water jacket and velocity tube. This assembly is lowered into a quartz envelope extended into the exposure chamber from the top. The assembly can be withdrawn to change lamps without disturbing the established vacuum. Unless a lamp ruptures, it is run for 100 hr and then replaced. Each test is begun with a new lamp. This procedure is followed because the A-H6 output decreases with time more in the 0.2- to 0.3- $\mu$  (2000- to 3000-Å) interval than in the 0.3- to 0.4- $\mu$  (3000- to 4000-Å) interval. Therefore, for materials that are degraded primarily by energy of wavelengths less than 0.3  $\mu$  (3000 Å), an old lamp will produce less degradation than a new lamp for the same total ultraviolet exposure, expressed in sun-hours. Some control over this effect is achieved by following this standard replacement procedure.

The ultraviolet intensity is monitored external to the vacuum chamber with a calibrated RCA 935 phototube in conjunction with a Corning 7-54 filter, which transmits only the near-ultraviolet output of the lamp. The output of the phototube is automatically measured and recorded for a few minutes each hour with a recording microammeter. The intervening quartz window and 7-54 filter are periodically checked for degradation in spectral transmittance and cleaned or replaced as necessary. When desired, a Corning 0-54 filter is used to compare the intensity in the 0.2- to 0.3- $\mu$  (2000- to 3000-Å) region with that in the 0.3- to 0.4- $\mu$  (3000- to 4000 Å) region as a measure of the relative degradation of lamp output in the shorter wavelength regions.

Section 6  
REFERENCES

1. "Teflon FEP Heat Sealing Principles," Technical Information Bulletin T-14, E. I. Dupont de Nemours and Co., Wilmington, Delaware.
2. A. E. Hultquist et al., Advanced Thermal Control Materials, LMSC-A967871, May 1970.
3. M. McCargo, S. A. Greenberg, and R. A. Breuch, Study of Environmental Effects on Spacecraft Thermal Control Materials, Final Report, NAS 2-4353, NASA Ames Research Center, January 1969.
4. Handbook of Geophysics, Chap. 16-3, "Solar Radiation Tables," Macmillan Company, 1960, pp. 16.16-16.17.
5. A. J. Hundhausen et al., J. Geophys. Res., Vol. 75, 1970, p. 643.
6. J. I. Vette, Electrons at Synchronous Altitudes, NASA SP-3024, Vol. III.

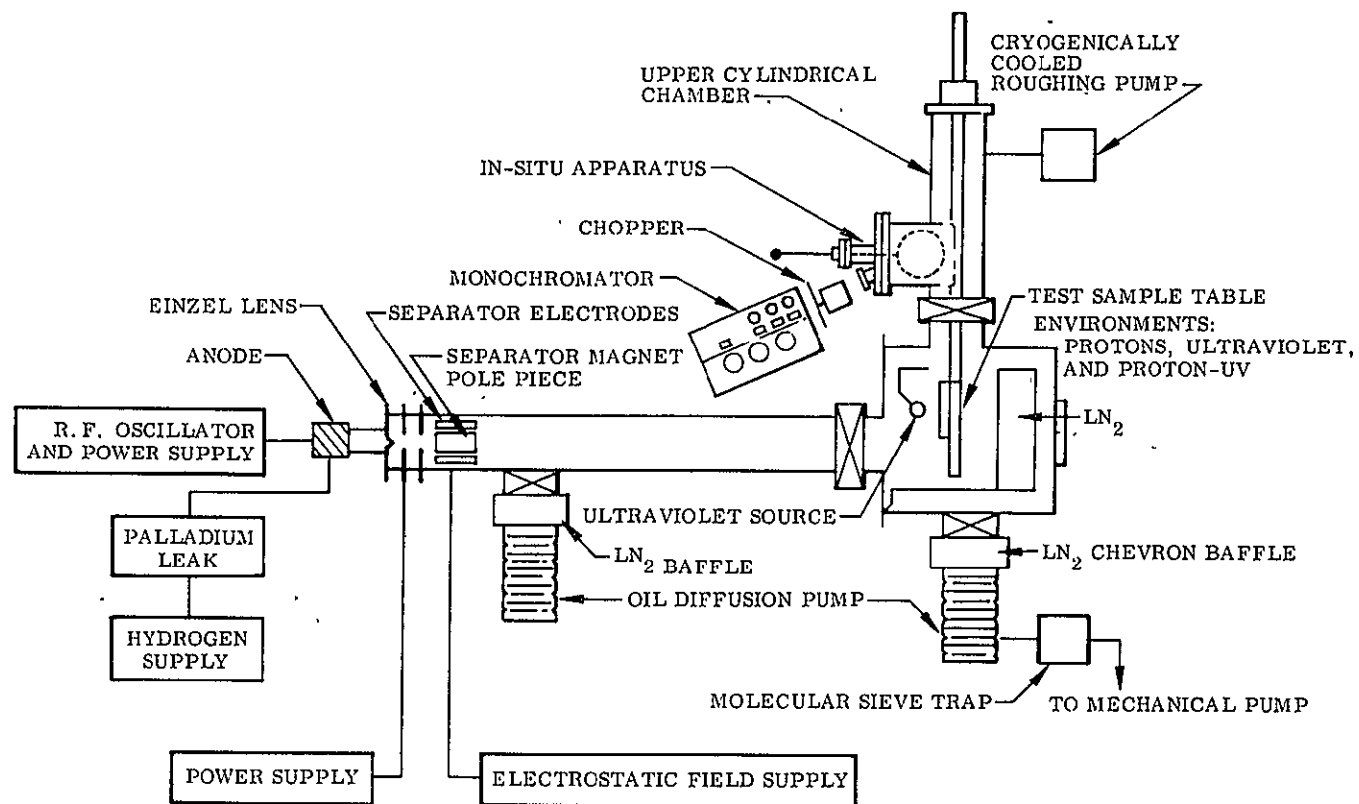


Figure 38. - Combined environments chamber

## A.2 PROTON EXPOSURE FACILITY

The Lockheed combined environments chamber was used for the proton exposures in this work. It has been described in detail (ref. 3) and is represented schematically in Figure 38.

The chamber, which affords simulation of three separate environments concurrently (proton only, ultraviolet only, and combined proton-plus-ultraviolet), is fabricated from 301 stainless steel with an extensive cryogenically cooled baffling system enclosing the test sample table during exposure. The sample table is so designed as to allow variation of exposure temperature from 77° to 423°K. The pumping is provided by suitably baffled diffusion pumps. The system is capable of maintaining a pressure of  $6.6 \times 10^{-9}$  N/cm<sup>2</sup> ( $5 \times 10^{-7}$  torr) during exposure conditions.

The proton source is an Ortec rf ion source and mass analyzer unit consisting of an rf source, an Einzel lens, and a crossed field (magnetic  $\times$  electrostatic) analyzer. The unit operates with an accelerating voltage of 0 to  $8 \times 10^{-16}$  J (5 keV), and absolute proton intensity at the test sample location is determined using a series of Faraday buttons which are interchangeable with the test table and can traverse the entire proton beam at the sample location.

## A.3 SOLAR SIMULATOR

The solar simulator used in this study is an Optical Coating Laboratory Solar Simulator Model 31. Radiation of wavelengths larger than  $0.65 \mu$  (6500 Å) is provided by a tungsten lamp; the remainder of the output is from a xenon arc lamp. The output from the two lamps is passed through an optical system containing suitable filters and combining optics. The output is in the form of a nearly parallel beam incident on the sample plane.

The simulator output was measured using a Cary Model 14 spectrophotometer equipped with a spectroradiometric accessory. The source was compared with a National Bureau of Standards calibrated tungsten-halogen lamp throughout the spectral range 0.25 to  $1.5 \mu$  (2500 to 15,000 Å). Figure 39 shows the simulator output compared with the Johnson sun (ref. 4). Figure 40 indicates the spectral deviation of the OCLI simulator from the spectral irradiance of the sun (AMO). The simulator is seen to agree within  $\pm 10\%$  over the spectral region of interest, 0.4 to  $1.2 \mu$  (4000 to 12,000 Å).

Following measurement of the spectral content of the solar simulator, the absolute intensity at the sample table position was calibrated using a NASA standard silicon cell (Standard Cell No. 168) supplied by the Jet Propulsion Laboratory. Secondary calibration of the spectral irradiance was routinely monitored using silicon solar cells equipped with wide-bandpass filters.

Sample cells to be measured were held on a water-cooled block by means of a vacuum holddown. Current-voltage curves were measured using a variable rheostat system in conjunction with a Moseley X-Y recorder. The reproducibility of the simulator-recorder system on a day-to-day basis was routinely  $\pm 1\%$ . Compensation for long-term lamp variations was achieved by adjustments of sample-to-lamp distances and lamp current.

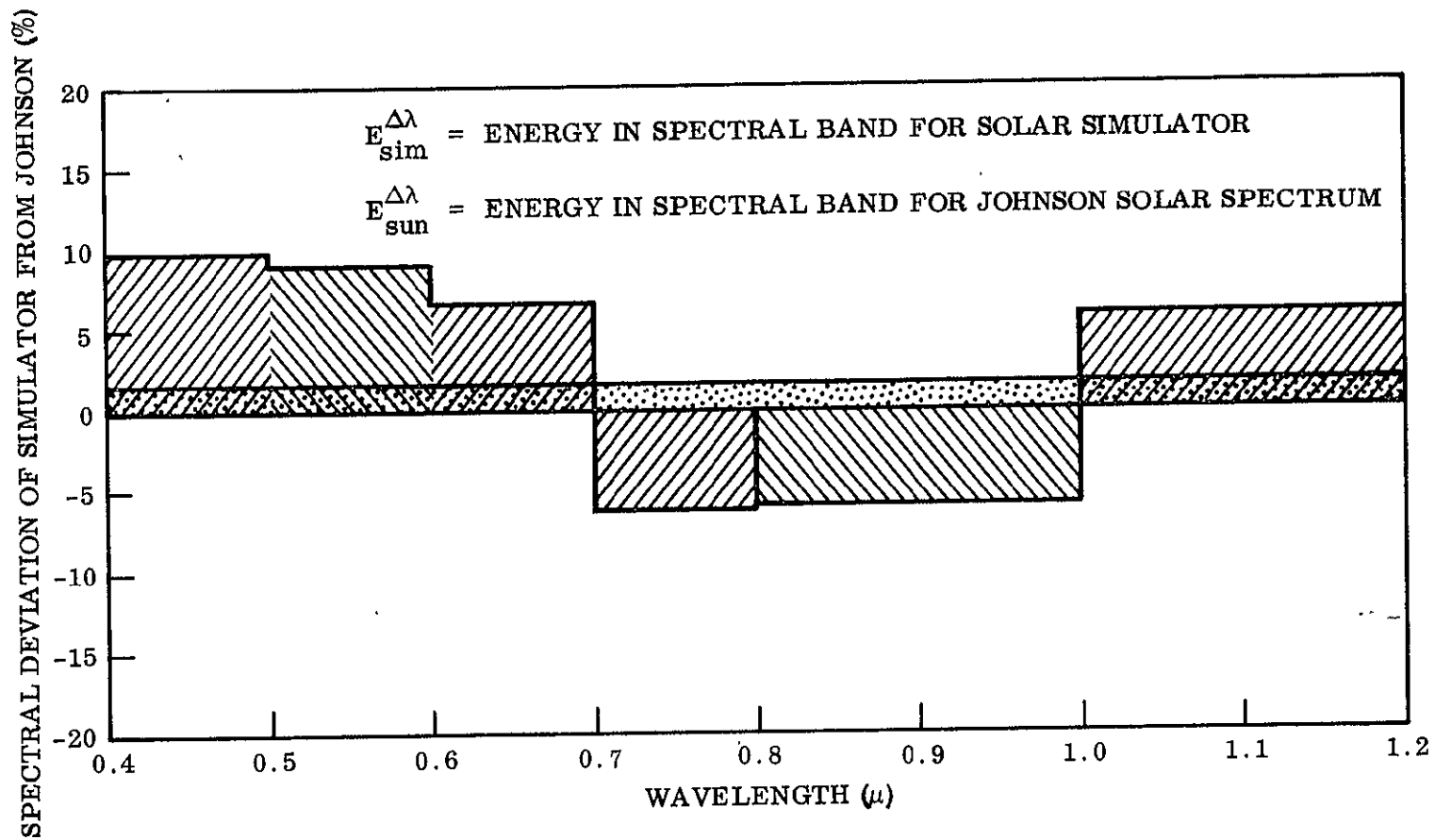


Figure 40. — Spectral deviation of simulator

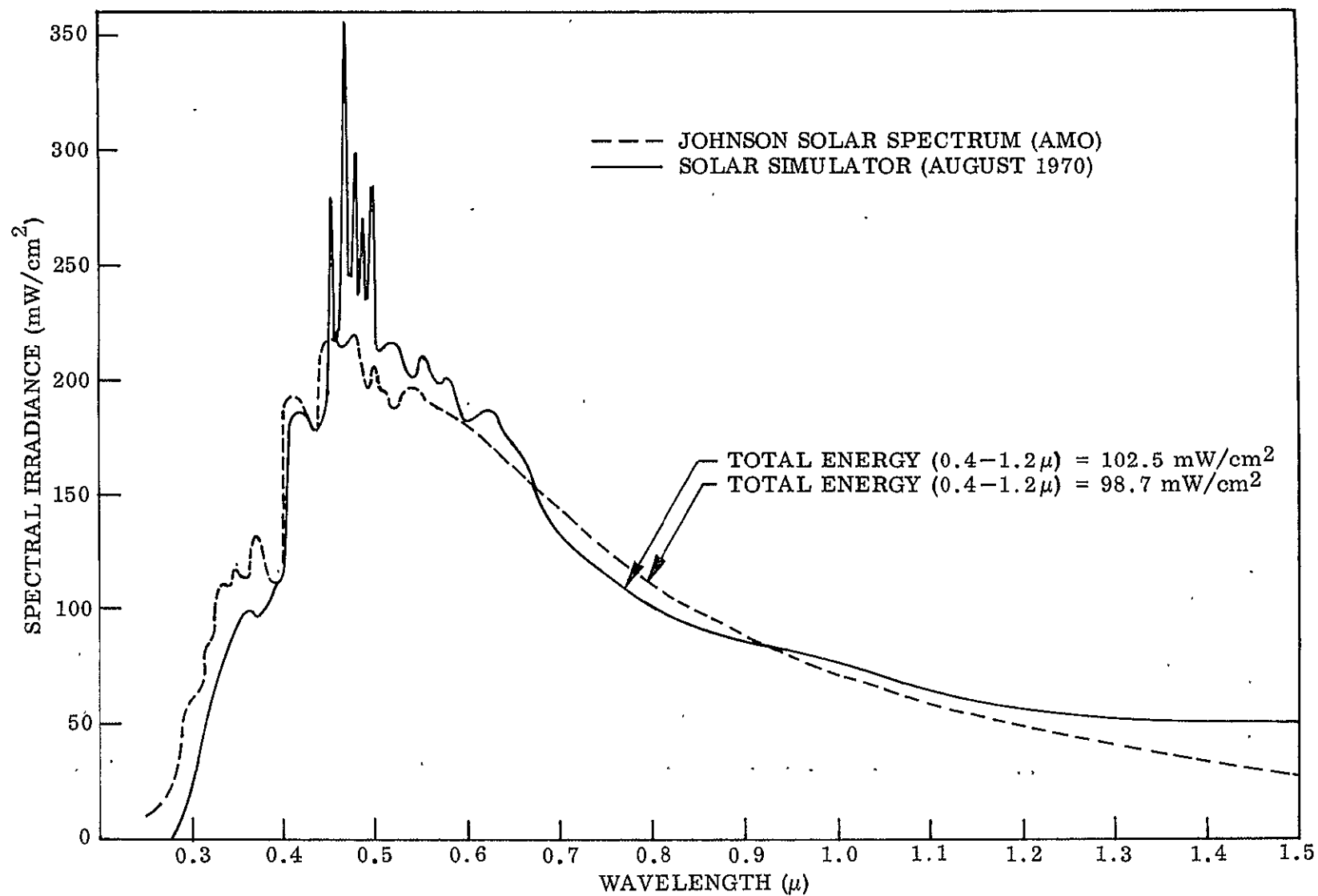


Figure 39. — Comparison of solar simulator with the Johnson solar spectrum



## Appendix B

### SPACE ENVIRONMENTAL CONSIDERATIONS

It is of some interest to compare the environmental test conditions with those likely to be encountered by solar cells operating on space vehicles. Although no single orbit is likely to encounter all the components evaluated, a comparison of typical space conditions and laboratory simulation parameters makes analysis of the test results more meaningful.

#### B.1 SOLAR ULTRAVIOLET RADIATION

The laboratory source used for the uv tests was a 1-kW mercury-argon A-H6 high-pressure arc lamp, which provides poor simulation of the solar ultraviolet spectrum. However, on an energy basis, the illumination was adjusted to provide 10 times the energy received at the surface in the spectral region 0.2 to 0.3  $\mu$  (2000 to 3000 Å). No evidence exists indicating spectral selectivity of FEP Teflon in this spectral band, although the FEP absorption edge (Figure 1) occurs in this region.

#### B.2 THERMAL CYCLING

The thermal cycle used in this study, 298° to 88°K (25° to -190°C) over a 70-min period approximates the "worst case" conditions likely to be encountered by a vehicle in a near-earth orbit. It is unlikely that such temperature extremes would be encountered on an operational vehicle. A minimum temperature of 163°K (-110°C) represents more nearly the realistic low bound likely to be experienced by a solar panel in a near-earth orbit, whereas the high bound may be closer to 373°K to (+100°C). Under special orbital conditions, however, for spinning panels and highly elliptical orbits, more extreme temperature excursions might be encountered.

#### B.3 LOW-ENERGY PROTONS

The interplanetary solar wind consists predominantly of  $H^+$  with a 4% contribution from  $He^+$ . In addition, the solar wind plasma has an electron component with energies in the vicinity of  $10^{-19}$  J. The energy of the protons spreads from  $0.8 \times 10^{-16}$  to  $4.8 \times 10^{-16}$  J (0.5 to 3.0 keV), with an average energy in the vicinity of  $1.9 \times 10^{-16}$  J (1.2 keV). From the Mariner IV and V data (ref. 5), the mean flux number at 1 AU is  $3 \times 10^8$  p/cm<sup>2</sup>-sec, which is equivalent to approximately  $9 \times 10^{15}$  p/cm<sup>2</sup>-year. This value is strongly dependent upon solar activity. The flux of  $1 \times 10^{-16}$  J (2-keV) protons used in this study was approximately  $2 \times 10^{12}$  p<sup>+</sup>/cm<sup>2</sup>-sec. The acceleration factor, therefore, was on the order of  $4.5 \times 10^3$ . Apparently, no complications from such a highly accelerated testing occurred during this effort. The total laboratory dose of  $2 \times 10^{17}$  p<sup>+</sup>/cm<sup>2</sup> corresponds to approximately 25 years in the interplanetary solar wind plasma.

#### A.4 THERMAL CYCLING APPARATUS

The thermal cycling facility consisted of a horizontally mounted copper block equipped with cooling coils and a 200-W resistance heater. A predetermined thermal cycling profile was prepared using a Datatrak system equipped with a silicon controlled rectifier, which specified requirements for cooling (liquid nitrogen) or heating in accordance with the thermal profile. The sample table with solar cell samples was enclosed in a bell jar housing. Pumping was provided by a liquid nitrogen trapped oil diffusion pump. Pressures on the order of  $6.6 \times 10^{-9}$  to  $1.3 \times 10^{-8}$  N/cm<sup>2</sup> ( $5 \times 10^{-7}$  to  $1 \times 10^{-6}$  torr) were routinely attained. Temperature-time records were maintained by continuously recording sample and table temperatures using a dual pen recorder in conjunction with copper-constantan thermocouples suitably referenced to ice bath junctions.

#### B.4 ELECTRON IRRADIATION

Electrons in the energy range  $0.8 \times 10^{-13}$  to  $4.8 \times 10^{-13}$  J (0.5 to 3.0 MeV) are found at synchronous altitudes (ref. 6). Table 6 shows the energy-flux distribution for these charged particles averaged over local time, where  $E_{th}$  is the threshold energy above which the specified flux is valid.

TABLE 6. - ELECTRONS AT SYNCHRONOUS ALTITUDES

$E_{th}$ , $10^{-13}$ J (MeV)	Flux, $e^-/\text{cm}^2\text{-day}$
0.8 (0.5)	$4.2 \times 10^{11}$
1.6 (1.0)	$4.0 \times 10^{10}$
3.2 (2.0)	$3.7 \times 10^8$
4.8 (3.0)	$3.5 \times 10^6$

At  $1.6 \times 10^{-13}$  J (1 MeV), the flux converted to a per-second basis is on the order of  $1.2 \times 10^5$   $e^-/\text{cm}^2\text{/sec}$ ; on an annual basis, this is approximately  $3.7 \times 10^{12}$   $e^-/\text{cm}^2$ . Thus,  $1 \times 10^{14}$   $e^-/\text{cm}^2$  (the lowest electron dose in the laboratory study) is equivalent to 30 years in the synchronous environment. The dose rate in the simulation studies ( $9.2 \times 10^{11}$   $e^-/\text{cm}^2\text{-sec}$ ) is nearly 7 orders of magnitude greater than the natural fluence. It is not surprising that stability problems were associated with the high electron dose rate employed for simulation. Evidently, the electron environment was greatly oversimulated.